

**SYNTHESIS AND STUDY OF PHOTOPHYSICAL AND
METAL ION BINDING PROPERTIES OF A FEW NOVEL
SEMISQUARAININE AND CROCONAINE DYES**

**Thesis submitted to
Cochin University of Science and Technology
in Partial Fulfillment of the Requirements for the Degree of**

**DOCTOR OF PHILOSOPHY
in Chemistry under the Faculty of Science**

By

REKHA RACHEL AVIRAH

**Under the Supervision of
Dr. D. RAMAIAH**



**Photosciences & Photonics
Chemical Sciences & Technology Division
National Institute for Interdisciplinary Science & Technology
(Formerly, Regional Research Laboratory), CSIR,
Trivandrum 695 019, KERALA**

APRIL 2010

STATEMENT

I hereby declare that the matter embodied in the thesis entitled: "**Synthesis and Study of Photophysical and Metal Ion Binding Properties of a Few Novel Semisquaraine and Croconaine Dyes**" is the result of investigations carried out by me at the Photosciences and Photonics, Chemical Sciences and Technology Division of the National Institute for Interdisciplinary Science and Technology (*formerly*, Regional Research Laboratory), CSIR, Trivandrum, under the supervision of Dr. D. Ramaiah and the same has not been submitted elsewhere for a degree.

In keeping with the general practice of reporting scientific observations, due acknowledgement has been made wherever the work described is based on the findings of other investigators.

(Rekha Rachel Avirah)

National Institute for Interdisciplinary Science and Technology



Photosciences and Photonics
Chemical Sciences and Technology Division
CSIR, Trivandrum 695019, India



Dr. D. Ramaiah
Scientist

Tel: +91 471 2515362; Fax: +91 471 2490186
E-mail: rama@niist.res.in

April 30, 2010

CERTIFICATE

This is to certify that the work embodied in the thesis entitled: **“Synthesis and Study of Photophysical and Metal Ion Binding Properties of a Few Novel Semisquaraine and Croconaine Dyes”** has been carried out by Ms. Rekha Rachel Avirah under my supervision at the Photosciences and Photonics, Chemical Sciences and Technology Division of the National Institute for Interdisciplinary Science and Technology (NIIST), CSIR, Trivandrum and the same has not been submitted elsewhere for a degree.

(D. Ramaiah)

Thesis Supervisor

ACKNOWLEDGEMENTS

I have great pleasure in placing on record my deep sense of gratitude to Dr. D. Ramaiah, my thesis supervisor, for suggesting the research problem and for his guidance, support and encouragement, leading to the successful completion of this work.

I would like to express my thanks to Professor M. V. George for being an inspiration.

I wish to thank Dr. Suresh Das, Director and Professor T. K. Chandrashekar and Dr. B. C. Pai, former Directors of the National Institute for Interdisciplinary Science and Technology (NIIST) for providing the necessary facilities for carrying out the work.

I sincerely thank Dr. A. Ajayaghosh, Dr. K. R. Gopidas, Dr. K. George Thomas and Dr. A. Srinivasan, Scientists of the Photosciences and Photonics, Chemical Sciences and Technology Division, for all the help and support.

I thank Professor Prashant V. Kamat, University of Notre Dame for the help in carrying out the light harvesting studies.

I thank all the members of the Photosciences and Photonics and in particular, Dr. M. Hariharan, Dr. E. Kuruvilla, Dr. J. Kuthanapillil, Dr. P. N. Prakash, Ms. V. S. Jisha, Mr. A. K. Nair, Mr. C. K. Suneesh, Mr. P. C. Nandajan, Mr. K. S. Sanju, Ms. T. J. Dhanya, Mr. N. Adarsh, Ms. M. Betsy, Mr. A. K. Paul, Mr. H. Shankar, Mr. P. Rafeeqe, Mr. P. K. Mandali, Ms. K. P. Divya and Mr. S. Mahesh for their help and cooperation. I also thank members of other Divisions of NIIST. I would like to thank Mr. Robert Philip for his help and support and also Mrs. Saumini Shoji, Mr. A. Adarsh and Mrs. S. Viji for NMR, mass spectral and CHN analyses.

My Family and friends have been a constant source of support and encouragement. Words are insufficient to express my heartfelt

thanks for their love, guidance, motivation and patience. I thank my teachers at Union Christian College, Alwaye for nurturing my love for the subject.

Financial assistance from the CSIR and DST is gratefully acknowledged.

Rekha Rachel Avirah

Dedicated to

Ammachi, Pappa and Mamma

For you have given me more than your name...

CONTENTS

	Page
Statement	i
Certificate	ii
Acknowledgements	iii
Preface	ix
Chapter 1. Semisquaraine and Croconaine Dyes: An Overview	
1.1. Introduction	1
1.2. Synthesis of Semisquaraine Dyes	4
1.3. Photophysical Properties of Semisquaraine Dyes	11
1.4. Semisquaraine Dyes as Probes and Sensitizers	13
1.5. Synthesis and Applications of Croconaine Dyes	19
1.6. Objectives of the Present Investigations	21
1.7. References	22
Chapter 2. Synthesis and Reactivity of a Few Novel Semisquaraine Derivatives	
2.1. Abstract	35
2.2. Introduction	36
2.3. Results	39
2.3.1. Synthesis of Semisquaraine Dyes	39
2.3.2. Characterization of Semisquaraine Dyes	44
2.3.3. Reactivity of Semisquaraine Isomers	53

2.4.	Discussion	56
2.5.	Conclusions	59
2.6.	Experimental Section	60
2.7.	References	75
Chapter 3. Novel Semisquaraines and Study of their Interactions with Mono- and Divalent Metal Ions		
3.1.	Abstract	81
3.2.	Introduction	82
3.3.	Results	86
3.3.1.	Synthesis and Photophysical Properties	86
3.3.2.	Interactions of Semisquaraine Dyes with Metal Ions	88
3.3.3.	Stoichiometry and Reversibility of Complexation	93
3.3.4.	Nature of Complexation	96
3.3.5.	Selectivity of Recognition of Hg²⁺ Ions	100
3.3.6.	Detection of Hg²⁺ Ions in Aqueous Medium Containing Micelles	102
3.3.7.	Selectivity of Hg²⁺ Ions Recognition in Aqueous Medium	106
3.4.	Discussion	109
3.5.	Conclusions	113
3.6.	Experimental Section	114
3.7.	References and Notes	116

Chapter 4. Novel Croconaine Dyes and Study of their Metal Ion Binding and Light Harvesting Properties	
4.1. Abstract	123
4.2. Introduction	125
4.3. Results	127
4.3.1. Synthesis of Croconaine Dyes	127
4.3.2. Photophysical Properties of Croconaine Dyes	129
4.3.3. Study of Interactions with Mono- and Divalent Metal Ions	134
4.3.4. Characterization of Metal Ion Complexation	139
4.3.5. Light Harvesting Properties of Croconaine Dyes	141
4.3.6. Photocurrent Generation at Dye Modified TiO ₂ Electrode	147
4.4. Discussion	149
4.5. Conclusions	152
4.6. Experimental Section	154
4.7. References	159
List of Publications	169

PREFACE

Semisquaraine, squaraine and croconaine dyes have been the subject of many recent investigations owing to their excellent optical and electronic properties. The intramolecular charge-transfer (CT) character of the S_0 - S_1 electronic excitation combined with an extended conjugated π -electron network gives rise to the intense bands observed in the visible to near-infrared (NIR) region for these dyes. These peculiar spectral features along with remarkable stability and wide molecular structure diversity promoted their exploitation in a number of applications including photoconductivity, data storage, light emitting field-effect transistors, solar cells, non-linear optics, fluorescent probes, fluorescent NIR dyes, sensors, fluorescence patterning, photodynamic therapy (PDT) and in two-photon absorption (TPA) applications. Photochemistry of these systems has been extensively studied and many derivatives of the parent squaraine and croconaine moieties have been synthesized mostly for improvements in various applications. In this context, the present thesis entitled *“Synthesis and Study of Photophysical and Metal Ion Binding Properties of a Few Novel Semisquaraine and Croconaine*

Dyes” describes our efforts towards the design of a few novel semisquaraine and croconaine dyes and study of their metal ion binding and light harvesting properties under different conditions.

The thesis has been divided into four chapters, of which the first chapter describes a brief account on semisquaraine and croconaine dyes. Focus was placed on the various methods reported for these derivatives. Further, emphasis has been given to the various applications reported in the literature for the semisquaraine and croconaine dyes.

The second chapter of the thesis describes the synthesis and characterization of a few novel quinaldine based semisquaraine dyes **1a-k** and **2a-k** derived from dibutyl squarate and squaric acid, respectively. Reaction of the quinaldinium salts containing electron withdrawing groups with squaric acid gave the corresponding squaraine dyes in quantitative yields, whereas the semisquaraine dye intermediates were isolated in quantitative yields from the quinaldinium salts containing electron donating groups. Surprisingly, when the quinaldinium salts substituted with electron donating groups were reacted with dibutyl squarate, we isolated semisquaraine derivatives, which were found to be structurally

different from those obtained with squaric acid. Characterization of these dyes on the basis of spectroscopic and analytical evidence including the single crystal X-ray structure analysis indicated that the semisquaraine dyes obtained through squaric acid and dibutyl squarate were found to be Z- and E-isomers, respectively.

Theoretical calculations showed that the geometrical semisquaraine dye E-isomer showed a dihedral angle of 9.5° between the quinoline and squaryl rings, whereas a dihedral angle of 32° was observed for the Z-isomer. Both the semisquaraine derivatives showed intense absorption maxima in the region of 450-550 nm with negligible fluorescence quantum yields. Notably, the structural differences of the semisquaraine isomers were manifested in the different reactivity exhibited by these two dyes. The Z-isomer of the semisquaraine dye reacted readily with a second nucleophilic enamine to form the unsymmetrical squaraine dye, while the E-isomer required the hydrolysis of the butyl adduct before the dye reaction. The uniqueness of this study is that, although semisquaraine dyes have been understood to be the intermediates formed during the squaraine dye reaction, this is for

the first time the existence of semisquaraine isomers have been proposed and observed.

The squaryl ring of the semisquaraine dyes have electron rich oxygen atoms, which enable them to act as stable bidentate ligands for various metal ions. In this regard, a comparative study of the metal ion binding properties of the semisquaraine dye Z-isomers **1a-e** and E-isomers **2a-e** is presented in the third chapter of the thesis. Among the various mono and divalent metal ions, it was observed that these semisquaraine dyes showed significant interactions with mercuric ions. The addition of one equivalent of mercuric ions to semisquaraine Z-isomer in acetone, resulted in the formation of a new blue shifted band in the absorption spectrum, together with a concomitant increase in the fluorescence intensity of ca. 18-fold. This resulted in a color change of the solution from deep red to orange and visual 'turn on' fluorescence intensity in the presence of Hg^{2+} ions.

Similarly, the addition of mercuric ions to a solution of the E-isomer, caused a decrease in the absorption maximum of the dye at 475 nm with a concomitant ca. 42-fold enhancement in the fluorescence intensity. In the presence of Hg^{2+} ions, we observed

change in color from deep orange to colorless solution and visual 'turn on' emission intensity at 467 nm. The association constants for the binding of mercuric ions with the semisquaraine Z- and E-isomers for 1:1 stoichiometry have been estimated and are found to be $2.4 \pm 0.1 \times 10^5 \text{ M}^{-1}$ and $2.2 \pm 0.1 \times 10^4 \text{ M}^{-1}$, respectively. The Z-isomer- Hg^{2+} complex was found to be one order more stable than the E-isomer- Hg^{2+} complex, indicating the importance of the orientation of groups in the complexation. The binding site of the two semisquaraine dyes was characterized through various experimental techniques such as FT-IR, ^1H NMR and ^{13}C NMR spectral analysis, which showed that these dyes bind to Hg^{2+} ions through the electron rich carbonyl groups.

To understand whether the semisquaraine dyes can act as selective probes for mercuric ions under aqueous medium, the interaction of the semisquaraine dyes with various mono and divalent metal ions were studied under different micellar conditions. Of all the conditions examined, it has been observed that a solvent system consisting of a mixture (9:1) of water and acetone containing sodium dodecyl sulfate (SDS) has been found to be very effective with respect to the stability of the semisquaraine dye as

well as to the selectivity and sensitivity of the metal ion binding event. Our results indicated that the Z-isomer, which showed high binding affinity towards the mercuric ions in acetone, showed selective binding interactions under the aqueous medium as well with an association constant (K) of $4.0 \pm 0.1 \times 10^4 \text{ M}^{-1}$. In contrast, the E-isomer, which showed one order lower binding affinity, exhibited negligible interactions with Hg^{2+} ions under identical conditions. The selectivity of semisquaraines towards Hg^{2+} ions can be attributed to the soft acid nature as well as the size of the metal cation. Results of these investigations reveal that the semisquaraine dyes selectively interact with Hg^{2+} ions as compared to other biologically and environmentally relevant metal ions like Li^+ , Na^+ , K^+ , Ag^+ , Ca^{2+} , Mg^{2+} , Zn^{2+} , Pb^{2+} , Cd^{2+} , Cu^{2+} and Fe^{3+} ions, thereby indicating their potential use as efficient dual chromogenic and fluorogenic probes for Hg^{2+} ions.

The synthesis and study of metal ion binding and light harvesting properties of a few quinaldine-based croconaine dyes **1a-d** form the subject matter of chapter four of the thesis. These dyes were synthesized in quantitative yields by the condensation reaction between the quinaldinium salts and croconic acid and have

been characterized based on spectroscopic and analytical evidence. These dyes showed absorption maximum in the infrared region (IR, 840-870 nm) with high molar extinction coefficients ($\epsilon = 1-5 \times 10^5 \text{ M}^{-1} \text{ cm}^{-1}$). As observed in the case of the semisquaraine dyes, the croconaine dyes could also act as bidentate ligands for various metal ions. The addition of divalent metal ions resulted in decrease in the absorption maximum of the dye at around 870 nm with the formation of a new blue shifted band at 735-805 nm. These dyes exhibited negligible fluorescence emission, but upon binding with metal ions showed an enhancement in fluorescence intensity in the infrared region at around 810-820 nm. These dyes showed high affinity for divalent metal ions with high association constants in the order of 10^5-10^7 M^{-1} , while the monovalent metal ions showed negligible affinity. The stoichiometry of the complexes with divalent metal ions was found to be 2:1 and exhibited selectivity in the order $\text{Zn}^{2+} > \text{Pb}^{2+} \gg \text{Cd}^{2+} \gg \text{Mg}^{2+} \approx \text{Hg}^{2+} \approx \text{Ca}^{2+} \approx \text{Ba}^{2+}$.

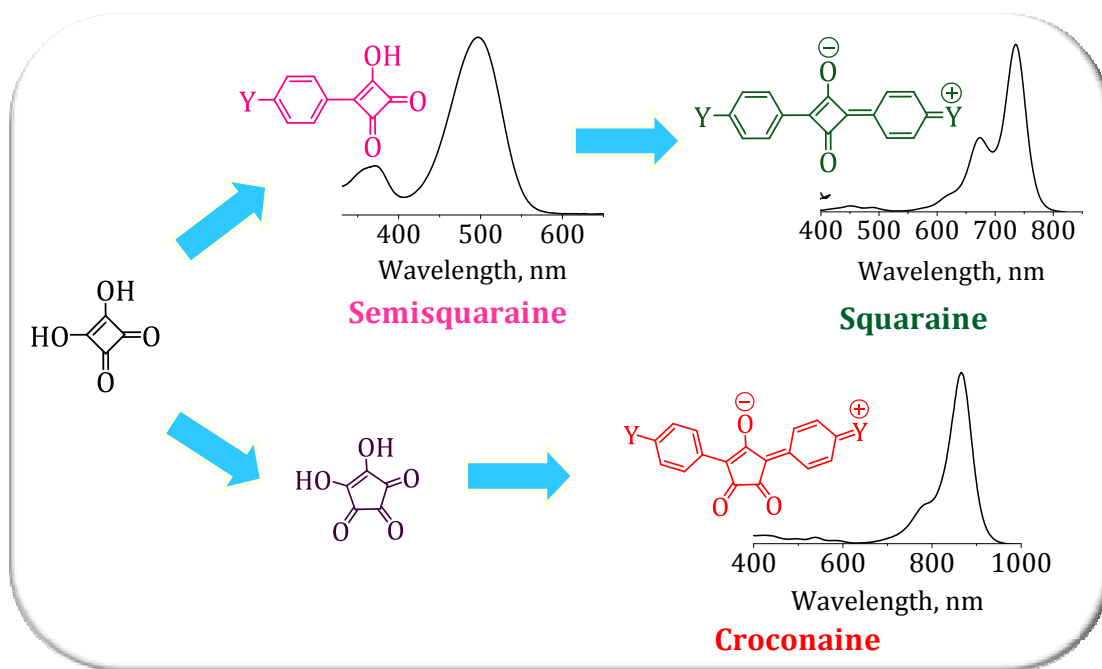
As the croconaine dyes have strong absorption in the infrared region, we have investigated their potential applications in light harvesting systems. These dye molecules found to undergo intermolecular interactions and form H-type aggregates. By making

use of this property, we have demonstrated the possibility of tuning the absorptive range of a photoelectrochemical cell using the croconaine dyes. The excited singlet of the monomeric dye quickly deactivated (4-7 ps) without undergoing intersystem crossing to generate triplet excited state. The triplet excited-state of the croconaine dye produced via triplet-triplet energy transfer method showed relatively a long lifetime of 7.2 μ s.

The dye molecules when deposited as thin film on optically transparent electrodes or on nanostructured TiO₂ film, they formed H-aggregates with a blue-shifted absorption maximum around 660 nm. The excitons formed upon excitation of the dye aggregates resulted in charge separation at the TiO₂ and SnO₂ interface. The H-aggregates in the thin film were photoactive and produced anodic current when employed in a photoelectrochemical cell. These studies reveal that the suitably substituted croconaine dyes with electron rich carbonyl groups at the croconyl moiety can have potential applications as molecular probes for divalent metal ions and as sensitizers in light harvesting devices.

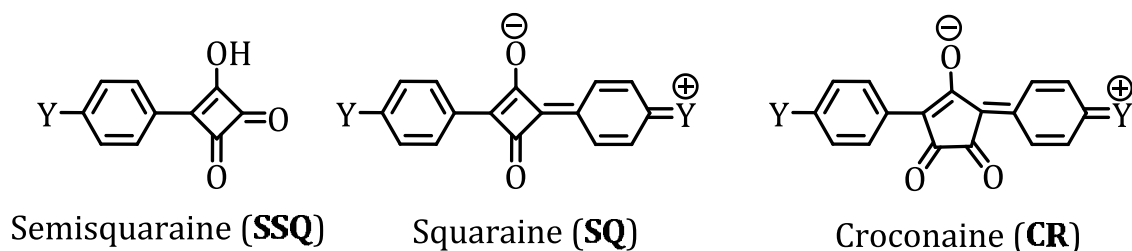
Note: *The numbers of various compounds given here correspond to those given under the respective Chapters.*

CHAPTER 1. SEMISQUARINE AND CROCONAINE DYES: AN OVERVIEW



1.1. INTRODUCTION

Squaraines and croconaines belong to a class of dyes having resonance stabilized zwitterionic structure, while semisquaraine dyes are the intermediate structure in the squaraine dye formation reaction (Chart 1.1).^{1,2} These dyes have attracted increasing attention in recent years due to their favourable spectroscopic properties such as narrow absorption bands with high molar absorption coefficients ($\epsilon > 10^5 \text{ M}^{-1}\text{cm}^{-1}$) and moderate fluorescence quantum yields in polar and aqueous media.³ Attracted by these features, the squaraine and croconaine dyes have been utilized as

**Chart 1.1**

deeply coloured and fluorescent materials for various applications such as optical recording,⁴ solar energy conversion,^{5,6} electrophotography,⁷ nonlinear optics,⁸ photodynamic therapy,⁹ multiphoton absorption,¹⁰ biochemical labelling¹¹ and chromo- and/or fluorogenic probes¹² for sensing of pH,¹³ cations,^{14,15} anions¹⁶ and neutral molecules^{17,18} as well as for the study of self-assembled dye aggregates.¹⁹

The ground (S_0) and the excited (S_1) electronic states of these systems are intramolecular charge transfer (CT) in nature.²⁰ The aromatic/heterocyclic moiety and the oxygen atoms are electron donors and the central four membered ring is an acceptor. The S_0 - S_1 electronic excitation involves a charge transfer character (CT) process that is primarily confined to the central C_4O_2 or C_5O_3 rings in squaraines and croconaines, respectively. In these cases, the intramolecular charge transfer takes place from the oxygen atoms of the squaryl ring and the aromatic/heterocyclic moiety to the central acceptor C_4O_2 or C_5O_3 unit. Thus the squaraine and croconaine dyes can be generally described as

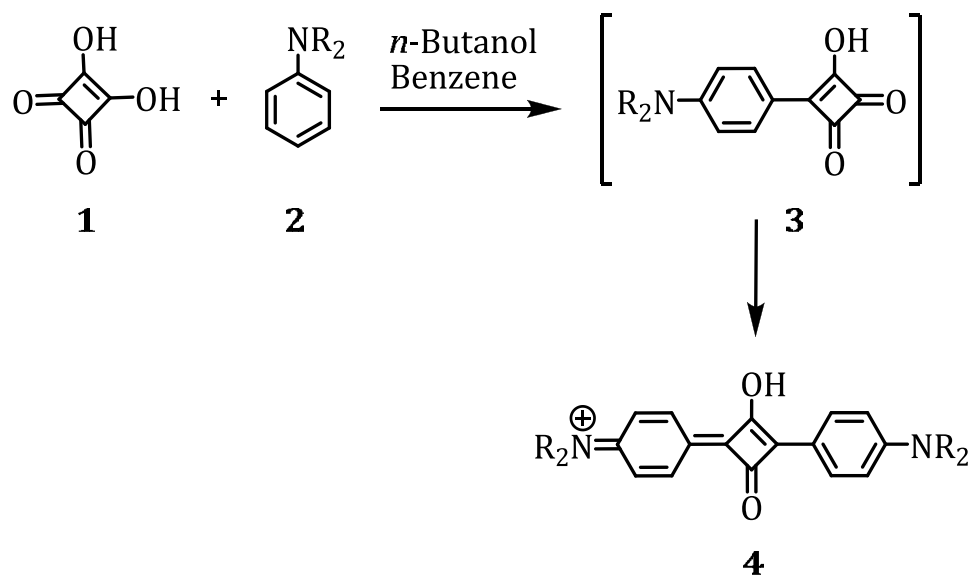
compounds containing two donor moieties (D) connected to a central C_4O_2 or C_5O_3 electron withdrawing group (A) forming a donor-acceptor-donor (D-A-D) system, whereas the semisquaraines may be considered to be a donor (D) in conjugation with an acceptor C_4O_2 (A) unit.²¹ The intramolecular charge transfer character of the S_0-S_1 transition combined with an extended π -electron network, gives rise to the observed sharp and intense bands in the visible to infrared region for these dyes.

Due to the favourable photophysical properties, the squaraine chemistry has been at the centre stage of research from both fundamental and technological viewpoints. In contrast, the potential of the semisquaraine dyes has been limited only to the synthesis of unsymmetrical squaraine dyes and their applicability has remained unexplored. Similarly, the croconaine dyes, which are the higher homologues of squaraine dyes, have received less attention due to the difficulties associated with their synthesis. Due to these reasons, the design and development of novel semisquaraine and croconaine dyes are of paramount importance for potential optoelectronic applications. This Chapter presents a brief overview on the various synthetic strategies adopted for the synthesis of semisquaraine derivatives and their applications. In addition, the importance of the croconaine dyes is discussed with particular emphasis on the applications of this class of dyes.

Further, the objectives of the present investigations are also briefly described in this Chapter.

1.2. SYNTHESIS OF SEMISQUARINE DYES

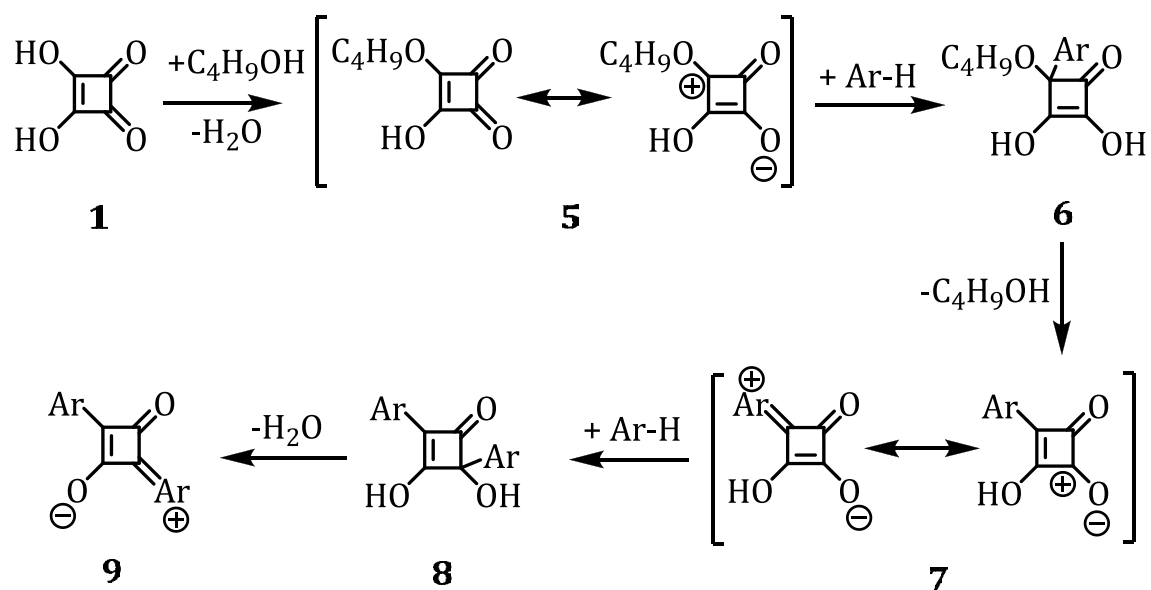
The reaction between squaric acid and an electron rich aromatic or heterocyclic species yields squaraine dyes through the intermediacy of the semisquaraine dyes. The typical squaraine synthesis is carried out by condensation of 1 equivalent of squaric acid (**1**) with 2 equivalents of aromatic or heterocyclic compounds. For example, the synthesis of aniline based dye **4** has been achieved by the reaction of two equivalents of the corresponding aniline derivative **2** with 1 equivalent of squaric acid in an azeotropic solvent mixture of butanol-benzene (Scheme 1.1).¹ The reaction



Scheme 1.1

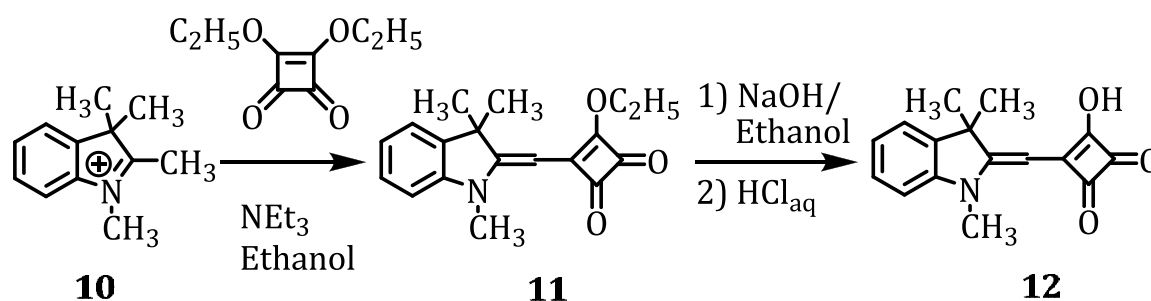
mechanism for the squaraine dye reaction proposed by Sprenger and Ziegenbein, shows that this reaction takes place through the formation of an intermediate system formed by the nucleophilic attack of the aromatic compound (Ar-H) at the carbonyl carbon in the half- ester of squaric acid (Scheme 1.2).²² This intermediate system is popularly known as the semisquaraine dye. The subsequent attack of another Ar-H followed by dehydration gives the squaraine dye. However, the separation of the semisquaraine, thus formed, from the squaraine dye was difficult and performed only by means of special procedures and under different conditions.²³

Later, alternate reaction strategies have been reported for the synthesis of semisquaraine derivatives in quantitative yields by employing

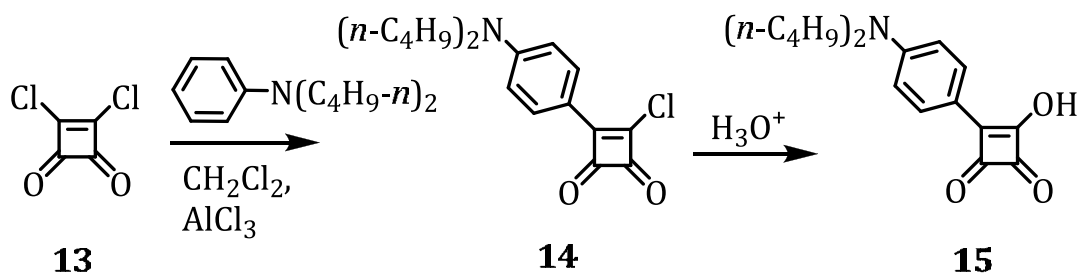


Scheme 1.2

derivatives of squaric acid.²⁴ Among them, the most widely employed method is the use of dialkyl squarates reported by Terpetschnig and Lakowicz.²⁵ In this strategy, the equimolar amounts of heterocyclic compounds such as 1,2,3,3-tetramethylindolium salt **10** is reacted with diethyl or dibutyl squarates, followed by hydrolysis to afford indolinyldenemethyl- substituted semisquaraine dye **12**. (Scheme 1.3).^{11a} This procedure was applicable to benzothiazolium and benzoselenazolium salts with an active methyl group at the 2-position.

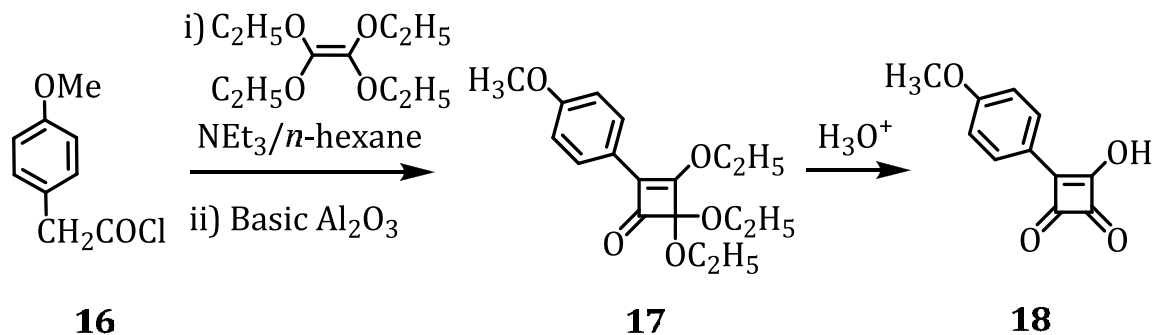
**Scheme 1.3**

Green and Neuse²⁶ reported a Friedel-Crafts type reaction of aromatic systems with 3,4-dichloro-3-cyclobutene-1,2-dione in the presence of AlCl_3 to obtain semisquaraine derivatives in quantitative yields (Scheme 1.4). Squaryl chloride or 3,4-dichloro-3-cyclobutene-1,2-dione (**13**) employed in the reaction was prepared from squaric acid through chlorination with thionyl chloride.²⁷ The monosubstituted squaryl chlorides obtained were converted to semisquaric acids **15** by hydrolysis under acidic conditions.



Scheme 1.4

Law and Bailey²⁸ have employed [2+2] cycloaddition reaction of tetraethoxyethane with arylacetylchloride **16** to obtain semisquaraine dye **18** (Scheme 1.5). The semisquaraine dyes prepared through the various reaction pathways are converted to the unsymmetrical squaraine dyes by condensation with a second different aromatic or heterocyclic derivative. The synthesis and isolation of the semisquaraine derivatives through the various reaction pathways indicated above enabled the easy synthesis of different unsymmetrical squaraine dyes with varying donor strengths. Such effective procedures provide immense possibilities to design a variety of

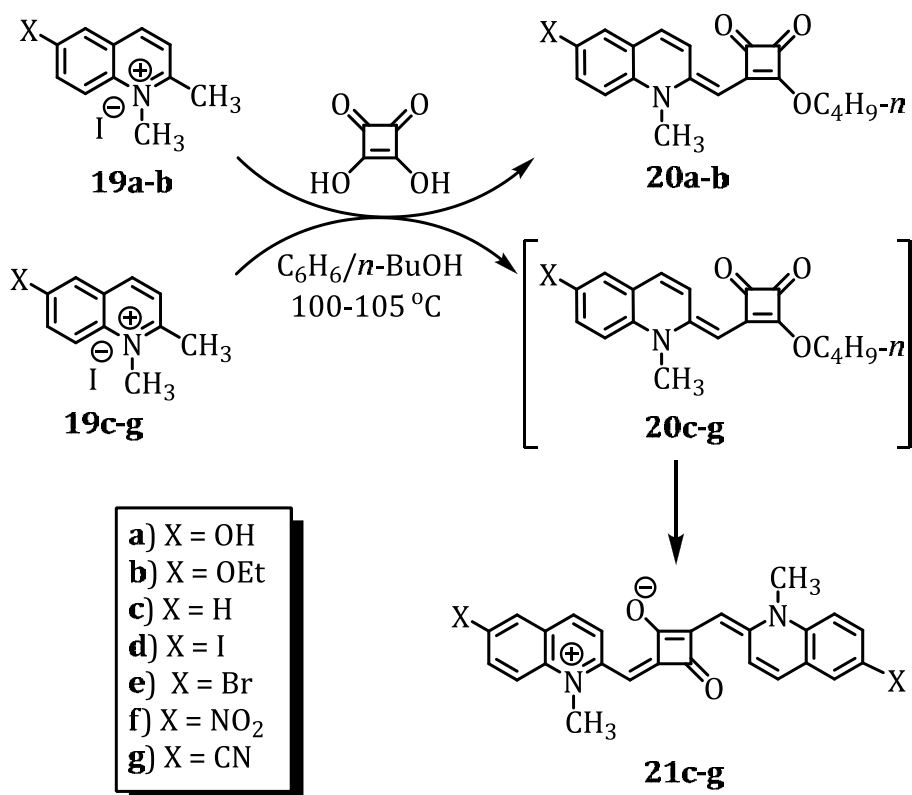


Scheme 1.5

squaraine dyes with tunable optical properties in the visible to the near-infrared (NIR) range.

Even though the reaction of aromatic or heterocyclic systems with squaric acid takes place through the intermediacy of semisquaraine, the isolation of the semisquaraine dye as the exclusive product was not observed in this reaction pathway. In this context, we observed that the isolation of the intermediate products in the squaraine dye reaction depends mostly on the nucleophilicity of the heterocyclic system used. For example, when we carried out the condensation reaction between the quinaldinium salt **19a** and squaric acid in 2:1 equivalents, (Scheme 1.6),²⁹ we did not get the expected squaraine dye; instead a different product having much shorter wavelength absorption was obtained quantitatively.

Since squaraine dyes, in general, are brightly coloured compounds with absorption in the near-infrared region, the progress of the reaction was monitored by absorption spectroscopy in addition to the thin layer chromatography. No absorption band in the near-infrared region was observed during the initial stages of the reaction. However, an absorption band around 485 nm was observed within 4 h of the reaction and this band increased in intensity with reaction time. The reaction mixture following work up and column chromatography after 30 h, gave the semisquaraine dye **20a** as the major product.



Scheme 1.6

Further investigation of the effect of various substituents revealed that substituents with electron donating groups such as the hydroxyl or the ethoxy (**19a,b**) gave only the corresponding semisquaraine dyes **20a-b** in quantitative yields. In contrast, the salts with electron withdrawing substituents (**19c-g**) like the halogen substituted, nitro or the cyano gave the corresponding squaraine dyes **21c-g**, through the intermediacy of the semisquaraine dyes **20c-g** under analogous conditions. The variation in the reactivity of the substituted quinaldinium salts **19a-g** in the dye reaction can be explained on the basis of the electronic effects of the different substituents.

Squaraine dye forming reaction involves the reaction between an electron rich aromatic derivative and squaric acid. The success of the reaction depends mainly on the nucleophilicity of the aryl species. In the present study, the nucleophile is an enamine formed from the quinaldinium salt, which reacts with squaric acid resulting in the formation of the semisquaraine dye. Subsequently, the semisquaraine undergoes further reaction with another moiety of the enamine to give the squaraine dye. The presence of electron-donating groups on the benzene ring of the quinaldinium salts **19a-b** reduces the acidity of the hydrogen atoms of the 2-methyl group, thereby, decreasing the formation of the enamine nucleophile. Nevertheless, the enamine formed reacts with squaric acid resulting in the corresponding semisquaraine dyes **20a-b**. Furthermore, the electrophilic terminus of these semisquaraines is rendered less reactive by the electron-donating substituents and hence further reaction with the less acidic salts becomes extremely difficult. As a result, the reaction stops with the formation of the semisquaraine only in the case of the salts **19a-b**.

In contrast, in the presence of neutral (**19c**), electronegative (**19d,e**) and electron-withdrawing substituents (**19f,g**), the hydrogen atoms of the 2-methyl group of the quinaldine moiety are relatively more acidic and thereby favours the formation of the enamine nucleophile very efficiently. These salts yield higher concentrations of the nucleophile and hence results in the formation of the corresponding squaraine dyes **21c-g** in quantitative

yields through the intermediacy of the semisquaraine intermediates **20c-g**. Thus, by proper tuning of the nucleophilicity of the quinaldinium salt employed in the squaraine dye reaction, one can obtain semisquaraine or squaraine dye in quantitative yields.

1.3. PHOTOPHYSICAL PROPERTIES OF SEMISQUARINE DYES

Semisquaraine dyes have an absorption in the region 350-500 nm region depending on the aromatic donor group present. For example, the semisquaraine based on *N,N*-dialkylated aniline derivatives have absorption maxima in the region 400-450 nm and emission maxima at 450-500 nm,³⁰ whereas semisquaraine dyes based on heterocycles such as benzothiazoles or indoles have absorption in the range 450-500 nm.³¹ Recently, Hecht and co-workers³² reported semisquaraine dye **22** having *ortho*-dialkylamino substituents (Chart 1.2). This semisquaraine dye exhibited absorption maxima at 355 nm in nonpolar (methylene chloride) and polar nonprotic solvents (acetonitrile), while polar protic solvents (methanol) induced a dramatic hypsochromic shift to 269 nm. Furthermore, they observed that strong emission occurs only in methanol ($\lambda_{\text{ex}} = 269$ nm, $\lambda_{\text{em}} = 354$ nm). These results suggest the presence of an intramolecular N-H-O hydrogen bonding in nonprotic media, while in protic solvents such a bonding is inhibited, resulting in the formation of a

decoupled system with strongly altered electronic and photophysical properties.

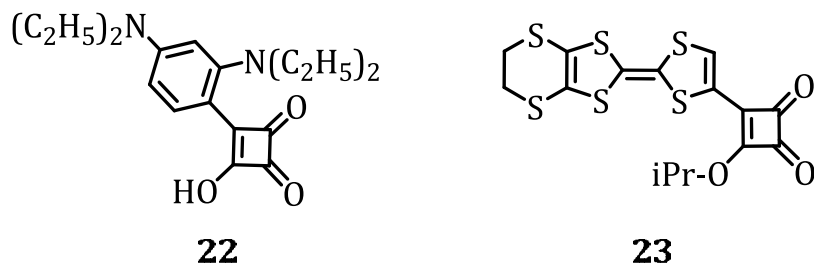


Chart 1.2

Tetrathiafulvalene-based semisquaraine **23** reported by Miyazaki *et al.*^{31c} shows solvatochromic behaviour in different solvents with an absorption maximum at 490, 514, 529 nm in acetone, toluene and chloroform, respectively (Chart 1.2). Theoretical calculations showed that intramolecular charge transfer from the tetrathiafulvalene (TTF) unit to the squaraine ring is negligibly small without UV-light irradiation. Despite the closed-shell electron configuration, this molecule showed conductive behaviour in the range $10^6 \Omega$ even in the neutral state. The MO calculations showed that the HOMOs of these molecules are mainly delocalized in the TTF skeleton, whereas the LUMOs are mainly populated on the four membered squaric acid ring. Therefore, the electronic charge redistribution from the TTF to the squaryl ring corresponds to a HOMO–LUMO excitation and gives a small electron deficiency in the TTF columns to produce the electrical conductivity.

1.4. SEMISQUARAIN DYES AS PROBES AND SENSITIZERS

The semisquaraine dyes have been synthesized with a view to prepare unsymmetrical squaraine dyes.³³ Although a number of semisquaraine dyes have been synthesized by various research groups, the applications of this versatile class of compounds remained unexplored. In the following section a brief account of the applications of the semisquaraine dyes reported in the literature are presented.

Squaric acid can act as a ligand due to the presence of the carbonyl group which, not only provides proton acceptor sites for hydrogen bonding with other molecules, but also presents a potential binding site for divalent metal ions. Due to this unique structure, systematic and exhaustive research work has been carried out to exploit their potential use as exceptionally versatile scaffolds for molecular recognition. Although large number of metal complexes of squarate dianions have been reported,³⁴ where it acts as a potential bridging ligand with possible μ -2 to μ -4 between the metals, only a few reports have appeared in the literature,³⁵ where the semisquaraine dyes have been utilized as probes for metal ions.

Recently, Kim *et al.*³⁵ have reported benzothiazolium based semisquaraine dye **24** as a selective sensor for mercuric ions in 9:1 DMSO-water mixture (Chart 1.3). Titration studies showed that the dye **24** forms a 1:1 complex with the metal ions. The addition of Hg²⁺ ions resulted in

decrease in the absorption as well as emission spectra of the semisquaraine dye as compared to other metal ions such as Ca^{2+} , Pb^{2+} , Al^{3+} , Ce^{3+} , Ba^{2+} , Ni^{2+} , Cd^{2+} , Zn^{2+} and Mg^{2+} ions. Theoretical studies carried out on the system revealed that HOMO-LUMO excitation moved the electron distribution from the thiazole moiety to the cyclobutene moiety, which reflect a strong migration of the intramolecular charge-transfer character of the dye **24**. It is proposed that the sulfur atom of the benzothiazole moiety is important for an effective complexation with Hg^{2+} ions in this system. The complexation of the Hg^{2+} ions to the sulfur atom reduces the electron density on the sulfur atom and lowers the electron donating ability of the thiazole moiety. Later on, the same group reported another probe **25**, which forms a 2:1 complex with mercuric ions, resulting in the decrease in its absorption and emission intensity.³⁶

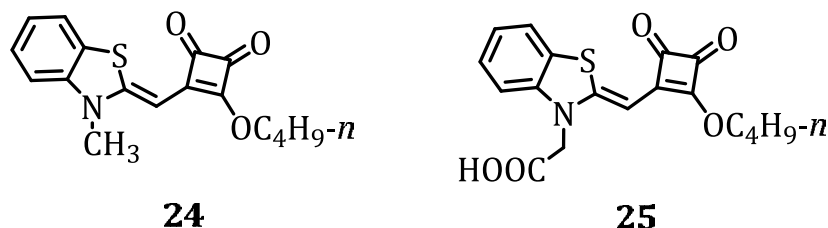


Chart 1.3

Since the discovery of the highly efficient dye-sensitized solar cell (DSSC) by Grätzel *et al.*,³⁷ much attention has been paid to the development of organic dye sensitizers. A schematic presentation of the operating principles of the DSSC is given in Figure 1.1. In the TiO_2 based DSSC cell

design, the mesoscopic semiconductor oxide film, coated on an ITO electrode, is placed in contact with a redox electrolyte or an organic hole conductor. A monolayer of the sensitizer (**S**) is coated on the surface of the nanocrystalline TiO_2 film. Upon photoexcitation, electrons are injected into the conduction band of TiO_2 and these travels across the nanocrystalline film to the conducting glass support serving as a current collector. The sensitizer dye is regenerated by electron donation from the electrolyte, usually an organic solvent containing a redox system, such as the I_3^-/I^- couple. The regeneration of the sensitizer by the iodide intercepts the recapture of the conduction band electron by the oxidized dye. The iodide is regenerated, in turn, by the reduction of triiodide at the counter electrode, with the circuit being completed via electron migration through

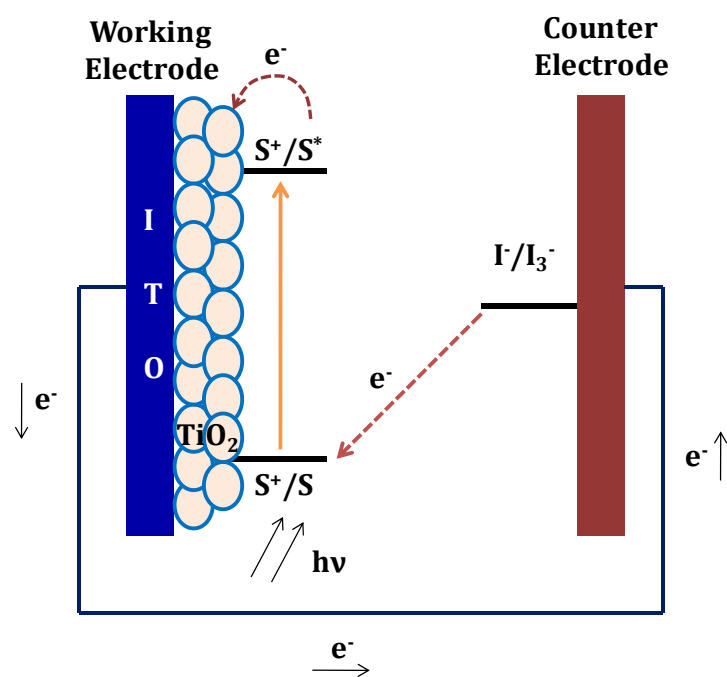
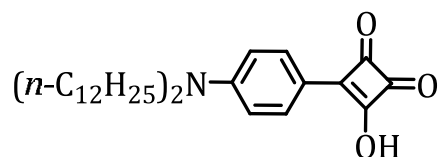


Figure 1.1. Principle of operation of a dye-sensitized solar cell (DSSC).

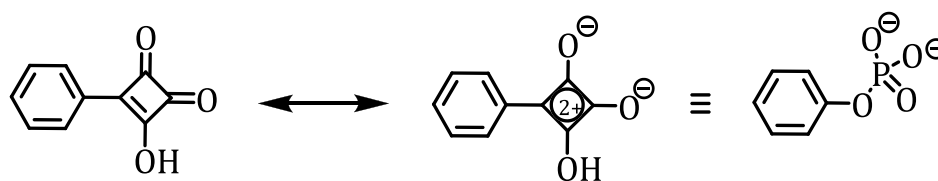
the external load. Among the various sensitizers investigated, polypyridyl complexes of ruthenium, such as N3 dye, *cis*-bis(isothiocyanato)bis(2,2'-bipyridyl-4,4'-dicarboxylate) ruthenium(II) and the more recently reported 'black dye', tris(isothiocyanato)-2,2,2'-terpyridyl-4,4,4'-tricarboxylate ruthenium(II) have been reported to have solar energy to electricity conversion of up to 10.4%.

Recently, various coumarin,³⁸ merocyanine,³⁹ squaraine⁴⁰ and styryl⁴¹ dyes have been proposed as sensitizers for solar cells. Semisquaraine dyes have been also reported to act as sensitizers, for a TiO₂ based solar cell.⁴² In this regard, Matsui and co-workers³⁰ have studied the photochemistry and solar cell applications of a series of semisquaraine derivatives. Cyclic voltammetric studies of these compounds showed that the E_{red} of the semisquaraines was sufficiently negative to inject electrons into the conduction band of TiO₂. In addition, the E_{ox} was positive enough to accept electrons from the electrolyte (I₃⁻/I⁻). Among the various semisquaraine dyes, the semisquaraine dye **26** with the longest alkyl chain showed the highest efficiency (Chart 1.4). These semisquaraine dyes were found to undergo aggregation on the TiO₂ surface due to strong intermolecular interactions involving polar carbonyl moieties. Furthermore, it was hypothesized that, π-π interactions between the aryl moieties as well as hydrophobic interactions between the long alkyl chains assist the self-assembly of **26** on the TiO₂ surface and thereby, increase the conversion

efficiency. The incident photon to charge carrier generation efficiency (IPCE) of **26** was found to be 48% with a photocurrent and photovoltage of 2.88 mA cm⁻² and 0.59 V, respectively.

**26****Chart 1.4**

Semisquaric acids can be considered as good electrostatic mimics for the phosphate group⁴³ and can be used to design effective inhibitors of protein tyrosine phosphatases (PTPases) (Chart 1.5). In this regard, Seto *et al.*⁴⁴ have studied a series of semisquaraine derivatives which provide a good electrostatic mimic of protein tyrosinase (pTyr) and bear a reduced negative charge at neutral pH, when compared to many of the other dianionic pTyr analogues. It is proposed that the squaric acid binds in the active site of the PTPase in a conformation that mimics the binding of aryl

**27****28****29****Chart 1.5**

phosphate ester substrates.⁴⁵ The anion of the squaric acid could form an electrostatic interaction with Arg-409 of the protein. This residue along with Cys-403 and Asp-356 make up the key catalytic residues of the enzyme.⁴⁶ The aromatic portion of the inhibitor undergoes hydrophobic contacts with Phe-229 of the protein. The larger aromatic ring of inhibitor, as in the case of **30**, strengthens these hydrophobic contacts and lead to the enhanced inhibition of the enzyme activity (Chart 1.6). In addition, favourable electrostatic interactions between Phe-229 and the electron-poor aromatic rings of compounds **31a-b** result in the enhanced activity of these inhibitors when compared to their electron rich counterparts **31c-e**.

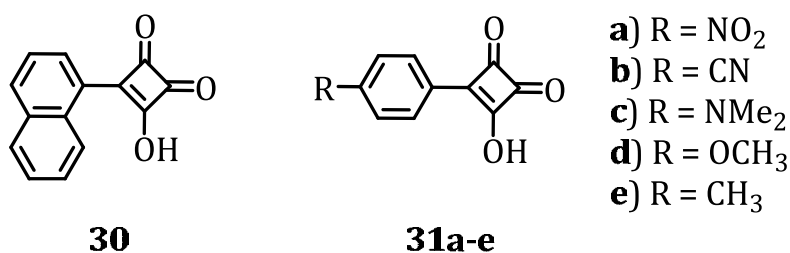
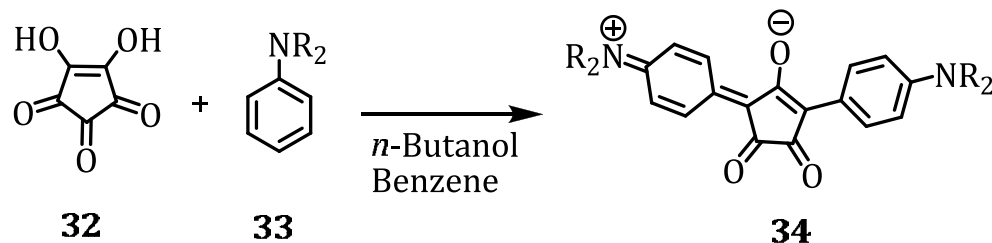


Chart 1.6

1.5. SYNTHESIS AND APPLICATIONS OF CROCONAINE DYES

Croconaine dyes are the higher homologues of the well-studied squaraine dyes having a highly efficient electron accepting croconyl moiety as the central core. These dyes are prepared by the reaction between highly reactive aromatic and heterocyclic compounds with croconic acid **32**

(Scheme 1.7).⁴⁷ Although, the croconaine dyes are known since the last decade, they have been investigated to a much lesser degree than the analogous squaraine dyes.⁴⁸ The replacement of the central four membered ring in the squaraine dyes by a croconyl ring with strong acceptor ability



Scheme 1.7

shifts the absorption maxima of the croconaines dyes to longer wavelengths compared to the homologues squaraines. Theoretical calculations and experiments have shown that the croconaine dyes have absorption maxima that are approximately 100 nm red-shifted than the corresponding squaraine dyes.⁴⁹ Bhanuprakash and Jayathirtha Rao *et al.*⁵⁰ have carried out the structural analysis of these dyes and have explored the role of oxyallyl substructures in tuning the absorption and hyperpolarizability of the croconaine dyes.

The longer wavelength absorption in the croconaines as compared to the squaraines is clearly due to the larger diradical nature in the former. The croconaine dyes are known to have narrow and intense absorption bands that peak in the 800 nm spectral region. These features make the

croconaine dyes attractive for many of applications especially as infrared (IR) probes and non-linear optical (NLO) materials.⁵¹ However, as compared to the corresponding squaraine dyes, their applications are yet to be explored.

Recently, Wang *et al*⁵² have synthesized croconaine dye **35** as a colourimetric chemodosimeter for biological thiols and cyanide ion (Chart 1.7). The dye has an absorption maximum at 823 nm, which decreases in intensity with the addition of 10 equivalents of cysteine at pH 5.7 when compared to other amino acids. However, at pH 6.8, other amino acids like glutathione, cysteine-glycine, homocysteine also showed similar changes in its absorption. In the absence of the amino acid nucleophiles, **35** can also

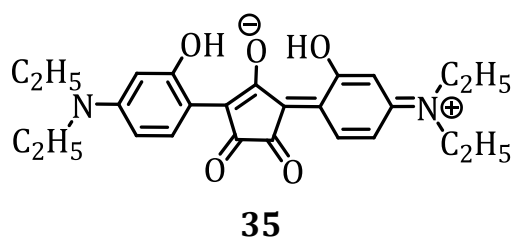


Chart 1.7

act as a chemosensor for the cyanide ion. In the presence of 2 equivalents of cyanide ions, the dye **35** showed a decrease in its absorption maximum at 823 nm with the formation of a new band in the 550-725 nm region in CH₂Cl₂:CH₃CN (98:2). Similar changes were observed in aqueous ethanol solutions at pH 9.0 with detection limit of (0.13 ppm) in water.

1.6. OBJECTIVES OF THE PRESENT INVESTIGATIONS

Development of functional molecules with favourable photophysical properties and exhibiting selective interactions towards different metal ions has great significance in optoelectronic, environmental and medicinal applications. In this context, the synthesis of semisquaraines that are intermediates in the preparation of squaraine dyes has immense significance in the development of novel dyes for various applications. In addition, the synthesis of croconaine dyes with absorption in the infrared region extends the applicability to the infrared region. Our main objective of the present investigations has been to design a few novel semisquaraine and croconaine dyes that can selectively bind and recognize various metal ions. Our strategy was to design novel quinaldine based semisquaraine and croconaine dyes substituted with different functional groups. It was proposed that these systems would act as bidentate ligands for various metal ions, by virtue of the presence of electron rich carbonyl groups. Another objective of the thesis has been to understand the structural differences of the different semisquaraine dyes. Since the donor-acceptor-donor character of the croconaine dyes makes them suitable candidates as sensitizers in solar cell applications, it was also of our interest to investigate the light harvesting properties of these dyes.

We synthesized a series of novel semisquaraine and croconaine dyes and have investigated their interactions with various metal ions through photophysical, electrochemical and NMR techniques. Our results indicate that the semisquaraine derivatives, synthesized through different reaction pathways are isomeric to each other and exhibit selective interactions with mercuric ions in both organic as well as aqueous medium and can have potential use as probes. In addition, our investigations on the photophysical properties of the croconaine dyes reveal that these dyes can act as potential sensitizers for solar cell applications as well as probes for bivalent metal ions.

1.7. REFERENCES

1. Treibs, A.; Jacob, K. *Angew. Chem.* **1965**, *77*, 680; *Angew. Chem., Int. Ed. Engl.* **1965**, *4*, 694.
2. (a) Yagi, S.; Nakazumi H. in *Functional Dyes* (Ed.: S.-H. Kim), Elsevier, Amsterdam, **2006**, pp. 215 – 255. (b) Kuzyk, M. G. *J. Mater. Chem.* **2009**, *19*, 7444.
3. (a) Das, S.; Thomas, K. G.; George, M. V. in *Organic Photochemistry* (Eds.: V. Ramamurthy, K. S. Schanze), CRC, Boca Raton, FL (USA), pp. 467–517. (b) Law, K.-Y. in *Organic Photochemistry* (Eds.: V. Ramamurthy, K. S. Schanze), CRC, Boca Raton, FL (USA), pp. 519 –

584. (c) Law, K. Y. *J. Chem. Phys.* **1987**, *91*, 5184. (d) Das, S.; Thomas, K. G.; Ramanathan, R.; George, M. V.; Kamat, P. V. *J. Chem. Phys.* **1993**, *97*, 13625. (e) Beverina, L.; Salice, P. *Eur. J. Org. Chem.* **2010**, 1207.
4. (a) Jipson, V. B.; Jones C. R. *J. Vac. Sci. Technol.* **1981**, *18*, 105. (b) Emmelius, M.; Pawlowski, G.; Vollmann, H. W. *Angew. Chem.* **1989**, *101*, 1475; *Angew. Chem. Int. Ed. Engl.* **1989**, *28*, 1445. (c) Tian, M.; Furuki, M.; Iwasa, I.; Sato, Y.; Pu, L. S.; Tatsuura, S. *J. Phys. Chem. B* **2002**, *106*, 4370.
5. (a) Zhao, W.; Hou, Y. J.; Wang, X. S.; Zhang, B. W.; Cao, Y.; Yang, R.; Wang, W. B.; Xiao, X. R. *Sol. Energy Mater. Sol. Cells* **1999**, *58*, 173. (b) Alex, S.; Santhosh, U.; Das, S. *J. Photochem. Photobiol. A* **2005**, *172*, 63. (c) Burke, A.; Schmidt-Mende, L.; Ito, S.; Gratzel, M. *Chem. Commun.* **2007**, 234. (d) Yum, J. H.; Walter, P.; Huber, S.; Rentsch, D.; Geiger, T.; Nlesch, F.; De Angelis, F.; Gratzel, M.; Nazeeruddin, M. K. *J. Am. Chem. Soc.* **2007**, *129*, 10320. (e) Wu, J.; Huo, E.; Wu, Z.; Lu, Z.; Xie, M.; Jiang, Q. *e-Polym.* **2007**, no. 077. (f) Silvestri, F.; Irwin, M. D.; Beverina, L.; Facchetti, A.; Pagani, G. A.; Marks, T. J. *J. Am. Chem. Soc.* **2008**, *130*, 17640. (g) Geiger, T.; Kuster, S.; Yum, J.-H.; Moon, S.-J.; Nazeeruddin, M. K.; Gratzel, M.; Nuesch, F. *Adv. Funct. Mater.* **2009**, *19*, 1.

6. (a) Merritt, V. Y.; Hovel, H. J. *Appl. Phys. Lett.* **1976**, *29*, 414. (b) Piechowski, A. P.; Bird, G. R.; Morel, D. L.; Stogryn, E. L. *J. Phys. Chem.* **1984**, *88*, 934. (c) Kamat, P. V.; Das, S.; Thomas, K. G.; George M. V. *J. Phys. Chem.* **1992**, *96*, 195. (d) Burke, A.; Schmidt-Mende, L.; Ito, S.; Gratzel, M. *Chem. Commun.* **2007**, 234. (e) Silvestri, F.; Lopez-Duarte, I.; Seitz, W.; Beverina, L.; Martinez-Diaz, M. V.; Marks, T. J.; Guldi, D. M.; Pagani, G. A.; Torres, T. *Chem. Commun.* **2009**, 4500. (f) Mor, G. K.; Kim, S.; Paulose, M.; Varghese, O. K.; Shankar, K.; Basham, J.; Grimes, C. A. *Nano Lett.* **2009**, *9*, 4250.
7. (a) Tam, A. C. *Appl. Phys. Lett.* **1980**, *37*, 978. (b) Law, K. Y. *J. Imaging Sci.* **1987**, *31*, 83. (c) Hwang, S. H.; Kim, N. K.; Koh, K. N.; Kim, S. H. *Dyes Pigm.* **1998**, *39*, 359.
8. (a) Chen, C. T.; Marder, S. R.; Cheng, L. T. *J. Am. Chem. Soc.* **1994**, *116*, 3117. (b) Chen, C. T.; Marder, S. R.; Cheng, L. T. *J. Chem. Soc. Chem. Commun.* **1994**, 259. (c) Ashwell, G. J.; Jefferies, G.; Hamilton, D. G.; Lynch, D. E.; Roberts, M. P. S.; Bahra, G. S.; Brown, C. R. *Nature* **1995**, *375*, 385. (d) Ajayaghosh, A. *Chem. Soc. Rev.* **2003**, *32*, 181. (e) Ashwell, G. J.; Ewington, J.; Moczko, K. *J. Mater. Chem.* **2005**, *15*, 1154. (f) Beverina, L.; Crippa, M.; Salice, P.; Ruffo, R.; Ferrante, C.; Fortunati, I.; Signorini, R.; Mari, C. M.; Bozio, R.; Facchetti, A. Pagani, G. A. *Chem. Mater.* **2008**, *20*, 3242.

9. (a) Ramaiah, D.; Joy, A.; Chandrasekhar, N.; Eldho, N. V.; Das, S.; George, M. V. *Photochem. Photobiol.* **1997**, *65*, 783. (b) Bonnett, R. *Chemical Aspects of Photodynamic Therapy*, Gordon and Breach, Amsterdam, **2000**, Chapter. 11. (c) Santos, R. F.; Reis, L. V.; Almeida, P.; Oliveira, A. S.; Vieira Ferreira, L. F. *J. Photochem. Photobiol. A* **2003**, *160*, 159. (d) Beverina, L.; Abbotto, A.; Landenna, M.; Cerminara, M.; Tubino, R.; Meinardi, F.; Bradamante, S.; Pagani, G. A. *Org. Lett.* **2005**, *7*, 4257. (e) Beverina, L.; Crippa, M.; Landenna, M.; Ruffo, R.; Salice, P.; Silvestri, F.; Versari, S.; Villa, A.; Ciaffoni, L.; Collini, E.; Ferrante, C.; Bradamante, S.; Mari, C. M.; Bozio, R.; Pagani, C. A. *J. Am. Chem. Soc.* **2008**, *130*, 1894. (f) Devi, D. G.; Cibir, T. R.; Ramaiah, D.; Abraham, A. *J. Photochem. Photobiol. B: Biol.* **2008**, *153*. (g) Quatarolo, A. D.; Sicilia, E.; Russo, N. *J. Chem. Theory Comput.* **2009**, *5*, 1849. (h) Rapozzi, V.; Beverina, L.; Salice, P.; Pagani, G. A.; Camerin, M.; Xodo, L. E. *J. Med. Chem.* **2010**, *53*, 2188.
10. (a) Meyers, F.; Chen, C.-T.; Marder, S. R.; Bredas, J.-L. *Chem. Eur. J.* **1997**, *3*, 530. (b) Chung, S.-J.; Zheng, S.; Odani, T.; Beverina, L.; Fu, J.; Padilha, L. A.; Biesso, A.; Hales, J. M.; Zhan, X.; Schmidt, K.; Ye, A.; Zojer, E.; Barlow, S.; Hagan, D. J.; Stryland, E. W. V.; Yi, Y.; Shuai, Z.; Pagani, G. A.; Bredas, J.-L.; Perry, J. W.; Marder, S. R. *J. Am. Chem. Soc.* **2006**, *128*, 14444. (c) Ohira, S.; Rudra, I.; Schmidt, K.; Barlow, S.;

- Chung, S.-J.; Zhang, Q.; Matichak, J.; Marder, S. R.; Bredas, J.-L. *Chem. Eur. J.* **2008**, *14*, 11082. (d) Beverina, L.; Crippa, M.; Salice, P.; Ruffo, R.; Ferrante, C.; Fortunati, I.; Signorini, R.; Mari, C. M.; Bozio, R.; Facchetti, A.; Pagani, G. A. *Chem. Mater.* **2008**, *20*, 3242. (e) Odom, S. A.; Webster, S.; Padilha, L. A.; Peceli, D.; Hu, H.; Nootz, G.; Chung, S.-J.; Ohira, S.; Matichak, J. D.; Przhonska, O. V.; Kachkovski, Barlow, S.; Bredas, J.-L.; Anderson, H. L.; Hagan, D. J.; Stryland, E. W. V.; Marder, S. R. *J. Am. Chem. Soc.* **2009**, *131*, 7510.
11. (a) Terpetschnig, E.; Szmecinski, H.; Lakowicz, J. R. *Anal. Chim. Acta* **1993**, *282*, 633. (b) Oswald, B.; Patsenker, L.; Duschl, J.; Szmecinski, H.; Wolfbeis, O. S.; Terpetschnig, E. *Bioconjugate Chem.* **1999**, *10*, 925. (c) Sun, C.; Yang, J.; Li, L.; Wu, X.; Liu, Y.; Liu, S. *J. Chromatogr. B* **2004**, *803*, 173. (d) Jisha, V. S.; Arun, K. T.; Hariharan, M.; Ramaiah, D. *J. Am. Chem. Soc.* **2006**, *128*, 6024. (e) Smith and co-workers have published a series of studies on the performance of squaraine-rotaxane dyes as biochemical labels; see for example, Gassensmith, J. J.; Arunkumar, E.; Barr, L.; Baumes, J. M.; DiVittorio, K. M.; Johnson, J. R.; Noll, B. C.; Smith, B. D. *J. Am. Chem. Soc.* **2007**, *129*, 15054. (f) Reddington, M. V. *Bioconjugate Chem.* **2007**, *18*, 2178. (g) Wang, B.; Fan, J.; Sun, S.; Wang, L.; Song, B.; Peng, X. *Dyes Pigments* **2010**, *85*, 43. (h) Lee, J.-J.; White, A. G.; Baumes, J. M.; Smith, B. D.

- Chem. Commun.* **2010**, 46, 1068.
12. (a) Arun, K. T.; Ramaiah, D.; *J. Phys. Chem. A* **2005**, 109, 5571. (b) Basheer, M. C.; Santhosh, S.; Alex, S.; Thomas, K. G.; Suresh, C. H.; Das, S. *Tetrahedron*, **2007**, 1617. (c) Renard, B.-L.; Aubert, Y.; Asseline, U. *Tetrahedron Lett.* **2009**, 50, 1897. (d) Matveeva, E. G. Terpetschnig, E. A.; Stevens, M.; Patsenker, L.; Kolosova, O. S.; Gryczynski, Z.; Gryczynski, I. *Dyes Pigments* **2009**, 80, 41. (e) Hilderbrand, S. A.; Weissleder *Curr. Opin. Chem. Biol.* **2010**, 14, 71. (f) Escobedo, J. O.; Rusin, O.; Lim, S.; Strongin, R. M. *Curr. Opin. Chem. Biol.* **2010**, 14, 64.
13. (a) Isgor, Y. G.; Akkaya, E. U. *Tetrahedron Lett.* **1997**, 38, 7417. (b) Snee, P. T.; Somers, R. C.; Nair, G.; Zimmer, J. P.; Bawendi, M. G.; Nocera, D. G. *J. Am. Chem. Soc.* **2006**, 128, 13320.
14. (a) Akkaya, E. U.; Turkyilmaz, S. *Tetrahedron Lett.* **1997**, 38, 4513. (b) Chenthamarakshan, C. R.; Ajayaghosh, A. *Tetrahedron Lett.* **1998**, 39, 1795. (c) Oguz, U.; Akkaya, E. U. *Tetrahedron Lett.* **1998**, 39, 5857. (d) Arunkumar, E.; Chithra, P.; Ajayaghosh, A. *J. Am. Chem. Soc.* **2004**, 126, 6590. (e) Balbo Block, M. A.; Hecht, S. *Macromolecules* **2004**, 37, 4761. (f) Wallace, K. J.; Gray, M.; Zhong, Z.; Lynch, V. M.; Anslyn, E. V. *Dalton Trans.* **2005**, 2436. (g) Arunkumar, E.; Ajayaghosh, A.; Daub, J. *J. Am. Chem. Soc.* **2005**, 127,

- 3156.
15. (a) Ros-Lis, J. V.; Martinez-Manez, R.; Rurack, K.; Sancenon, F.; Soto, J.; Spieles, M. *Inorg. Chem.* **2004**, *43*, 5183. (b) Ros-Lis, J. V.; Marcos, M. D.; Martinez-Manez, R.; Rurack, K.; Soto, J. *Angew. Chem.* **2005**, *117*, 4479; *Angew. Chem. Int. Ed.* **2005**, *44*, 4405. (c) Ros-Lis, J. V.; Casau, R.; Comes, M.; Coll, C.; Marcos, M. D.; Martinez-Manez, R.; Sancenon, F.; Soto, J.; Amoros, P.; Haskouri, J. E.; Garro, N.; Rurack, K. *Chem. Eur. J.* **2008**, *14*, 8267. (d) Climent, E.; Casaus, R.; Marcos, M. D.; Martinez-Manez, R.; Sancenon, F.; Soto, J. *Dalton Trans.* **2009**, 4806.
16. (a) Ros-Lis, J. V.; Martinez-Manez, R.; Soto, J. *Chem. Commun.* **2002**, 2248. (b) Jimenez, D.; Martinez-Manez, R.; Sancenon, F.; Ros-Lis, J. V.; Benito, A.; Soto, J. *J. Am. Chem. Soc.* **2003**, *125*, 9000. (c) Gassensmith, J. J.; Matthys, S.; Lee, J.-J.; Wojcik, A.; Kamat, P. V.; Smith, B. D. *Chem. Eur. J.* **2010**, *16*, 2916.
17. (a) Kukrer, B.; Akkaya, E. U. *Tetrahedron Lett.* **1999**, *40*, 9125. (b) Suzuki, Y.; Yokoyama, K. *Angew. Chem.* **2007**, *119*, 4175; *Angew. Chem. Int. Ed.* **2007**, *46*, 4097. (c) Thomas, J.; Sherman, D. B.; Amiss, T. J.; Andaluz, S. A.; Pitner, J. B. *Bioconjugate Chem.* **2007**, *18*, 1841. (d) Hewage, H. S.; Anslyn, E. V. *J. Am. Chem. Soc.* **2009**, *131*, 13099.
18. (a) Ros-Lis, J. V.; Garcia, B.; Jimenez, D.; Martinez-Manez, R.;

- Sancenon, F.; Soto, J.; Gonzalvo, F.; Valdecabres, M. C. *J. Am. Chem. Soc.* **2004**, *126*, 4064. (b) Ros-Lis, J. V.; Martinez-Manez, R.; Soto, J. *Org. Lett.* **2005**, *7*, 2337. (c) Sreejith, S.; Divya, K. P.; Ajayaghosh, A. *Angew. Chem. Int. Ed.* **2008**, *120*, 8001. (d) Climent, E.; Calero, P.; Marcos, M. D.; Martinez-Manez, R.; Sancenon, F.; Soto, J. *Chem. Eur. J.* **2009**, *15*, 1816.
19. (a) Stoll, R. S.; Severin, N.; Rabe, J. P.; Hecht, S. *Adv. Mater.* **2006**, *18*, 1271. (b) Ajayaghosh, A.; Chithra, P.; Varghese, R. *Angew. Chem.* **2007**, *119*, 234; *Angew. Chem. Int. Ed.* **2007**, *46*, 230. (c) Hsueh, S.-Y.; Lai, C.-C.; Liu, Y.-H.; Peng, S.-M.; Chiu, S.-H. *Angew. Chem.* **2007**, *119*, 2059; *Angew. Chem. Int. Ed.* **2007**, *46*, 2013. (d) Jyothish, K.; Hariharan, M.; Ramaiah, D. *Chem. Eur. J.* **2007**, *13*, 5944. (e) Ajayaghosh, A.; Chithra, P.; Varghese, R.; Divya, K. P. *Chem. Commun.* **2008**, 969.
20. (a) Farnum, D. G.; Neuman, M. A.; Suggs, W. T. *J. Cryst. Mol. Struct.* **1974**, *4*, 199. (b) Bigelow, R. W.; Freund, H.-J. *Chem. Phys.* **1986**, *107*, 159. (c) Kobayashi, Y.; Goto, M.; Kurahashi, M., *Bull. Chem. Soc. Jpn.* **1986**, *59*, 311. (d) Bernstein, J.; Goldstein, E., *Mol. Cryst. Liq. Cryst.* **1988**, *164*, 213. (e) Dirk, C. W.; Herndon, W. C.; Cervantees-Lee, P.; Selnau, H.; Martinez, S.; Kalamehgam, P. A.; Campos, G.; Velez, M. Z.; Ledoux, I.; Cheng, L. T. *J. Am. Chem. Soc.* **1995**, *117*,

- 2214.
21. (a) Sreejith, S.; Carol, P.; Chithra, P.; Ajayaghosh, A. *J. Mater. Chem.* **2008**, *18*, 264. (b) Law, K. Y. *Chem. Rev.* **1993**, *93*, 449. (c) Kamat, P. V.; Das, S.; Thomas, K. G.; George, M. V. *J. Chem. Phys.* **1992**, *96*, 195. (d) Bigelow, R. W.; Freund, H. J. *Chem. Phys.* **1986**, *107*, 159.
22. Ziegenbein, W.; Sprenger, H.-E. *Angew. Chem., Int. Ed. Engl.* **5**, **1966**, 893.
23. Treibs, A.; Jacob, K. *Liebigs Ann. Chem.* **1968**, 712, 123.
24. Yagi, S.; Hyodo, Y.; Matsumoto, S.; Takahashi, N.; Kono, H.; Nakazumi, H. *J. Chem. Soc. Perkin Trans. 1* **2000**, 599.
25. Terpetschnig, E. & Lakowicz, J.R., *Dyes Pigments* **1993**, *21*, 227.
26. Green, B.R.; Neuse, E.W. *Synthesis* **1974**, 46.
27. de Selms, R.C.; Fox, C.J.; Riordan, R.C. *Tetrahedron Lett.* **1970**, *10*, 781.
28. (a) Law, K.-Y.; Bailey, F.C. *J. Chem. Soc. Chem. Commun.* **1990**, 863. (b) Law, K.-Y.; Bailey, F.C. *J. Org. Chem.*, **1992**, *57*, 3278.
29. (a) Jyothish, K.; Arun, K. T.; Ramaiah, D. *Org. Lett.* **2004**, *6*, 3965. (b) Jyothish, K.; Avirah, R, R.; Ramaiah, D. *Org. Lett.* **2007**, *8*, 111. (c) Jyothish, K.; Avirah, R, R.; Ramaiah, D. *Arkivoc* **2007**, *8*, 296.
30. Matsui, M.; Nagasaka, K.-I; Tokunaga, S.-Y.; Funabiki, K.; Yoshida, T.; Minoura, H. *Dyes Pigments* **2003**, *58*, 219.

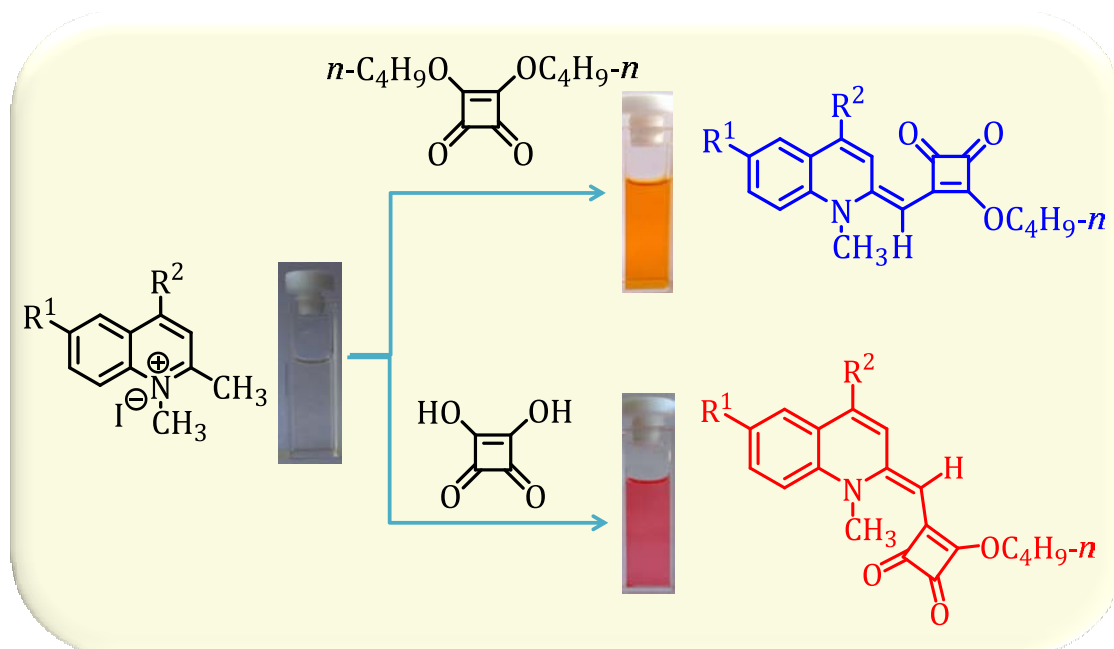
31. (a) Keil, D. Hartmann, H. *Dyes Pigments* **2001**, *49*, 161. (b) Tatarets, A. L.; Fedyunyaeva, I. A.; Terpetschnig, E.; Patsenker, L. D. *Dyes Pigments* **2005**, *64*, 125. (c) Miyazaki, A.; Enoki, T. *New J. Chem.* **2009**, *33*, 1249.
32. Block, M. A. B., Khan, A.; Hecht, S. *J. Org. Chem.* **2005**, *69*, 184.
33. Beverina, L. Ruffo, R.; Patriacra, g.; Angelis, F. D.; Roberto, D.; Righetto, S.; Ugo, R.; Pagani, G. A. *J. Mater. Chem.*, **2009**, *19*, 8190.
34. (a) Gerstein, B. C.; Habenschuss, M. *J. Appl. Phys.* **1972**, *43*, 5155. (b) Weiss, A.; Riegler, E.; Alt, I.; Bohme, H.; Robl. Ch. *Z. Naturforsch.* **1986**, *41B*, 18. (c) Weiss, A.; Riegler, E.; Robl. Ch. *Z. Naturforsch.* **1986**, *41B*, 1333. (d) Frankenbach, G. M.; Beno, M. A.; Kini, A. M.; Williams, J. M.; Welp, U.; Thompson, J. E.; Whangbo, M.-H. *Inorg. Chim. Acta* **1992**, *192*, 195. (e) Lee, C.-R.; Wang, C.-C.; Chen, K.-C.; Lee, G.-H.; Wang, Y. *J. Phys. Chem. A* **1999**, *103*, 156.
35. Bae, J.-S.; Son, Y.-A.; Kim, S.-H. *Fibers Polym.* **2009**, *10*, 403.
36. Bae, J.-S.; Gwon, S.-Y.; Son, Y.-A.; Kim, S.-H. *Dyes Pigments* **2009**, *83*, 324.
37. (a) O'Regan, B.; Gratzel, M. *Nature* **1991**, *353*, 737. (b) Grätzel, M. *Nature* **2001**, *338*, 414. (c) Nazeeruddin, M. K. Pechy, P.; Renouard, T.; Zakeeruddin, S. M.; Humphry-Baker, R.; Comte, P.; Liska, P.; Cevey, L.; Costa, E.; Shklover, V.; Spiccia, L.; Deacon, G. B.; Bignozzi,

- C. A.; Gratzel, M. *J. Am. Chem. Soc.* **2001**, *123*, 1613. (d) Gratzel, M. *Inorg. Chem.* **2005**, *44*, 6841. (d)
38. Hara, K.; Sayama, K.; Ohga Y, Shinpo, A.; Suga, S.; Arakawa, H. *Chem Commun.* **2001**, 569.
39. Sayama, K.; Hara, K.; Mori, N.; Satsuki, M.; Suga, S.; Sugihara, S.; Arakawa, H. *Chem Commun.* **2000**, 1173.
40. (a) Fuji Film. Gel electrolytes, gel electrolytes for photoelectrochemical cells, and the cells. JP 2000-058140. (b) Kamat, P. V.; Das, S.; Thomas, K. G.; George, M. V. *Chem. Phys. Lett.* **1991**, *178*, 75. (c) Takechi, K.; Sudeep, S.; Kamat, P. V. *J. Phys. Chem. B* **2006**, *110*, 16169. (d) Sudeep, P. K.; Takechi, K.; Kamat, P. V. *J. Phys. Chem. C* **2007**, *111*, 488.
41. Wang, Z. S.; Li, F. U.; Huang, C. H. *J. Phys. Chem. B* **2001**, *105*, 9210.
42. Fuji Film. Photoelectric converters and photoelectrochemical cells. JP 2000-251958.
43. (a) Smutney, E. J.; Caserio, M. C.; Roberts, J. D. *J. Am. Chem. Soc.* **1960**, *82*, 1793. (b) Patton, E.; West, R. *J. Am. Chem. Soc.* **1973**, *95*, 8703.
44. Xie, J.; Comeau, A. B.; Seto, C. T. *Org. Lett.* **2004**, *6*, 83.
45. Salmeen, A.; Andersen, J. N.; Myers, M. P.; Tonks, N. K.; Barford, D. *Mol. Cell* **2000**, *6*, 1401.

46. Stuckey, J. A.; Schubert, H. L.; Fauman, E. B.; Zhang, Z.-Y.; Dixon, J. E.; Saper, M. A. *Nature* **1994**, *370*, 571.
47. (a) Yasui, S.; Matsuoka, M.; Kitao, T. *Dyes Pigments* **1988**, *10*, 13. (b) Simard, T. P.; Yu, J. H.; Zebrowski-Young, J. M.; Haley, N. F.; Detty, M. R. *J. Org. Chem.* **2000**, *65*, 2236. (c) Encinas, C.; Otazo, E.; Rivera, L.; Miltsov, S.; Alonso, J. *Tett. Letters*, **2002**, *43*, 8391. (d) Panda, J.; Virkler, P. R.; Detty M. R. *J. Org. Chem.* **2003**, *68*, 1804. (e) Puyol, M.; Encinas, C.; Rivera, L.; Miltsov, S.; Alonso, J. *Dyes Pigments* **2007**, *73*, 383. (f) Song, X.; Foley, J. W. *Dyes Pigments* **78**, **2008**, 60.
48. Keil, D.; Hartmann, H.; Reichardt, Ch. *Liebigs Ann. Chem.* **1993**, 935.
49. Kim, S. H.; Hwang, S. H.; Song, H. C.; Yoon, Nam Sik *J. Korean Chem. Soc.* **1996**, *40*, 741.
50. (a) Prabhakar, Ch.; Yesudas, K.; Chaitanya, K. G.; Sitha, S.; Bhanuprakash, K.; Rao, V. J. *J. Phys. Chem. A* **2005**, *109*, 8604. (b) Prabhakar, Ch.; Chaitanya, K. G.; Sitha, S.; Bhanuprakash, K.; Jayathritha Rao, V. *J. Phys. Chem. A* **2005**, *109*, 2614. (c) Yesudas, K.; Chaitanya, K. G.; Prabhakar, Ch.; Bhanuprakash, K.; Rao, V. J. *J. Phys. Chem. A* **2006**, *110*, 11717. (d) Srinivas, K.; Prabhakar, C.; Devi, C. L.; Yesudas, K.; Bhanuprakash, K.; Rao, V. J. *J. Phys. Chem. A* **2007**, *111*, 3378. (e) Yesudas, K.; Bhanuprakash, K. *J. Phys. Chem. A* **2007**, *111*, 1943. (f) Prabhakar, Ch.; Yesudas, K.; Bhanuprakash, K.; Rao, V. J.;

- Kumar, R. S. S.; Rao, N. D. *J. Phys. Chem. C* **2008**, *112*, 13272. (g)
- Thomas, A.; Srinivas, K.; Prabhakar, Ch.; Bhanuprakash, K.; Rao, V. J. *Chem. Phys. Lett.* **2008**, *454*, 36.
51. Li, Z.; Jin, Z.-H.; Kasatani, K.; Okamoto, H. *Physica B* **2006**, *382*, 229.
52. Zhang, X.; Li, C.; Cheng, X.; Wang, X.; Zhang, B. *Sensors Actuators* **2008**, *129*, 152.

CHAPTER 2. SYNTHESIS AND REACTIVITY OF A FEW NOVEL SEMISQUARINE DERIVATIVES



2.1. ABSTRACT

Squaraine dye reaction is a well-studied one, where the dye formation takes place by the condensation of electron rich aromatic systems and squaric acid through the formation of the intermediate semisquaraine dyes. However, the isolation of the semisquaraine is decided by the nucleophilicity of the aromatic system. In this regard, it was observed that the reaction of quinaldinium salts substituted with electron withdrawing groups with squaric acid yielded the squaraine dyes due to

the higher electrophilicity of the semisquaraine intermediate formed during the dye reaction. In contrast, the reaction of the quinaldinium salts with electron donating groups and squaric acid yielded the butyl adducts of the semisquaraine dyes only. Interestingly, the reaction between the quinaldinium salts having either electron withdrawing or electron donating substituents and dibutyl squarate yielded the semisquaraine dye intermediates; which were found to be isomeric (E-isomer) to the semisquaraine dyes (Z-isomer) isolated from squaric acid. An interesting aspect of these isomers is that, not only do they differ in their reactivity pattern but also in their photophysical as well as metal ion binding properties. Notably, the Z-isomer formed from squaric acid readily reacts further to furnish the unsymmetrical squaraine dyes, while its isomer undergoes further dye reaction only after hydrolysis of the butyl adduct. Our results demonstrate that the occurrence of E- and Z-isomers have immense implications in the synthesis of novel symmetrical and unsymmetrical squaraine dyes, which opens up new avenues for the design of novel materials for various optoelectronic applications.

2.2. INTRODUCTION

Squaraine and semisquaraine dyes have been the subject of many recent investigations owing to their excellent optical and electronic properties.¹⁻¹³ The intramolecular charge-transfer (CT) character of the

S_0 - S_1 electronic excitation combined with an extended conjugated π -electron network gives rise to the intense bands observed in the near-infrared (NIR) region for the squaraine dyes.¹⁴ These dyes are generally prepared by the condensation of electron rich aromatic or heterocyclic compounds such as N,N-dialkylanilines, benzothiazoles, phenols, azulenes and pyrroles with 3,4-dihydroxy-3-cyclobutene-1,2-dione (squaric acid) to give the 1,3-disubstituted squaraine dyes.¹⁵ However, the reaction of these nucleophiles with squaric acid under these conditions yields only the symmetrical squaraine dyes. To synthesize unsymmetrical squaraine dyes, the most useful and widely employed method involves the preparation of the semisquaraine derivatives.¹⁶ These can be prepared by the reaction of activated squaric acid derivatives, such as dibutyl squarate or squaryl chloride, with electron rich compounds. The reaction of dibutyl squarate or squaryl chloride yields the butyl or chloride adducts of the semisquaraine dyes, which when hydrolyzed can react with a different electron rich component to give the unsymmetrical squaraine dyes.¹⁷

Recently, we have proposed that squaraine dyes could be used as potential sensitizers in photodynamic therapy (PDT).^{11a-c} During the course of our efforts to prepare quinaldine based systems, we observed that the quinaldinium salts with electron withdrawing groups exclusively form the squaraine dyes as the main product.¹⁸ Surprisingly, the quinaldinium salts with electron donating groups gave the intermediate semisquaraine dyes

as the sole product. Further investigation on the effect of substituents revealed that the product formed upon dye reaction with the squaric acid is decided by the nucleophilicity of the salt taking part in the reaction. This was the first report, which highlighted the role of the electronic factors in governing the squaraine dye reactions. Further, we could also tune the synthesis of the unsymmetrical squaraine dyes by modulating the nucleophilicity of the quinaldinium salt employed in the dye reaction. Interestingly, the reaction of the quinaldinium salts with dibutyl squarate gives exclusively semisquaraines as the reaction products, irrespective of the nucleophilicity of the quaternary salt employed in the reaction. In this context, it is important to understand the structural differences between the two semisquaraine dyes isolated from the quinaldinium salts through the different reaction routes. Our results indicate that the two semisquaraine derivatives formed are geometric isomers (Chart 2.1).

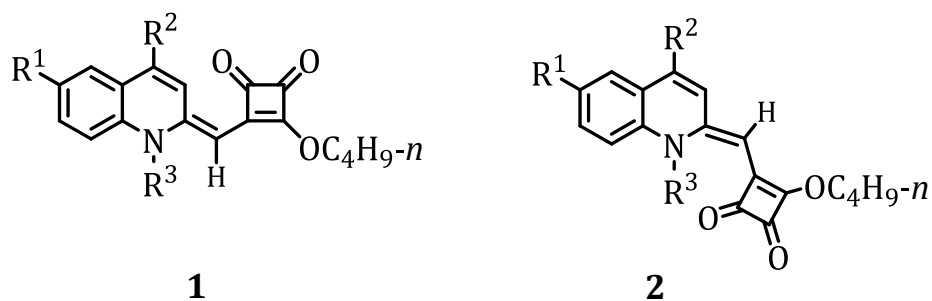


Chart 2.1

Interestingly, these two semisquaraine isomers are found to differ in their photophysical properties as well as in their reactivity pattern.

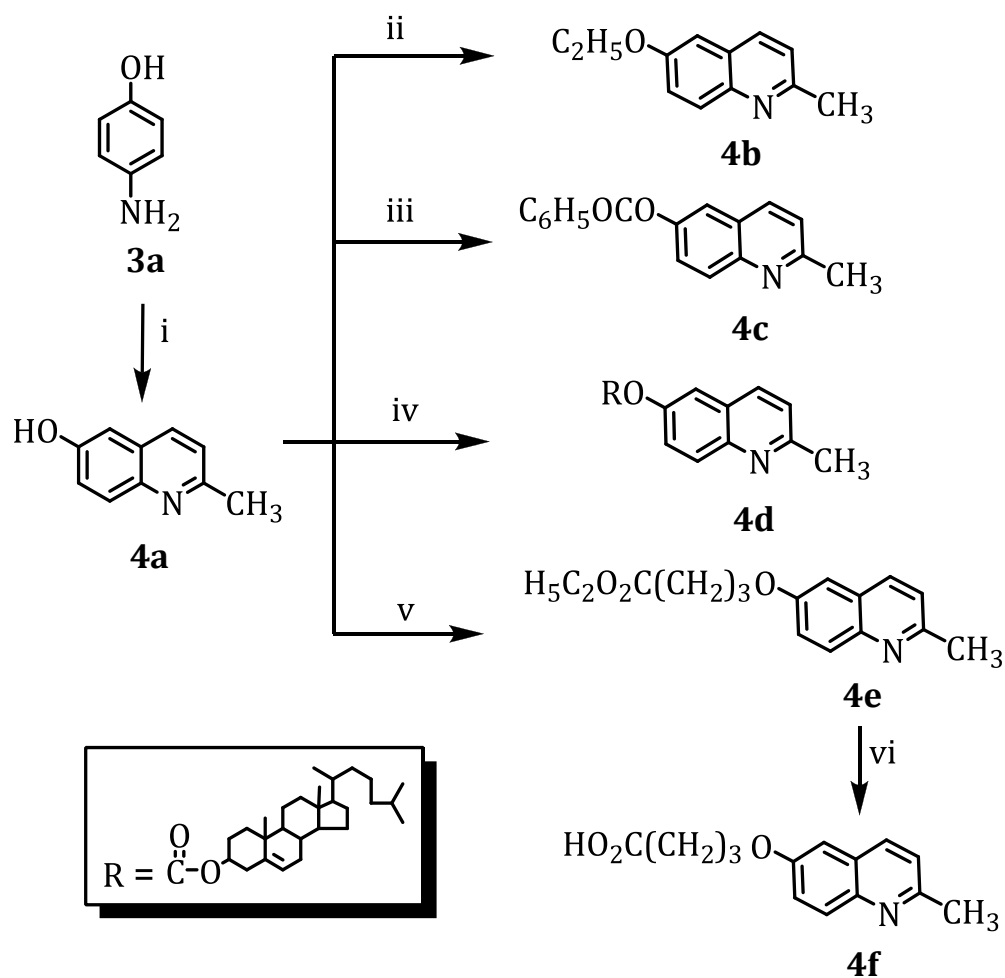
2.3. RESULTS

2.3.1. Synthesis of Semisquaraine Dyes

The synthesis of various quinaldine derivatives was achieved starting from 6-hydroxyaniline (**3a**) as shown in the Scheme 2.1. The reaction of **3a** with crotonaldehyde in 6N HCl for 12 h gave the 6-hydroxyquinoline (**4a**) in 40% yield, which was subsequently converted to various 6-substituted quinaldine derivatives. The ethoxy substituted quinaldine derivative **4b** was prepared by the reaction **4a** with ethyl bromide in sodium hydride and THF at 80 °C for 8 h, whereas the benzoyl derivative (**4c**) was prepared in 85% yield using benzoyl chloride. The reaction of **4a** with cholesteryl chloroformate in dichloromethane in presence of pyridine at 60 °C yielded the cholesterol linked quinaldine **4d** in 80% yields. Further, when **4a** was reacted with 4-bromobutyrate in DMF and Cs₂CO₃ at 25 °C, **4e** was obtained in quantitative yields, which was subsequently hydrolyzed using NaOH in methanol to give the corresponding acid derivative **4f** in 75% yields.

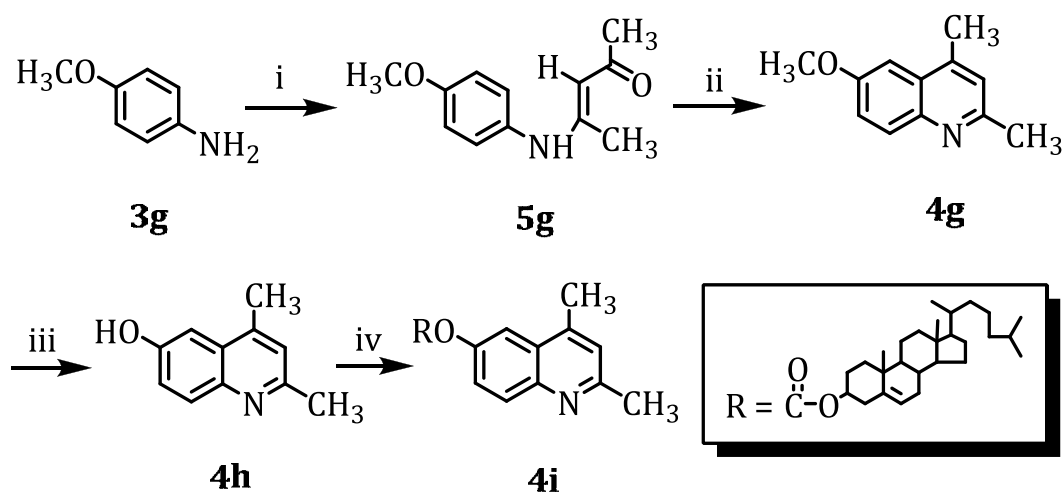
The synthesis of the 2,4-dimethylquinoline derivatives (**4g-i**) is shown in Scheme 2.2. As shown in the scheme, the reaction of the 6-substituted aniline derivative **3g** with pentane-2,4-dione in the presence of

anhydrous calcium sulphate under reflux gave 80% of the corresponding 6-substituted enamine derivative **5g**. Subsequently, the reaction of enamine with H_2SO_4 at $80\text{ }^\circ\text{C}$ yielded the corresponding 6-methoxy-2,4-dimethylquinolines (**4g**) in quantitative yields. The product **4g** obtained was further hydrolyzed with BBr_3 in dichloromethane at $0\text{ }^\circ\text{C}$ to give the



- i) Crotonaldehyde, 6N HCl, $100\text{ }^\circ\text{C}$; ii) $\text{C}_2\text{H}_5\text{Br}$, NaH, THF, $80\text{ }^\circ\text{C}$, 8 h; iii) benzoyl chloride, CH_2Cl_2 , pyridine, $0\text{ }^\circ\text{C}$, 4 h; iv) cholesteryl chloroformate, CH_2Cl_2 , pyridine, $60\text{ }^\circ\text{C}$, 12 h; v) $\text{Br}(\text{CH}_2)_3\text{COOC}_2\text{H}_5$, DMF, Cs_2CO_3 , $25\text{ }^\circ\text{C}$, 8 h; vi) CH_3OH , NaOH, $25\text{ }^\circ\text{C}$, 8 h.

Scheme 2.1

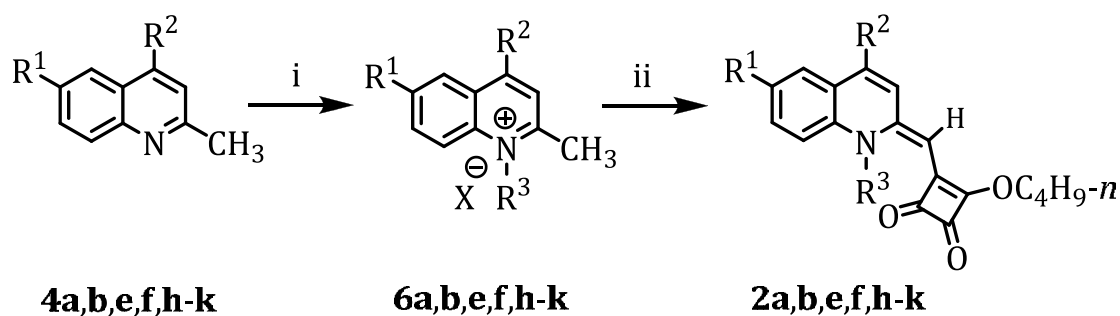


i) Pentane-2,4-dione, anhydrous calcium sulphate, reflux, 1 h; ii) H_2SO_4 , reflux, 3 h; iii) BBr_3 , CH_2Cl_2 , 0 °C; iv) cholesteryl chloroformate, triethylamine, 80 °C, 12 h.

Scheme 2.2

hydroxy derivative **4h**. This was subsequently reacted with cholesteryl chloroformate at 80 °C to give the quinoline derivative **4i**. The synthesis of the quinaldine based semisquaraine dyes was carried out as shown in the Scheme 2.3. The reaction of the substituted quinoline derivatives **4a,b**, **4e,f** and **4h-k** with methyl iodide or bromoethanol gave the corresponding *N*-quaternized quinolinium derivatives **6a,b,e,f,h-k** in 85-95% yields. Subsequent condensation reaction of the quinolinium salts with squaric acid at 100-105 °C in a 1:1 mixture of benzene and *n*-butanol using quinoline as catalyst yielded the corresponding substituted semisquaraine dyes **2a,b,e,f,h-k** in quantitative yields.

The reaction between the quinaldinium salts and squaric acid affords the semisquaraine derivatives only in the case of the electron donating group substituted quinaldinium salts, while the electron withdrawing salts yielded the squaraine dyes.^{18a-c} In order to overcome this limitation, an alternate reaction pathway was adopted to prepare the semisquaraine



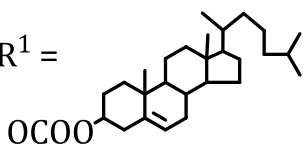
a) $R^1 = \text{OH}$, $R^2 = \text{H}$, $R^3 = \text{CH}_3$

b) $R^1 = \text{OC}_2\text{H}_5$, $R^2 = \text{H}$, $R^3 = \text{CH}_3$

e) $R^1 = \text{OC}_3\text{H}_6\text{COOC}_2\text{H}_5$, $R^2 = \text{H}$, $R^3 = \text{CH}_3$

f) $R^1 = \text{OC}_3\text{H}_5\text{COOH}$, $R^2 = \text{H}$, $R^3 = \text{CH}_3$

h) $R^1 = \text{OH}$, $R^2 = \text{CH}_3$, $R^3 = \text{CH}_3$

i) $R^1 =$  , $R^2 = \text{CH}_3$, $R^3 = \text{CH}_3$

j) $R^1 = \text{H}$, $R^2 = \text{H}$, $R^3 = \text{CH}_2\text{CH}_2\text{OH}$

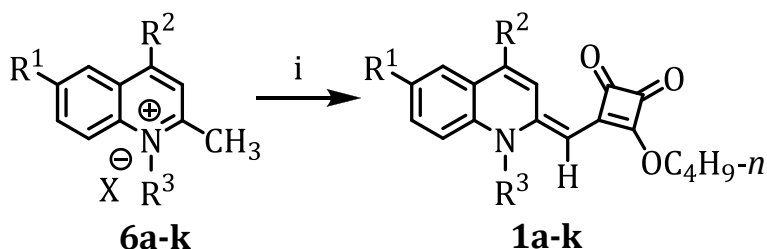
k) $R^1 = \text{Br}$, $R^2 = \text{H}$, $R^3 = \text{CH}_2\text{CH}_2\text{OH}$

$X = \text{Br}, \text{I}$

i) $\text{CH}_3\text{I}/\text{BrCH}_2\text{CH}_2\text{OH}$, 100 °C, 12 h; ii) squaric acid, *n*-BuOH/ C_6H_6 (1:1), quinoline, 100-105 °C, 12 h.

Scheme 2.3

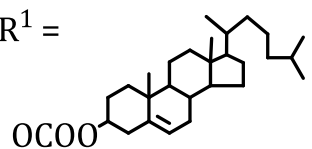
derivatives with electron withdrawing substituents by employing activated squaric acid derivatives.¹⁶ Following the same strategy, the reaction between various quinaldinium salts (**6a-k**) and dibutylsquarate was carried out as shown in the Scheme 2.4. The reaction of the various substituted quinolinium salts with dibutylsquarate in *n*-butanol at 25 °C



a) $R^1 = \text{OH}, R^2 = \text{H}, R^3 = \text{CH}_3$

b) $R^1 = \text{OC}_2\text{H}_5, R^2 = \text{H}, R^3 = \text{CH}_3$

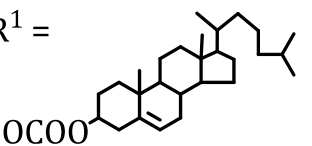
c) $R^1 = \text{OCOC}_6\text{H}_5, R^2 = \text{H}, R^3 = \text{CH}_3$

d) $R^1 =$  $, R^2 = \text{H}, R^3 = \text{CH}_3$

e) $R^1 = \text{OC}_3\text{H}_6\text{COOC}_2\text{H}_5, R^2 = \text{H}, R^3 = \text{CH}_3$

f) $R^1 = \text{OC}_3\text{H}_5\text{COOH}, R^2 = \text{H}, R^3 = \text{CH}_3$

h) $R^1 = \text{OH}, R^2 = \text{CH}_3, R^3 = \text{CH}_3$

i) $R^1 =$  $, R^2 = \text{CH}_3, R^3 = \text{CH}_3$

j) $R^1 = \text{H}, R^2 = \text{H}, R^3 = \text{CH}_2\text{CH}_2\text{OH}$

k) $R^1 = \text{Br}, R^2 = \text{H}, R^3 = \text{CH}_2\text{CH}_2\text{OH}$

i) 3,4-Dibutyl squarate, *n*-BuOH, 25 °C, 12 h.

Scheme 2.4

using triethylamine as a catalyst yielded the isomeric semisquaraine dyes **1a-k**. Characterization of the product through ^1H NMR indicated that the semisquaraine dyes obtained through this reaction pathway exist as butyl adducts. Interestingly, ^1H , ^{13}C NMR, FT-IR and HRMS spectral analysis indicate that the products obtained from the reaction of the quinaldinium salts with dibutyl squarate are different from the semisquaraine dyes obtained from the reaction of squaric acid with quinaldinium salts containing electron withdrawing substituents.

2.3.2. Characterization of Semisquaraine Dyes

The semisquaraines obtained from the reaction of the quinaldinium salts with dibutyl squarates (**1a-k**) and squaric acid (**2a,b,e,f,h-k**) have been characterized through various analytical and spectral techniques. For example, the ^1H NMR spectrum of the semisquaraine dye **1b** showed well-resolved peaks corresponding to the aromatic protons in the region between δ 6.8-7.4 ppm and a broad signal at δ 8.5 ppm. The olefinic protons and *N*-methyl protons, on the other hand, appeared at δ 5.2 and 3.7 ppm, respectively (Figure 2.1A). The broadening of the aromatic proton shows a dynamic process and was, therefore, further investigated by variable temperature ^1H NMR experiments. Figure 2.1B shows the NMR spectrum of a solution of **1b** in CDCl_3 at 233 K. Interestingly, the broad

aromatic band at δ 8.5 ppm splits into a well resolved doublet at δ 8.7 ppm with $J = 9.5$ Hz with a shift ($\Delta\delta$) of 0.2 ppm. This proton is assigned as the 3-H proton of the quinoline ring, which is capable of undergoing hydrogen bonding interactions with the carbonyl group.

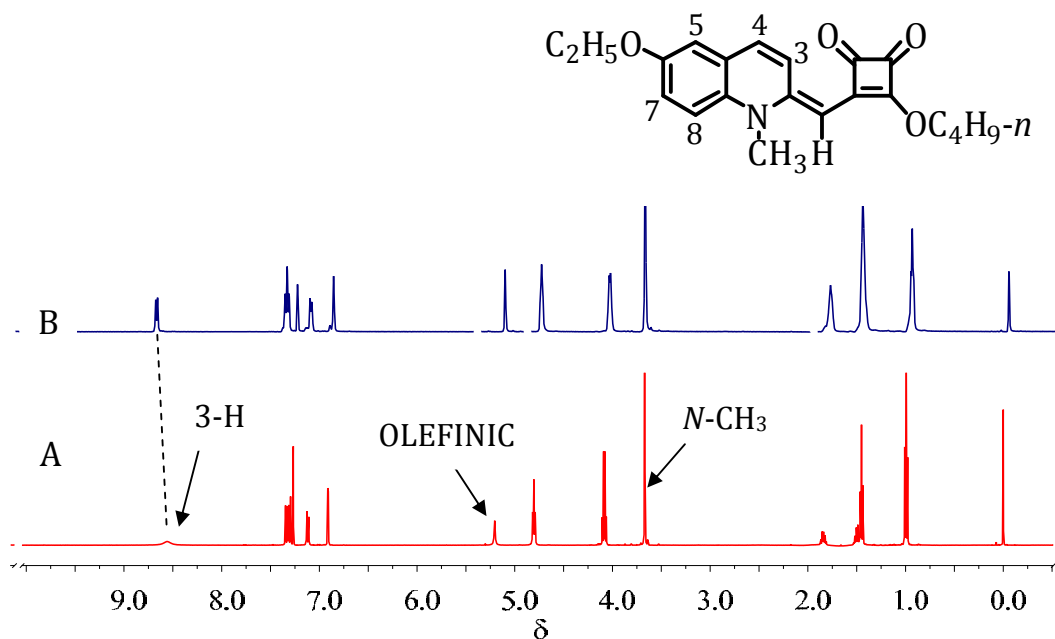


Figure 2.1. ^1H NMR spectrum of **1b** in CDCl_3 at A) 298 K and B) 233 K.

In contrast, in the ^1H NMR spectrum of the isomeric semisquaraine dyes (**2a,b,e,f,h-k**), the characteristic olefinic proton appear in the range from 6.1–6.2 ppm, whereas the *N*-methyl protons appear at 4.0–4.2 ppm. For example, the ^1H NMR spectrum of the semisquaraine dye **2b** in CDCl_3 showed well-resolved peaks corresponding to the aromatic protons in the range from δ 7.1–7.8 ppm with the 3-H proton appearing at δ 9.5 ppm having $J = 9.5$ Hz (Figure 2.2). In addition, the olefinic proton can be seen

as a sharp signal at δ 6.2 ppm, while the *N*-methyl protons appeared at δ 4.1 ppm.

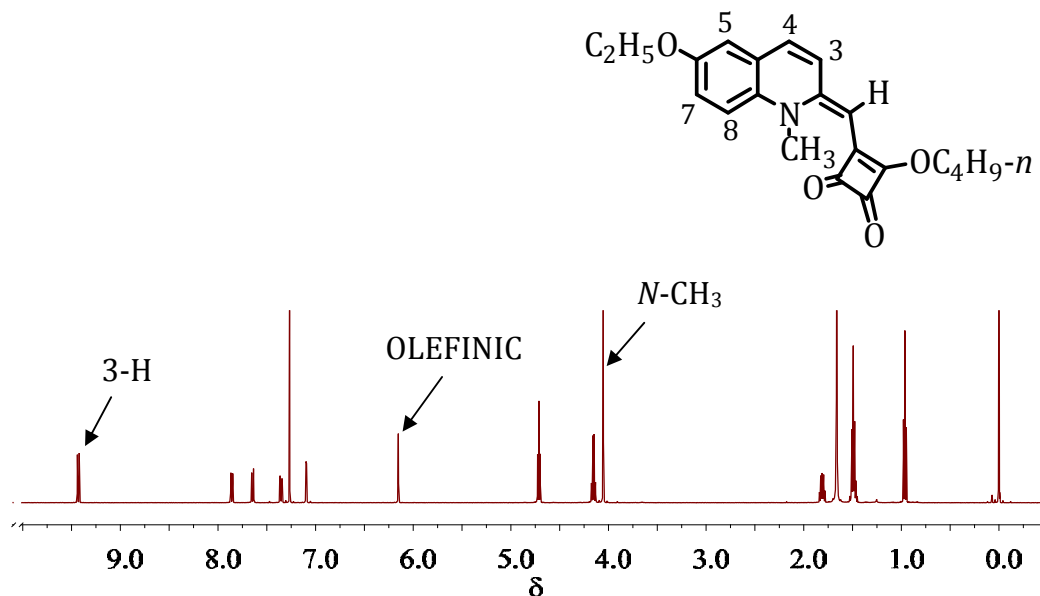


Figure 2.2. ^1H NMR spectrum of **2b** in CDCl_3 .

The ^{13}C NMR peaks corresponding to the squarone carbonyl carbons appeared at δ 193 and 185 ppm, for **1b**, while it is at δ 184 and 176 ppm for **2b**. The downfield shift of the carbonyl carbons in **1b** further substantiates the presence of strong hydrogen bonding interactions involving the squarone oxygen. Furthermore, a molecular mass of 353.22 and 353.16, respectively, was obtained for **1b** and **2b**, which corresponds to the molecular formula $\text{C}_{21}\text{H}_{23}\text{NO}_4$. Both the CHN analysis and the FAB-MS indicate that **1b** and **2b** are isomeric in nature.

Further evidence for the structural difference between the semisquaraines **1** and **2** was obtained by analyzing the FT-IR spectra. For

example, the dye **1b** showed a sharp and strong characteristic stretching frequency corresponding to the carbonyl groups at 1766 and 1696 cm^{-1} . In contrast, for the Z-isomer (**2b**), the carbonyl stretching band appears at 1760 cm^{-1} . The lowering of the carbonyl stretching frequency of one of the carbonyl groups to 1696 cm^{-1} in **1b** could be due to the interactions of the carbonyl group with the quinoline proton which decreases the C-O bond order. Moreover, the broadening of the proton peak ($\delta = 8.5$ ppm) in the proton NMR spectrum suggests that such an interaction indeed exists in the semisquaraine dye **1** systems.

The structure of the semisquaraines was further analyzed through nuclear overhauser effect (NOE) and 2D NMR experiments. The NOE experiments demonstrated that irradiation of the olefinic peak at δ 5.2 ppm induced 15% enhancement at δ 3.7 ppm corresponding to the *N*-CH₃ group for **1b**. For **2b**, the irradiation of the peak at δ 6.2 ppm induced 12% enhancement of the *N*-CH₃ group at δ 4.1 ppm. Figure 2.3 shows the ROESY (rotating frame overhauser effect spectroscopy) spectra of the semisquaraine dyes **1b** and **2b**. As can be seen from the figure 2.3A, the *N*-CH₃ peak at δ 3.7 ppm shows a ROE cross peak with the olefinic proton of **1b**. This coupling could also be seen in the ROESY spectrum of the dye **2b** (Figure 2.3B). Similar ROE cross peaks between the olefinic protons and the *N*-CH₂-CH₂ protons can be observed for the dyes **1j** and **2j** (Figure 2.4).

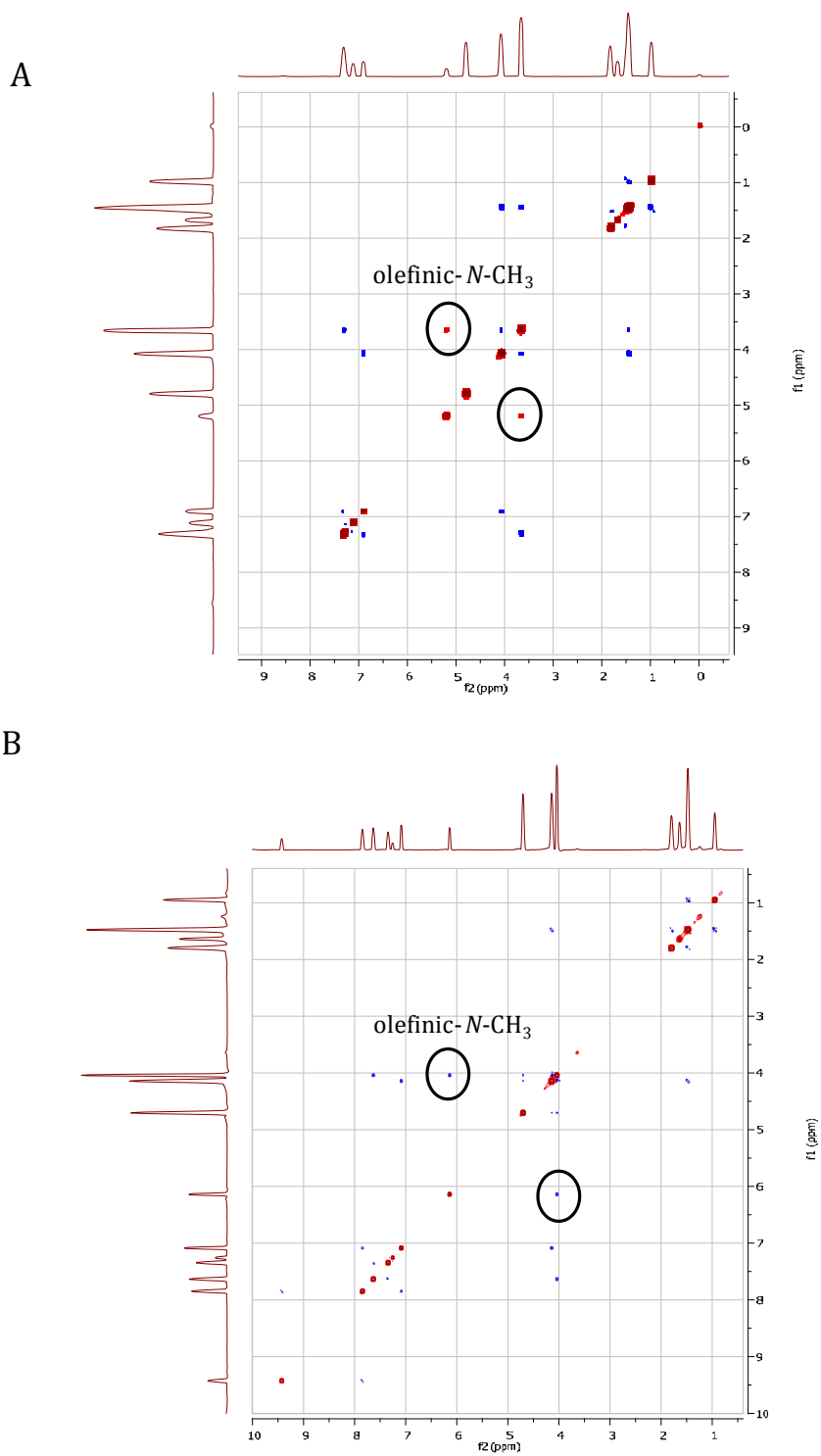


Figure 2.3. ROESY spectra of the semisquaraine dyes (A) **1b** and (B) **2b** in CDCl₃.

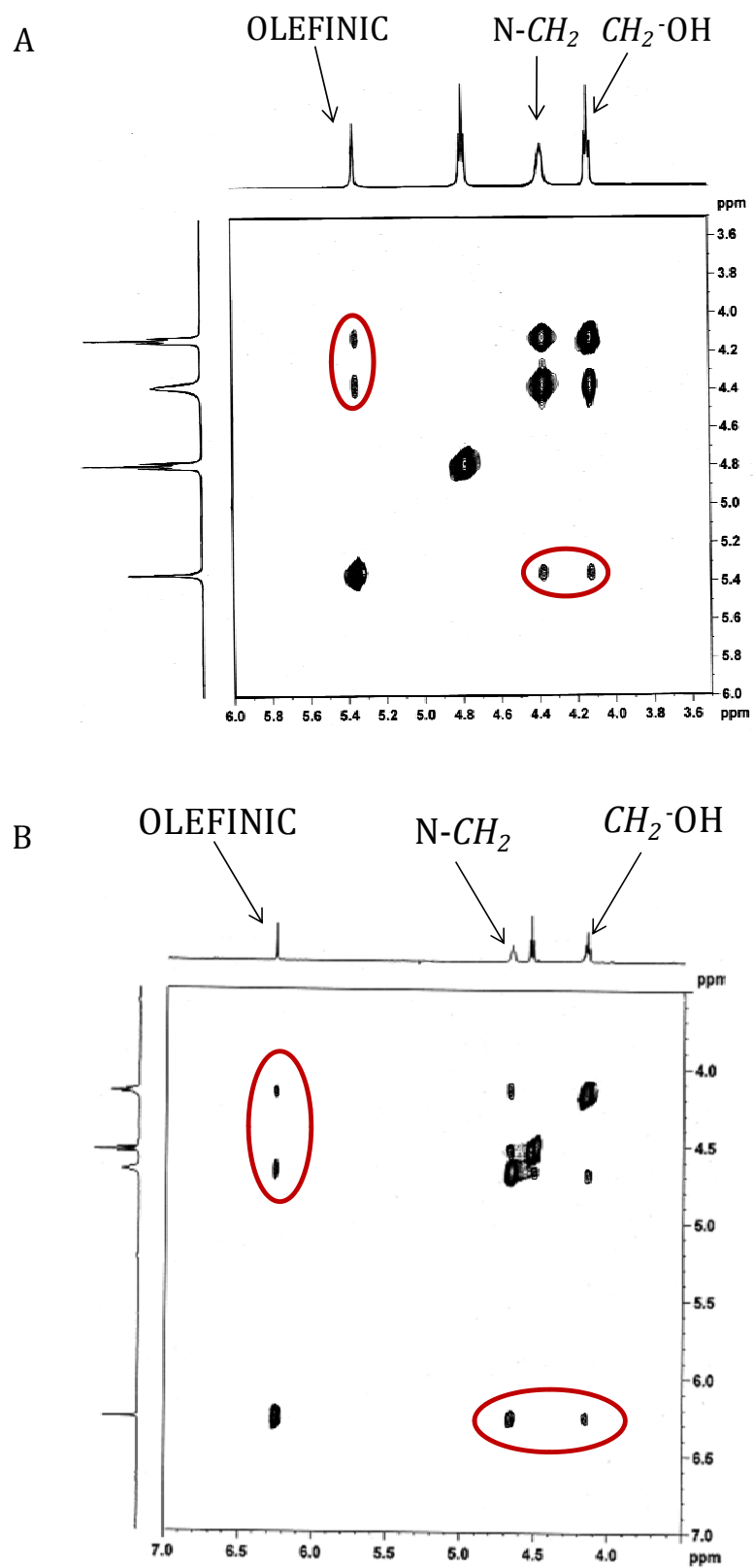


Figure 2.4. ROESY spectra of the semisquaraine dyes (A) **1j** and (B) **2j** in CDCl₃.

Based on these observations, we propose that the two semisquaraine derivatives could exist in either of the four isomeric forms as shown in Chart 2.2. To understand the stability of the various conformations, theoretical calculations were also carried out, which further, supports the existence of the four different conformers. Of all the possible structures for the dye **1a-k**, structure **1'** is the most probable structure. This structure was, further, conclusively determined by single crystal X-ray analysis of the representative semisquaraine dyes **1b** and **1j** (Figure 2.5) and their data has been summarized in Table 2.1.¹⁹ The semisquaraine dyes **1a-k** have an E-conformation as represented by **1'**. For example, the dye **1b** crystallized in the triclinic space group P-1 with cell parameters of $a = 8.78 \text{ \AA}$, $b = 9.15 \text{ \AA}$ and $c = 13.15 \text{ \AA}$. The angles α , β and γ have been found to be 85.53° , 76.52°

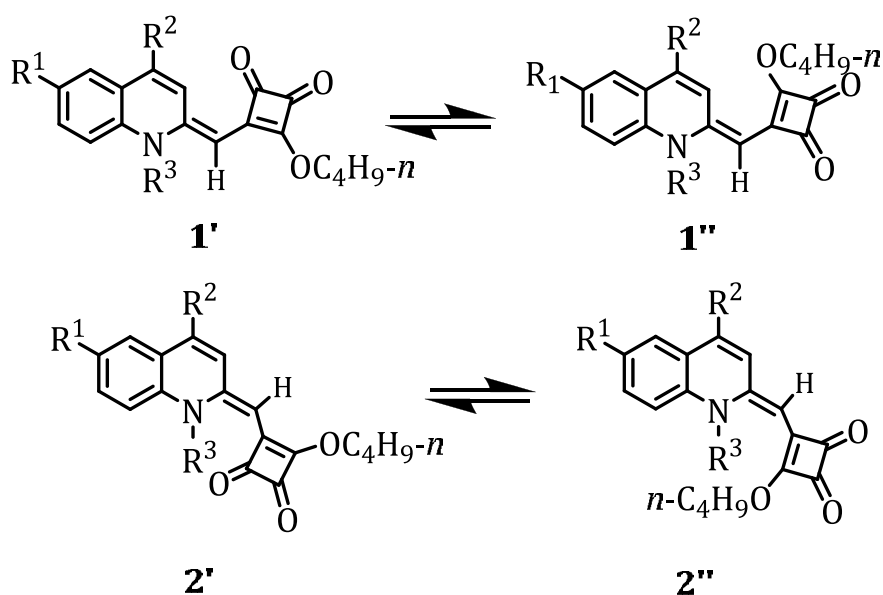


Chart 2.2

and 62.87° . Moreover, the dyes with E-conformation have a dihedral angle of around 10° between the quinoline and the squaryl ring.

Our attempts to unambiguously establish the structure of the Z-isomer through single crystal X-ray analysis were unsuccessful owing to its less stability, as compared to the E-isomer. Based on the analytical and spectral evidence we conclude that this isomer has a conformation represented by the stable structure **2'** with a dihedral angle of around 32° .

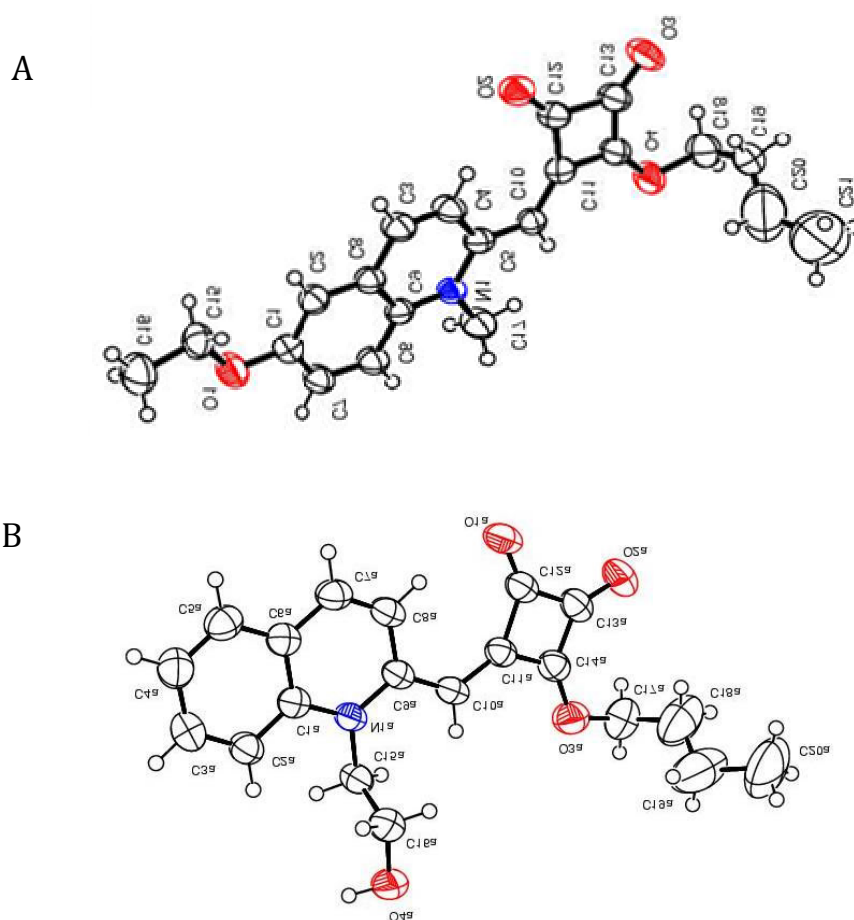


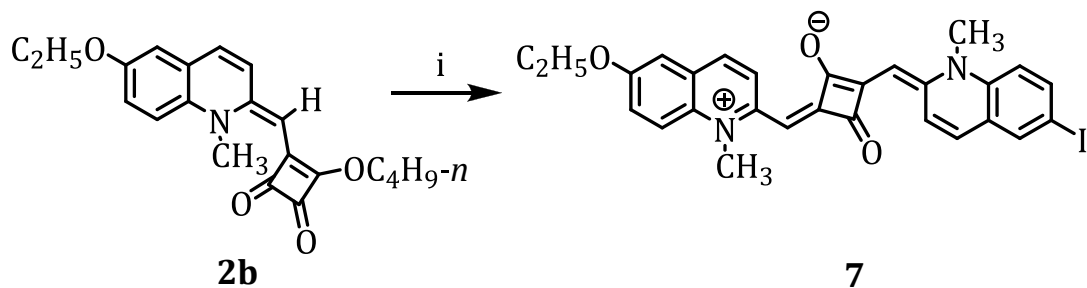
Table 2.1. Summary of crystallographic data for the semisquaraine dyes **1b** and **1j**.

Parameters	1b	1j
Empirical formula	C ₂₁ H ₂₃ NO ₄	C ₂₀ H ₂₁ NO ₄
Formula weight	353.40	339.38
Temperature, K	293(2)	293(2)
Wavelength, Å	0.71073	0.71073
Crystal system,	Triclinic	Triclinic
space group	P-1	P-1
a, Å	8.7796(2)	10.8220(8)
b, Å	9.1523(2)	12.8641(10)
c, Å	13.1484(3)	13.8618(11)
α, deg	85.5340(10)	65.888(2)
β, deg	76.5160(10)	87.750(2)
γ, deg	62.8700(10)	87.170(2)
Volume, Å ³	913.86(4)	1758.9(2)
Z	2	4
d _{calc} , mg/m ³	1.284	1.282
F(000)	376	720
Crystal size	0.30 x 0.20 x 0.20 mm	0.25 x 0.20 x 0.20 mm
Theta range for data collection, deg	2.50 to 29.07	1.61 to 26.03
Limiting indices	-12 ≤ h ≤ 11, - 12 ≤ k ≤ 12, -17 ≤ l ≤ 17	-13 ≤ h ≤ 13, - 15 ≤ k ≤ 15, -17 ≤ l ≤ 17
Reflections collected / unique	21943 / 4827	32888 / 6898
Data / restraints / parameters	4827 / 1 / 245	6898 / 0 / 462
Goodness-of-fit on F ²	1.047	1.032
Final R indices [I > 2σ(I)]	R1 = 0.0590, wR2 = 0.1833	R1=0.0653, wR2 = 0.1725
R indices (all data)	R1 = 0.0875, wR2 = 0.2109	R1=0.0994, wR2 = 0.2060

2.3.3. Reactivity of Semisquaraine Isomers

As indicated in Section 2.3.1, the quinaldine based squaraine dyes are prepared by the reaction between the corresponding quinaldinium salts and squaric acid through the intermediacy of the semisquaraine dye.^{18a-c} The intermediate semisquaraines formed readily undergoes further dye formation, unless the semisquaraine is rendered less electrophilic by the substituent present in the quinoline ring. In this context, the semisquaraine dyes **2a,b,e,f,h-k** were prepared by the reaction between squaric acid and the quinaldinium salts having electron donating substituents. Due to the presence of the electron donating substituent at the 6-position, there is a greater electron density at the squaryl carbonyl groups making them less electrophilic; as a result of which further reaction of the semisquaraine with a second weakly nucleophilic quinaldinium salt was inhibited. Nevertheless, the semisquaraine dye thus formed, can react directly with more reactive quinaldinium salts (ie, salts with electron withdrawing groups) to give the corresponding unsymmetrical squaraine dyes (Scheme 2.5). For example, the semisquaraine dye **2b** can undergo reaction with highly reactive quinaldinium salt to give the unsymmetrical dye **7** in 90% yield.

In contrast, the E-isomer (**1b**) did not undergo further condensation reaction with the *N*-methyl-6-iodo-2-quinaldinium salt under analogous

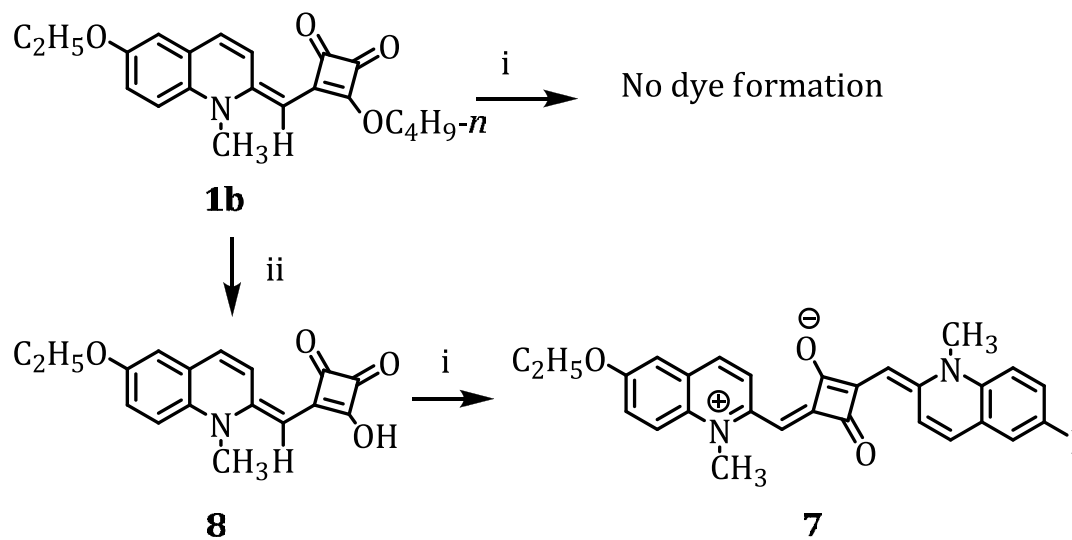


i) *N*-Methyl-6-iodo-2-methylquinolinium iodide, *n*-BuOH/ C₆H₆ (1:1), quinoline, 100-105 °C.

Scheme 2.5

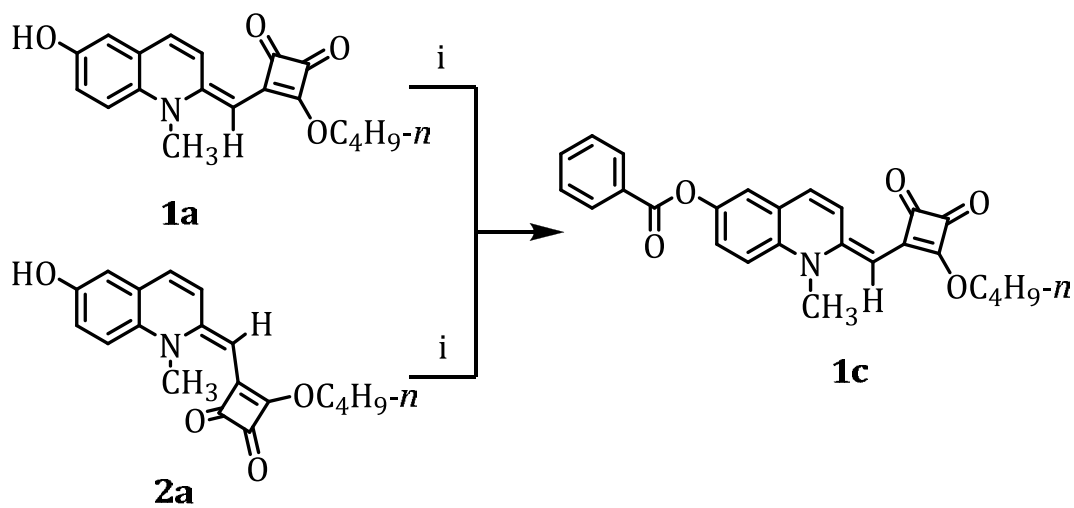
reaction conditions (Scheme 2.6). However, as shown in the scheme, it was observed that the dye reaction is feasible after hydrolysis of the semisquaraine dye. The dye **1b** was hydrolyzed in a mixture (50:50:1) of CH₃COOH:H₂O:4N HCl to yield the semisquaric acid **8**, which, then, readily reacted with the quinaldinium salt to form the unsymmetrical squaraine dye **7**.

To understand the reactivity pattern of the semisquaraine isomers, we have carried out the reaction of the hydroxy substituted semisquaraine **1a** and **2a** with benzoyl chloride in dichloromethane using pyridine as catalyst at 0 °C for 12 h (Scheme 2.7). Interestingly, the reaction of the semisquaraine derivative **2a** with benzoyl chloride under similar reaction conditions gave the E-conformer (**1c**) in quantitative yields; the formation of which may be explained by the acid catalyzed isomerization of the Z-isomer under the reaction conditions.



i) *N*-Methyl-6-iodo-2-methylquinolinium iodide, *n*-BuOH/C₆H₆ (1:1), quinoline, 100-105 °C, 12 h; ii) CH₃COOH:H₂O:4N HCl (50:50:1), 25 °C, 4 h.

Scheme 2.6



i) Benzoyl chloride, CH₂Cl₂, pyridine, 0 °C, 12 h.

Scheme 2.7

2.4. DISCUSSION

The quinaldinium salts with electron donating groups on reaction with dibutyl squarate and squaric acid respectively, gave the semisquaraine dyes **1a-k** and **2a,b,e,f,h-k**. Further, it was observed that on reaction with squaric acid, only the quinaldinium salts with electron donating groups yielded the semisquaraine derivatives, whereas the quinaldinium salts with electron withdrawing group, gave exclusively the corresponding squaraine dye. This difference in the reactivity of squaric acid towards the quinaldinium salts was explained in terms of the nucleophilicity of the salt taking part in the dye formation reaction. Interestingly, the reaction of the quinaldinium salts substituted with electron donating/withdrawing groups and dibutyl squarate yielded exclusively E-isomer of the semisquaraine dyes (**1a-k**); the structure of which was confirmed through single crystal X-ray analysis.

The minimum energy conformation of the dye **1a-k** obtained through molecular modeling studies were found to be consistent with the data obtained through single crystal X-ray structure analysis. For example, Figure 2.6 shows the optimized geometry of the rotomers of **1b**, which shows a distance of 2.096 Å between the 3-H proton of the quinoline ring and the squaryl oxygen atom, which is comparable to the value of 2.239 Å obtained through the crystallographic data. Of the two possible rotameric

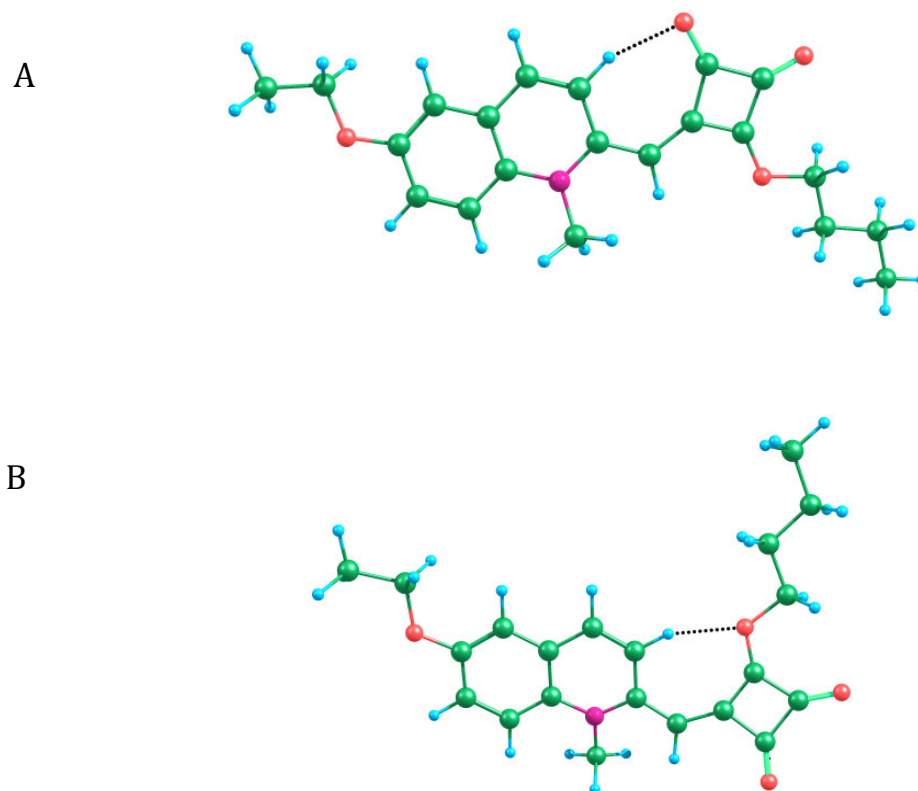
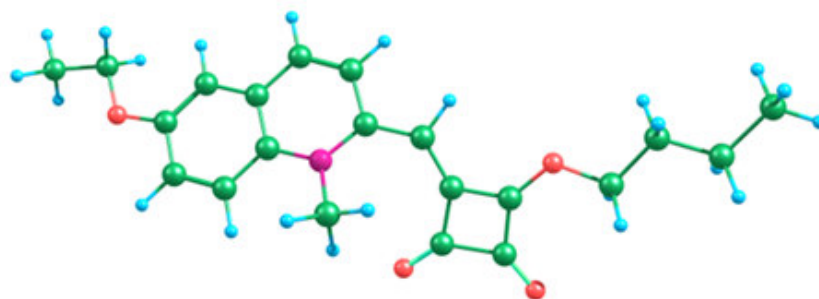


Figure 2.6. Optimized geometry of the rotamers of **1b** obtained with B3LYP/6-31G theoretical calculations. (A) **1b'** and (B) **1b''**.

structures for **1b**, the structure **1b'** is 1.83 kcal/mol more stable than the structure **1b''**. This is further substantiated by the single crystal structure analysis of **1b**. Similar to the E-isomer (**1b**), the Z-isomer (**2b**) can also exist in two rotameric forms (Figure 2.7); of which, the structure **2b'** is 2.38 kcal/mol more stable than the structure **2b''**. In **2b'** and **2b''**, the squaryl ring is twisted by an angle of 32° with respect to the quinoline ring. Theoretical calculations showed that the Z-isomer is 3.72 kcal/mol less stable than the E-isomer.

A



B

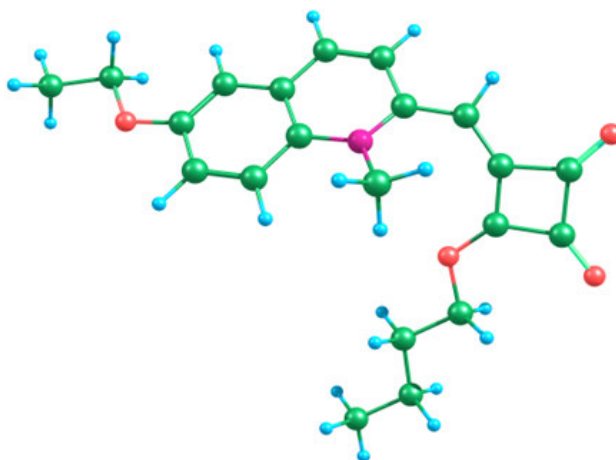


Figure 2.7. Optimized geometry of the rotamers of **2b** obtained with B3LYP/6-31G theoretical calculations. (A) **2b'** and (B) **2b''**.

The Z-conformation for the semisquaraine dyes (**2a,b,e,f,h-k**) was assigned based on the analytical and spectral evidence like 1D and 2D NMR, FTIR, FAB mass and elemental analysis. This was, further, confirmed by the presence of the cross peaks between the *N*-CH₃ and the olefinic group in the ROESY spectra. This can be attributed to the steric crowding between the carbonyl group and the *N*-CH₃ group, which result in the twisting of the squaryl ring with respect to the quinoline ring, as validated by the theoretical calculations. This would bring the olefinic and *N*-CH₃ protons

within a distance of 4Å, which, in turn, gives rise to the ROESY cross peak. This was further verified in the case of the semisquaraine derivative **2j**. Efforts are currently in progress to establish the structure of the Z-isomer unambiguously through single crystal X-ray analysis. We observed that the Z-isomer reacts readily with a strong nucleophilic salt to form the unsymmetrical squaraine dye, while the E-conformer should be hydrolyzed before it can react further. This is attributed to the greater reactivity of the Z-isomer, as compared to the E-isomer.

2.5. CONCLUSIONS

The synthesis of novel isomeric semisquaraine derivatives based on the quinaldine moiety has been achieved in quantitative yields. The reaction of the quinaldinium salts containing electron donating groups and squaric acid gave the Z-isomer of the semisquaraine derivative, while dibutyl squarate yielded the E-isomer. These dyes have been characterized based on various analytical and spectral evidences. In addition, the structure of the representative examples of the E-isomer has been established through single crystal X-ray analysis. These derivatives also, interestingly, showed different photophysical properties and reactivity patterns. Further, the existence of such isomers of semisquaraine dyes

opens up new avenues for the synthesis of novel symmetrical and unsymmetrical squaraine dyes for various optoelectronic applications.

2.6. EXPERIMENTAL SECTION

2.6.1. General Techniques

The equipment and procedure for spectral recordings are described elsewhere.²⁰ All melting points are determined on a Mel-Temp II melting point apparatus. The IR spectra were recorded on a Perkin Elmer Model 882 infrared spectrometer. Elemental analyses were done using a Perkin-Elmer series-II 2400 CHN analyzer. The electronic absorption spectra were recorded on a Shimadzu UV-3101 or 2401 PC UV-VIS-NIR scanning spectrophotometer. The fluorescence spectra were recorded on a SPEX-Fluorolog F112X spectrofluorimeter. ¹H and ¹³C NMR were recorded on a 300 MHz and 500 MHz Bruker advanced DPX spectrometer. All the solvents used were purified and distilled before use.

2.6.2. Materials

6-Hydroxy-2-quinaldine (**4a**), mp 262-264 °C (lit. mp 262-264 °C),^{19a} 6-ethoxy-2-quinaldine (**4b**), mp 71-72 °C (lit. mp 71-72 °C),^{19a} 6-cholester-3-yl-2-methylquinoline-6-yl carbonate (**4d**), mp 101-102 °C (lit. mp 101-102 °C),^{19b} 6-hydroxy-*N*-methyl-2-quinaldinium iodide (**6a**), mp 238-239 °C

(lit. mp 238-239 °C),^{19a} 6-ethoxy-*N*-methyl-2-quinaldinium iodide (**6b**), mp 182-183 °C (lit. mp 182-183 °C),^{19a} 6-iodo-*N*-methyl-2-quinaldinium iodide, mp 222-223 °C (lit. mp 222-224 °C)²¹ and cholesterol linked *N*-methylquinolinium iodide (**6d**), mp 216-217 °C (lit. mp 216-217 °C),^{19b} were prepared by modifying the reported procedures. 4-Aminophenol, cholesteryl chloroformate was purchased from Aldrich and used as such while squaric acid was a gift from Professor Waldemar Adam, University of Würzburg, Germany.

2.6.3. Preparation of Enamine 5g

A mixture of 2.5g (0.023 mol) of *p*-toluidine and 2.33 g (0.023 mol) of pentane-2,4-dione, 5 g of granular anhydrous calcium sulphate was refluxed for 1 h. The reaction mixture was cooled and filtered after adding 40 mL of ethyl ether. The precipitate obtained was washed with about 40 mL of ethyl ether and the combined filtrate was evaporated to get the product as a viscous liquid. **5g**: (80%); IR (KBr) ν_{\max} 3051, 1697, 1595 cm^{-1} ; ^1H NMR (300 MHz, CDCl_3) δ 12.47 (1H, s), 7.36 (2H, t, $J = 7.5$ Hz), 7.21 (1H, t, $J = 7.4$ Hz), 7.12 (2H, d, $J = 7.6$ Hz), 5.18 (1H, s), 2.10 (3H, s), 1.99 (3H, s); FAB-MS m/z Calcd for $\text{C}_{12}\text{H}_{15}\text{NO}_2$ 205.33, Found 205.25.

2.6.4. Preparation of 2-Methylquinolines 4c,e-f

Preparation of 6-benzoyl-2-methylquinoline 4c : To a mixture of

200 mg (1.25 mmol) of **3a** (in dichloromethane (10 mL) in presence of pyridine (0.5 mL), benzoyl chloride (2 mL) was added dropwise at 0 °C and stirred for 8 h. The resulting mixture was neutralized with NH₄OH and extracted with CHCl₃ to give a residue which was purified by column chromatography. Elution of the column with a mixture (9:1) of chloroform and methanol gave **4c** in 85% yield. mp 94-96 °C; IR (KBr) ν_{\max} 3061, 1697, 1598, 1450 cm⁻¹; ¹H NMR (500 MHz, CDCl₃) δ 8.17 (2H, d, J = 9 Hz), 7.7-7.4 (8H, m), 2.85 (3H, s); FAB-MS *m/z* Calcd for C₁₇H₁₃NO₂ 264.29 (M+1), Found 264.53.

Preparation of 6-hydroxy-2-methylquinoline derivative 4e : A mixture of **4a** (200 mg, 1.25 mmol), ethyl-4-bromobutyrate (190 mg, 1.25 mmol) and Cs₂CO₃ (1.22 g, 3.75 mol) was stirred in DMF (5 mL) at room temp under inert atmosphere for 12 h. The inorganic precipitate was filtered off, the filtrate was concentrated under reduced pressure. The residue was diluted with water and extracted with dichloromethane. The combined organic solution was washed with water and saturated aqueous NaCl, dried over Na₂SO₄ and evaporated. Chromatographed on silica gel and elution with a mixture (1:9) of ethyl acetate and hexane gave **4e** in 88% yield. mp 60-62 °C; IR (KBr) ν_{\max} 2920, 1735, 1602, 1375 cm⁻¹; ¹H NMR (300 MHz, CD₃CN) δ 7.94 (2H, d, J = 9.4 Hz), 7.33 (1H, d, J = 9.1 Hz), 7.23 (1H, d, J = 8.4 Hz), 7.02 (1H, s), 4.14 (4H, m), 2.69 (3H, s), 2.58 (2H, t), 2.21 (2H, m), 1.28

(3H, t); FAB-MS m/z Calcd for $C_{16}H_{19}NO_3$ 274.33 (M+1), Found 274.45.

Preparation of 6-hydroxy-2-methylquinoline derivative 4f: To a solution of **4e** (2.7 mg, 10 μ mol) in methanol (1 mL), 2N aq NaOH (0.1 mL, 0.2 mmol) was added. The mixture was stirred at 25 °C for 4 h and neutralized with 2N HCl. The solvent was evaporated off and chromatographed over silica gel. Elution of the column with a mixture (2:8) of ethyl acetate and hexane gave **4f**. (75%) mp 173-175 °C; IR (KBr) ν_{max} 2964, 1689, 1602, 1506, 1234 cm^{-1} ; 1H NMR (300 MHz, CD_3OD) δ 8.11 (1H, d, $J = 8.4$ Hz), 7.85 (1H, d, $J = 9.2$ Hz), 7.37-7.32 (2H, m), 7.20 (1H, s), 4.15 (2H, t), 2.67 (3H, s), 2.56 (2H, t), 2.18 (2H, t); FAB-MS m/z Calcd for $C_{14}H_{15}NO_3$ 245.27, Found 246.46.

2.6.5. Preparation of Dimethylquinolines 4g-i

Enamine **3g** (4g, 18.26 mmol) was added in portions to 6 mL conc. sulphuric acid and heated to 60-70 °C for 3 h. The reaction mixture was cooled to room temperature and 10 mL of ice water was added to the reaction mixture. Sodium carbonate was added until the reaction mixture turned alkaline. The reaction mixture was extracted with chloroform. The solvent was distilled off under reduced pressure to obtain a residue which was chromatographed over silica gel. Elution of the column with a mixture (1:10) of ethylacetate and hexane gave the dimethylquinoline derivative **4g**: (82 %); mp 85-87 °C; IR (KBr) ν_{max} 2974, 1560, 1444, 1232 cm^{-1} ;

^1H NMR (300 MHz, CDCl_3) δ 8.29 (1H, d, $J = 8.8$ Hz), 7.34 (1H, d, $J = 9.1$ Hz), 7.13-7.08 (2H, m), 3.90 (3H, s), 2.92 (3H, s), 2.60 (3H, s). FAB-MS m/z Calcd for $\text{C}_{12}\text{H}_{13}\text{NO}$ 187.24 (M+1), Found 187.36.

Preparation of 6-hydroxy-2,4-dimethylquinoline derivative 4h. To solution of **4g** (2 g, 10 mmol) in dichloromethane (10 mL) BBr_3 (2 mL, 21 mmol) was added at 0 °C and stirred overnight. 50 mL of distilled water was added to the reaction mixture. The reaction mixture was made basic by adding 1.5 N of NaOH gave **4h** which was recrystallised from methanol, (69 %); mp 220-222 °C; IR (KBr) ν_{max} 3061, 1618, 1568, 1446, 1238 cm^{-1} ; ^1H NMR (300 MHz, CD_3OD) δ 7.79 (1H, d, $J = 8.9$ Hz), 7.28-7.14 (3H, m), 2.58 (6H, s); FAB-MS m/z Calcd for $\text{C}_{11}\text{H}_{11}\text{NO}$ 174.21 (M+1), Found 174.38.

Preparation of cholesterol linked 6-hydroxy-2,4-dimethylquinoline derivative 4i. A mixture of 6-hydroxy-2,4-dimethylquinoline **4h** (250 mg, 1.4 mmol), cholesteryl chloroformate (1.2 g, 2.9 mmol) and triethylamine (10 mL) was heated at 90 °C for 12 h. Removal of the solvent gave a residue, which was then subjected to column chromatography over silica gel. Elution of the column with a mixture of ethyl acetate and petroleum ether (1:9) gave 85% of the quinoline derivative **4i**: mp 172-174 °C; IR (KBr) ν_{max} 2945, 1761, 1606, 1465, 1249 cm^{-1} ; ^1H NMR (300 MHz, CDCl_3) δ 8.01 (1H, d, $J = 9.1$ Hz), 7.76 (1H, s), 7.54 (1H, d, $J = 9.1$ Hz), 7.38 (1H, s), 5.43 (1H, s), 4.56 (1H, s), 2.69-0.61 (47H, m); FAB-MS m/z Calcd for

$C_{38}H_{55}NO_3$ 586.86 (M+1), Found 586.85.

2.6.6. General Procedure for Synthesis of Quinaldinium Salts 6c-k

A mixture of the corresponding quinaldine (1 mmol) and methyl iodide/2-bromoethanol (4 mmol) was heated in a sealed tube at 100-105 °C for 12 h. The precipitate formed was filtered, washed thoroughly with cold diethyl ether and recrystallized from methanol to give the corresponding quinaldinium salts **6c-k** in good yields.

6c: 90%; mp 100-102 °C; IR (KBr) ν_{\max} 3068, 1693, 1600, 1450, 1290 cm^{-1} ; 1H NMR (CD_3OD) δ 8.9 (1H, d, J = 8.5 Hz), 8.6 (1H, d, J = 9 Hz), 8.2-7.6 (8H, s), 4.7 (3H, s), 2.9 (3H, s); FAB-MS m/z Calcd for $C_{18}H_{16}NO_2^+$ 279.32 (M+1), Found 279.44.

6d: 95%; mp 216-217 °C; IR (KBr) ν_{\max} 1762, 1612 cm^{-1} ; 1H NMR (300 MHz, $CDCl_3:MeOH-d_4$) δ 8.92 (1H, d, J = 8.4 Hz), 8.57 (1H, d, J = 9.9 Hz), 8.17 (1H, s), 8.05 (1H, m), 7.47 (1H, s), 5.45 (1H, s), 4.60 (3H, s), 4.59 (1H, s), 3.35 (3H, s), 2.05-0.71 (43H, m); FAB-MS m/z Calcd for $C_{39}H_{56}NO_3^+$ 587.87 (M+1), Found 587.89.

6e: 92%; mp 163-165 °C; IR (KBr) ν_{\max} 2993, 1716, 1610, 1519, 1388, 1271 cm^{-1} ; 1H NMR (500 MHz, $DMSO-d_6$) δ 8.93 (1H, d, J = 8.5 Hz), 8.52 (1H, d, J = 9 Hz), 8.05 (1H, d, J = 8.5 Hz), 7.82 (2H, m), 4.42 (3H, s), 4.24 (2H, t), 4.10 (2H, m), 3.03 (3H, s), 2.55 (2H, m), 2.10 (2H, t), 1.20 (3H, t); 2.21 (2H,

m), 1.28 (3H, t); FAB-MS m/z Calcd for $C_{17}H_{22}NO_3^+$ 288.36, Found 288.59.

6f: 85 %; mp 178-180 °C; IR (KBr) ν_{\max} 3414, 1718, 1608, 1519, 1269 cm^{-1} ; 1H NMR (500 MHz, DMSO- d_6) δ 12.18 (1H, s), 8.91 (1H, d, $J = 8.5$ Hz), 8.51 (1H, d, $J = 9.5$ Hz), 8.04 (1H, d, $J = 8.5$ Hz), 7.82 (2H, m), 4.41 (3H, s), 4.23 (2H, t), 3.01 (3H, s), 2.47 (2H, t), 2.06 (2H, t); FAB-MS m/z Calcd for $C_{15}H_{18}NO_3^+$ 260.31, Found 260.52.

6h: 90%; mp 224-226 °C; IR (KBr) ν_{\max} 3435, 3099, 1610, 1537, 1431, 1261 cm^{-1} ; 1H NMR (CD_3OD) δ 8.36 (1H, d, $J = 9.5$ Hz), 7.82 (1H, s), 7.70 (1H, d, $J = 9.5$ Hz), 7.66 (1H, s), 4.82 (3H, s), 4.42 (3H, s), 2.86 (3H, s); FAB-MS m/z Calcd for $C_{12}H_{14}NO^+$ 188.25, Found 188.41.

6i: 85 %; mp 193-195 °C, IR (KBr) ν_{\max} 2935, 1761, 1616, 1465, 1253 cm^{-1} ; 1H NMR ($CDCl_3$) δ 8.63 (1H, d, $J = 9.6$ Hz), 8.06 (1H, s), 7.99 (2H, m), 5.44 (1H, s), 4.62 (3H, s), 3.24 (3H, s), 2.88 (3H, s), 2.02-0.67 (46H, s); FAB-MS m/z Calcd for $C_{40}H_{58}NO_3^+$ 600.58, Found 600.56.

6j: 90%; mp 128-130 °C; IR (KBr) ν_{\max} 3242, 1604, 1523, 1433, 1371, 1078 cm^{-1} ; 1H NMR (300 MHz, CD_3OD) δ 9.03 (1H, d, $J = 8.5$ Hz), 8.58 (1H, d, $J = 9$ Hz), 8.37 (1H, d, $J = 8$ Hz), 8.24 (1H, m), 8.06 (1H, d, $J = 8.5$ Hz), 7.99 (1H, t), 5.26 (2H, t), 4.20 (2H, t), 3.23 (3H, s); FAB-MS m/z Calcd for $C_{12}H_{14}NO^+$ 188.25, Found 188.27.

6k: 85 %; mp 194-196 °C, IR (KBr) ν_{\max} 3257, 1598, 1506, 1369 cm^{-1} ; 1H NMR (300 MHz, CD_3OD) δ 8.95 (1H, d, $J = 8.5$ Hz), 8.60-8.49 (2H, m),

8.30-8.21 (1H, m), 8.09 (1H, d, J = 8.6 Hz), 5.23 (2H, t), 4.17 (2H, t), 3.21 (3H, s); FAB-MS m/z Calcd for C₁₂H₁₃BrNO⁺ 267.14, Found 267.87.

2.6.7. General method for Synthesis of Semisquaraine Dyes 1a-k

A mixture of the corresponding quinaldinium salt (0.06 mmol), dibutylsquarate (0.06 mmol) and triethylamine (0.5 mL) in butanol (10 mL) was stirred at 25 °C for 12 h. The solvent was distilled off under reduced pressure to obtain a residue which was chromatographed over silica gel. Elution of the column with a mixture (1:10) of methanol and chloroform gave the semisquaraine derivative **1**.

1a: (95%) mp 205-207 °C; IR (KBr) ν_{\max} 3450, 1753, 1649, 1612, 1500, 1348 cm⁻¹; ¹H-NMR (500 MHz, DMSO-*d*₆) δ 8.39 (1H, bs), 7.65-7.59 (2H, m), 7.12 (1H, d, J = 9 Hz), 6.91 (1H, s), 5.2 (1H, s), 4.74 (2H, t), 3.7 (3H, s), 1.79 (2H, t), 1.55 (2H, m), 0.96 (3H, t); ¹³C NMR (125 MHz, DMSO-*d*₆) δ 192, 184, 182, 171, 153, 150, 132, 124, 120, 116, 111, 84, 72, 54, 35, 31, 17, 13; FAB-MS m/z Calcd for C₁₉H₁₉NO₄ 325.14, Found 325.37.

1b: (98%) mp 202-204 °C; IR (KBr) ν_{\max} 1766, 1696, 1529, 1462 cm⁻¹; ¹H-NMR (500 MHz, CDCl₃) δ 8.55 (1H, bs), 7.34-7.26 (2H, m), 7.12 (1H, d, J = 9 Hz), 6.91 (1H, s), 5.2 (1H, s), 4.81 (2H, t), 4.1 (2H, t), 3.66 (3H, s), 1.86 (2H, m), 1.51 (5H, m), 1.006 (3H, t); ¹³C NMR (125 MHz, CDCl₃) δ 193, 185, 184, 173, 155, 151, 134, 132, 124, 119, 115, 111, 85, 73, 64, 35, 32, 18, 14, 13;

FAB-MS m/z Calcd for $C_{21}H_{23}NO_4$ 353.163, Found 353.22. Anal. Calcd; C, 71.37; H, 6.56; N, 3.96. Found: C, 71.37; H, 7.04; N, 4.2.

1c: (90%) mp 188-190 °C; IR (KBr) ν_{\max} 2964, 1759, 1726, 1618, 1539, 1350 cm^{-1} ; 1H -NMR (500 MHz, $CDCl_3$) δ 8.57 (1H, bs), 8.22 (2H, d, $J = 8$ Hz), 7.68 (1H, t), 7.55 (2H, t), 7.38 (2H, s), 7.35 (2H, m), 5.27 (1H, s), 4.83 (2H, t), 3.68 (3H, s), 1.86 (2H, t), 1.52 (2H, m), 1.01 (3H, t); ^{13}C NMR (125 MHz, $CDCl_3$) δ 193, 186, 185, 173, 165, 151, 146, 138, 133, 132, 130, 130, 129, 128, 128, 125, 124, 124, 120, 115, 87, 73, 35, 32, 18, 13; FAB-MS m/z Calcd for $C_{26}H_{23}NO_5$ 426.46, Found 426.05.

1d: (95%) : mp 201-203 °C; IR (KBr) ν_{\max} 2945, 1762, 1539, 1232 cm^{-1} ; 1H NMR (300 MHz, $CDCl_3$) δ 8.57 (1H, bs), 7.32-7.26 (4H, m), 5.43 (1H, s), 5.25 (1H, s), 4.84 (2H, m), 4.61 (1H, s), 3.65 (3H, s), 2.50 (2H, d, $J = 6.3$ Hz), 2.01-0.90 (48H, m); ^{13}C NMR (75 MHz, $CDCl_3$) δ 192, 188, 186, 185, 173, 152, 151, 146, 138, 132, 125, 124, 123, 120, 118, 117, 116, 115, 114, 111, 110, 109, 108, 87, 79, 69, 56, 49, 49, 42, 41, 39, 37, 36, 35, 31, 31, 28, 27, 27, 24, 22, 21, 19, 18, 15, 11; FAB-MS m/z Calcd for $C_{47}H_{63}NO_6$ 738.00, Found 737.83.

1e: (96%) mp 146-148 °C; IR (KBr) ν_{\max} 2958, 1764, 1730, 1697, 1672, 1537, 1355 cm^{-1} ; 1H -NMR (500 MHz, $CDCl_3$) δ 8.37 (1H, bs), 7.64 (2H, m), 7.19 (2H, m), 5.18 (1H, s),), 4.72 (2H, t), 4.20 (4H, m), 4.07 (2H, s), 3.67 (3H, s), 2.00 (2H, m), 1.77 (2H, m), 1.42 (5H, m), 0.947 (3H, t); ^{13}C NMR

(125 MHz, DMSO-*d*₆) δ 193, 185, 182, 172, 171, 154, 150, 134, 133, 124, 123, 120, 117, 110, 85, 72, 66, 59, 35, 31, 30, 24, 18, 14, 13; FAB-MS *m/z* Calcd for C₂₅H₂₉NO₆ 440.50 (M+1), Found 440.35.

1f: (98%) mp 167-169 °C; IR (KBr) ν_{\max} 2962, 1764, 1668, 1602, 1533, 1465, 1354 cm⁻¹; ¹H-NMR (500 MHz, CDCl₃) δ 8.7 (1H, bs), 7.95 (1H, d, *J* = 7 Hz), 7.29-7.23 (2H, m), 7.05 (1H, s), 5.2 (1H, s), 4.52 (4H, m), 4.16 (3H, s), 2.57 (2H, m), 2.2-2.0 (2H, m), 1.78 (2H, m), 1.45 (2H, m), 1.0 (3H, m); ¹³C NMR (125 MHz, CDCl₃) δ 193, 188, 185, 184, 174, 155, 143, 135, 129, 127, 122, 106, 67, 66, 56, 35, 32, 30, 29, 24, 24, 18, 13; FAB-MS *m/z* Calcd for C₂₃H₂₅NO₆ 412.45 (M+1), Found 412.40.

1h: 95%, mp 230-232 °C; IR (KBr) ν_{\max} 3086, 1757, 1676, 1570, 1514, 1354, 1201 cm⁻¹; ¹H NMR (CD₃OD) δ 8.3 (1H, bs), 7.52-7.28 (3H, m), 5.27 (1H, s), 4.55 (2H, t), 3.8 (3H, s), 2.62 (3H, s), 1.76 (2H, m), 1.51 (2H, m), 1.01 (3H, t); ¹³C NMR (125 MHz, CD₃OD) δ 192, 184, 182, 172, 153, 150, 132, 124, 120, 116, 111, 85, 72, 54, 35, 31, 17, 14, 13; FAB-MS *m/z* Calcd for C₂₀H₂₁NO₄ 340.39 (M+1), Found 340.50.

1i: 80%, mp 205-207 °C; IR (KBr) ν_{\max} 2947, 1759, 1697, 1635, 1535, 1240 cm⁻¹; ¹H NMR (500 MHz, CDCl₃) δ 8.54 (1H, bs), 7.43-7.26 (3H, m), 5.43 (1H, s), 5.23 (1H, s), 4.83 (2H, t), 4.63 (1H, m), 3.66 (3H, s), 2.50-0.68 (53H, m); ¹³C NMR (125 MHz, CDCl₃) δ 192, 188, 186, 185, 173, 152, 150, 146, 139, 138, 137, 125, 124, 123, 123, 116, 115, 79, 73, 56, 56, 49, 42, 39,

39, 37, 36, 36, 36, 35, 35, 32, 31, 31, 28, 28, 27, 24, 23, 22, 22, 21, 19, 18, 15, 13, 13; FAB-MS m/z Calcd for $C_{48}H_{65}NO_6$ 752.03, Found 752.23.

1j: (95%) mp 170-172 °C, IR (KBr) ν_{\max} 3446, 1761, 1678, 1625, 1519, 1334 cm^{-1} . 1H -NMR (500 MHz, $CDCl_3$) δ 8.48 (1H, bs), 7.52 (2H, m), 7.47 (1H, d, $J = 7.5$ Hz), 7.39 (1H, d, $J = 9.5$ Hz), 7.25 (1H, m), 5.36 (1H, s), 4.81 (2H, t), 4.37 (2H, bs), 4.13 (2H, t), 1.86 (2H, m), 1.51 (2H, m), 1.01 (3H, t); ^{13}C NMR (125 MHz, $CDCl_3$) δ 193, 186, 185, 173, 151, 139, 133, 131, 128, 124, 123, 114, 99, 86, 73, 58, 49, 32, 18, 13; FAB-MS m/z Calcd for $C_{20}H_{21}NO_4$ 340.39 (M+1), Found 340.45.

1k: (88%) mp 230-232 °C; IR (KBr) ν_{\max} 1759, 1680, 1629, 1523, 1467, 1328 cm^{-1} ; 1H -NMR (500 MHz, $DMSO-d_6$) δ 8.35 (1H, bs), 7.83 (1H, s), 7.68 (1H, d, $J = 9.5$ Hz), 7.61-7.56 (2H, m), 5.42 (1H, s), 4.78 (2H, t), 4.37-4.24 (4H, m), 1.78 (2H, m), 1.41 (2H, m), 0.92 (3H, t); ^{13}C NMR (125 MHz, $DMSO-d_6$) δ 193, 186, 184, 172, 150, 139, 133, 132, 130, 125, 124, 118, 115, 94, 86, 73, 57, 31, 18, 13; FAB-MS m/z Calcd for $C_{20}H_{20}BrNO_4$ 418.28, Found 418.74.

2.6.8. General Procedure for Synthesis of Semisquaraine Dyes 2a-k

A mixture of the corresponding quinaldinium salt (0.06 mmol), squaric acid (0.06 mmol) and quinoline (0.5 mL) was refluxed in a mixture of *n*-butanol and benzene (6 mL each, 1:1) with azeotropic distillation of

water for 12 h. The solvent was distilled off under reduced pressure to obtain a residue which was chromatographed over silica gel. Elution of the column with a mixture (1:9) of methanol and chloroform gave the semisquaraine derivatives **2a,b,e,f,h-k**.

2a: (95%) mp 150-152 °C; IR (KBr) ν_{\max} 3412, 3042, 2963, 1761, 1606 cm^{-1} . $^1\text{H-NMR}$ (300 MHz, $\text{CDCl}_3+\text{DMSO-d}_6$, 1:4) δ 10.06 (1H, OH), 9.29 (1H, d, $J = 11.4$ Hz), 7.89 (1H, d, $J = 9.3$ Hz), 7.73 (1H, d, $J = 9.4$ Hz), 7.34 (1H, d, $J = 9.3$ Hz), 7.17 (1H, s), 6.16 (1H, s), 4.64 (2H, t, $J = 6.5$ Hz), 4.11 (3H, s), 1.78 (2H, m), 1.45 (2H, m), 0.93 (3H, m). $^{13}\text{C NMR}$ (DMSO-d_6 , 1:4) δ 185, 177, 175, 171, 155, 152, 137, 132, 127, 124, 123, 119, 111, 95, 70, 37, 31, 18, 13; FAB-MS m/z Calcd for $\text{C}_{19}\text{H}_{19}\text{NO}_4$ 325.139, Found 325.140.

2b: (90%) mp 184-186 °C; IR (KBr) ν_{\max} 3016, 2923, 1760, 1602 cm^{-1} . $^1\text{H-NMR}$ (500 MHz, CDCl_3) δ 9.45 (1H, d, $J = 9.3$ Hz), 7.84 (1H, d, $J = 9.3$ Hz), 7.63 (1H, d, $J = 9.4$ Hz), 7.33 (1H, d, $J = 9.5$ Hz), 7.09 (1H, s), 6.15 (1H, s), 4.71 (2H, t, $J = 6.6$ Hz), 4.14 (2H, t, $J = 6.9$ Hz), 4.05 (3H, s), 1.78 (5H, m), 1.49 (2H, m), 0.96 (3H, m). $^{13}\text{C NMR}$ (CDCl_3) δ 184, 176, 174, 170, 156, 153, 136, 126, 125, 122, 117, 109, 94, 71, 63, 37, 31, 18, 14, 13, 13; FAB-MS m/z Calcd for $\text{C}_{21}\text{H}_{23}\text{NO}_4$ 353.163, Found 353.164; Anal. Calcd; C, 71.37; H, 6.56; N, 3.96. Found: C, 71.02; H, 7.12; N, 4.24.

2e: (88%) mp 210-212 °C; IR (KBr) ν_{\max} 3412, 1762, 1726, 1597, 1354 cm^{-1} ; $^1\text{H-NMR}$ (300 MHz, CDCl_3) δ 9.43 (1H, d, $J = 9.33$ Hz), 7.86 (1H, d,

J = 9.3 Hz), 7.66 (1H, d, J = 9.47 Hz), 7.36 (1H, d, J = 9.43 Hz), 7.11 (1H, s), 6.14 (1H, s), 4.72 (2H, t), 4.20 (4H, m), 4.04 (3H, s), 2.57 (2H, t), 2.20 (2H, t), 1.83 (2H, t), 1.52 (2H, t), 1.29 (3H, t), 0.98 (3H, t); δ 198, 176, 172, 171, 169, 163, 161, 158, 152, 142, 134, 130, 127, 121, 108, 98, 72, 67, 59, 31, 29, 23, 18, 14, 13; FAB-MS m/z Calcd for $C_{25}H_{29}NO_6$ 439.50, Found 439.05.

2f: (85%) mp 152-154 °C; IR (KBr) ν_{\max} 2964, 1762, 1710, 1570, 1346, 1257 cm^{-1} ; 1H -NMR (300 MHz, $CDCl_3$) δ 9.23 (1H, d, J = 9.27 Hz), 8.05 (1H, d, J = 8.36 Hz), 7.89 (1H, d, J = 9.18 Hz), 7.73 (2H, m), 7.12 (1H, s), 6.15 (1H, s), 4.52 (4H, m), 4.17 (3H, s), 2.59 (2H, m), 2.22 (2H, m), 1.78 (2H, m), 1.45 (2H, m), 0.97 (3H, m); ^{13}C NMR (125 MHz, $DMSO-d_6$) δ 185, 177, 175, 173, 172, 156, 152, 137, 133, 126, 124, 123, 119, 109, 99, 95, 79, 70, 67, 66, 60, 37, 34, 31, 30, 29, 28, 24, 18, 18, 13, 13; FAB-MS m/z Calcd for $C_{23}H_{25}NO_6$ 412.45 (M+1), Found 412.35.

2h: (95%) mp 231-233 °C, IR (KBr) ν_{\max} 3126, 1759, 1618, 1564, 1442, 1224 cm^{-1} ; 1H NMR (CD_3OD) δ 9.01 (1H, s), 8.02 (1H, d, J = 9.5 Hz), 7.42 (1H, d, J = 9.5 Hz), 7.33 (1H, s), 6.19 (1H, s), 4.54 (2H, t), 4.18 (3H, s), 2.68 (3H, s), 1.78 (2H, m), 1.50 (2H, m), 1.00 (3H, t); ^{13}C NMR (125 MHz, $DMSO-d_6$) δ 185, 177, 175, 171, 155, 151, 145, 132, 127, 124, 122, 119, 116, 97, 79, 71, 31, 19, 18, 13; FAB-MS m/z Calcd for $C_{20}H_{21}NO_4$ 340.01 (M+1), Found 340.50.

2i: (80%) mp 228-230 °C, IR (KBr) ν_{\max} 2953, 1761, 1604, 1558, 1471, 1247 cm^{-1} ; ^1H NMR (500 MHz, CDCl_3) δ 9.26 (1H, s), 7.70-7.53 (3H, m), 6.32 (1H, s), 5.37 (1H, s), 4.66 (2H, m), 4.01 (3H, s), 2.60-0.61 (52H, m); ^{13}C NMR (125 MHz, CDCl_3) δ 189, 178, 178, 176, 154, 152, 148, 138, 136, 126, 126, 125, 123, 117, 117, 95, 79, 76, 72, 56, 56, 50, 42, 39, 39, 37, 37, 36, 36, 36, 35, 32, 31, 31, 28, 28, 27, 24, 23, 22, 22, 21, 19, 19, 18, 18, 13, 11; FAB-MS m/z Calcd for $\text{C}_{48}\text{H}_{65}\text{NO}_6$ 752.03, Found 752.37.

2j: (90%) mp 182-184 °C; IR (KBr) ν_{\max} 3330, 1761, 1593, 1560, 1342 cm^{-1} ; ^1H -NMR (500 MHz, CDCl_3) δ 9.36 (1H, d, $J = 9$ Hz), 7.95 (2H, d, $J = 9$ Hz), 7.78 (2H, d, $J = 10$ Hz), 7.53 (1H, m), 6.34 (1H, s), 4.75 (2H, t), 4.58 (2H, t), 4.24 (2H, t), 1.78 (2H, t), 1.46 (2H, m), 0.96 (3H, t); ^{13}C NMR (CD_3OD) δ 184, 181, 178, 172, 156, 140, 134, 130, 128, 123, 121, 119, 97, 73, 60, 52, 33, 19, 18, 14; FAB-MS m/z Calcd for $\text{C}_{20}\text{H}_{21}\text{NO}_4$ 340.39 (M+1), Found 340.45.

2k: (90%) mp 208-210 °C; IR (KBr) ν_{\max} 3062, 1764, 1597, 1554, 1435, 1350 cm^{-1} ; ^1H -NMR (500 MHz, CDCl_3) δ 9.1 (1H, d, $J = 9.5$ Hz), 7.9-7.5 (4H, m), 6.36 (1H, s), 4.7 (2H, t), 4.6 (2H, t), 4.25 (2H, t), 1.77 (2H, t), 1.46 (2H, m), 0.96 (3H, t); ^{13}C NMR (DMSO-d_6) δ 187, 182, 178, 171, 159, 146, 139, 131, 126, 125, 124, 111, 108, 93, 68, 49, 31, 19, 18, 14; FAB-MS m/z Calcd for $\text{C}_{20}\text{H}_{20}\text{BrNO}_4$ 419.28 (M+1), Found 419.74.

2.6.9. Synthesis of semisquaric acid **8**

A solution of **1b** or **2b** (1 mmol) in 5 mL acetic acid:water:2N HCl (50:50:4) is stirred for 4 h at room temperature. The resulting solution was extracted with CHCl₃ to give 30% of **8**. mp > 300 °C; IR (KBr) ν_{\max} 3095, 1753, 1602, 1562, 1492, 1363 cm⁻¹; ¹H-NMR (300 MHz, CDCl₃) δ 8.72 (1H, d, J = 9.6 Hz), 7.17 (1H, d, J = 8.6 Hz), 6.95 (3H, m), 5.10 (1H, s), 4.54 (3H, s), 4.27 (2H, m), 1.35 (3H, t); FAB-MS m/z Calcd for C₁₇H₁₅NO₄ 298.31 (M+1), Found 298.10.

2.6.10. Synthesis of unsymmetrical squaraine dye **7**

A solution of 1 mmol of **2b/8** is refluxed with 1 mmol of 6-iodo-*N*-methyl-2-quinaldinium iodide in 1:1 butanol:benzene (5 mL) at 100 °C for 12 h. The solvent was distilled off under reduced pressure to obtain a residue which was chromatographed over silica gel. Elution of the column with a mixture (1:9) of methanol and chloroform gave the unsymmetrical squaraine dye **7**. (90%) mp >300 °C; IR (KBr) ν_{\max} 2922, 1614, 1564, 1485, 1317 cm⁻¹; ¹H NMR (500 MHz, CDCl₃) δ 9.35 (1H, d, J = 9.5 Hz), 9.21 (1H, d, J = 9.5 Hz), 7.47-6.93 (8H, m), 5.82 (1H, s), 5.72 (1H, s), 4.11 (2H, m), 3.85 (3H, s), 3.70 (3H, s), 1.46 (3H, t); FAB-MS m/z Calcd for C₂₈H₂₃IN₂O₃ 563.40 (M+1), Found 563.21.

2.7. REFERENCES

1. (a) Grynyov, R. S.; Sorokin, A. V.; Guralchuk, G. Y.; Yefimova, S. L.; Borovoy, I. A.; Malyukin, Y. V. *J. Phys. Chem. C* **2008**, *112*, 20458. (b) Odom, S. A.; Webster, S.; Padiha, L. A.; Peceli, D.; Hu, H.; Nootz, G.; Chung, S.-J.; Ohira, S.; Matichak, J. D.; Przhonska, O. V.; Kachkovski, A. D.; Barlow, S.; Bredas, J.-L.; Anderson, H. L.; Hagan, D. J.; Stryland, E. W. V.; Marder, S. R. *J. Am. Chem. Soc.* **2009**, *131*, 7510.
2. (a) Law, K. Y. *J. Phys. Chem.* **1987**, *91*, 5184. (b) Law, K. Y.; Bailey, F. C. *J. Org. Chem.* **1992**, *57*, 3278. (c) Law, K. Y. *Chem. Rev.* **1993**, *93*, 449.
3. Emmelius, M.; Pawlowski, G.; Vollmann, H. W. *Angew. Chem.* **1989**, *101*, 1475.
4. Smits, E. C. P.; Setayesh, S.; Anthopoulos, T. D.; Buechel, M.; Nijssen, W.; Coehoorn, R.; Blom, P. W. M.; de Boer, B.; de Leeuw, D. M. *Adv. Mater.* **2007**, *19*, 734.
5. (a) Matsui, M.; Nagasaka, K.; Tokunaga, S.; Funabiki, K.; Yoshida, T.; Minoura, H. *Dyes Pigments* **2003**, *58*, 219. (b) Yum, J.-H.; Walter, P.; Huber, S.; Rentsch, D.; Geiger, T.; Nuesch, F.; De Angelis, F.; Gratzel, M.; Nazeeruddin, M. K. *J. Am. Chem. Soc.* **2007**, *129*, 10320. (c) Burke, A.; Schmidt-Mende, L.; Ito, S.; Graetzel, M. *Chem. Commun.* **2007**, *3*, 234. (d) Ohira, S.; Rudra, I.; Schmidt, K.; Barlow, S.; Chung, S.-J.; Zhang, Q.; Matichak, J.; Marder, S. R.; Bredas, J.-L. *Chem. Eur. J.* **2008**, *14*, 11082.

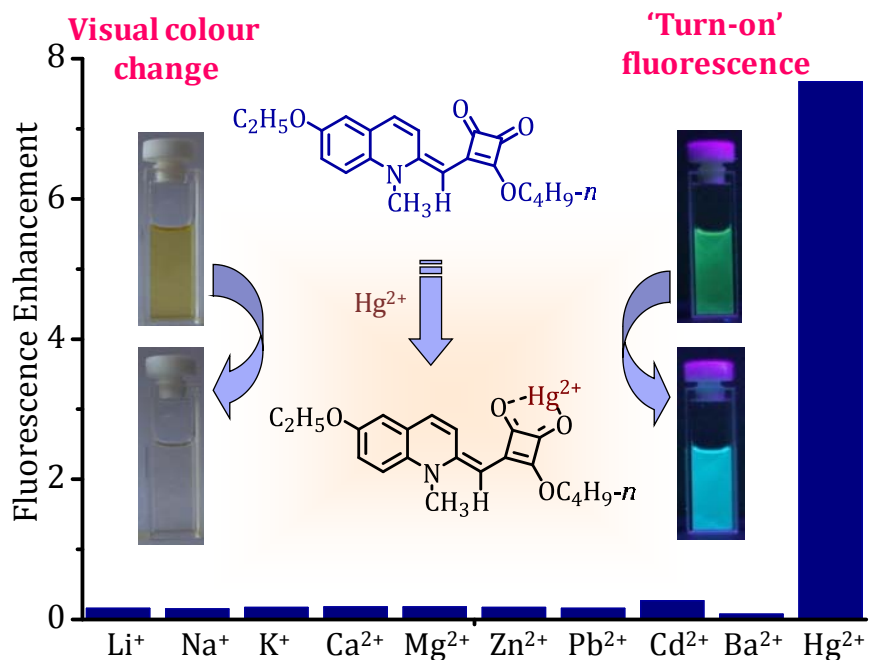
- (d) Silvestri, F.; Irwin, M. D.; Beverina, L.; Facchetti, A.; Pagani, G. A.; Marks, T. J. *J. Am. Chem. Soc.* **2008**, *130*, 17640. (e) Silvestri, F.; Irwin, M. D.; Beverina, L.; Facchetti, A.; Pagani, G. A. *J. Am. Chem. Soc.* **2008**, *130*, 17640.
6. (a) Chen, C.-T.; Marder, S. R.; Cheng, L. T. *Chem. Commun.* **1994**, 259. (b) Chen, C.-T.; Marder, S. R.; Cheng, L. T. *J. Am. Chem. Soc.* **1994**, *116*, 3117. (c) Meyers, F.; Chen, C.-T.; Marder, S. R.; Bredas, J.-L. *Chem. Eur. J.*, **1997**, *3*, 530. (d) Beverina, L.; Crippa, M.; Salice, P.; Ruffo, R.; Ferrante, C.; Fortunati, I.; Signorini, R.; Mari, C. M.; Bozio, R.; Facchetti, A.; Pagani, G. A. *Chem. Mater.* **2008**, *20*, 3242.
7. (a) Oswald, B.; Patsenker, L.; Duschl, J.; Szmecinski, H.; Wolfbeis, O. S.; Terpetschnig, E. *Bioconjugate Chem.* **1999**, *10*, 925. (b) Arun, K. T.; Ramaiah, D. *J. Phys. Chem. A* **2005**, *109*, 5571. (c) Basheer, M. C.; Santhosh, U. Alex, S.; Thomas, K. G.; Suresh, C. H.; Das, S. *Tetrahedron* **2007**, *63*, 1617. (d) Reddington, M. V. *Bioconjugate Chem.* **2007**, *18*, 2178.
8. (a) Meier, H.; Dullweber, U. *J. Org. Chem.* **1997**, *62*, 4821. (b) Yagi, S.; Hyodo, Y.; Matsumoto, S.; Takahashi, N.; Kono, H.; Nakazumi, H. *J. Chem. Soc., Perkin Trans. 1*, **2000**, 599. (c) Ajayaghosh, A. *Acc. Chem. Res.* **2005**, *38*, 449. (d) Arunkumar, E.; Fu, N.; Smith, B. D. *Chem. Eur. J.* **2006**, *12*, 4684. (e) Johnson, J. R.; Fu, N.; Arunkumar, E.; Leevy, W. M.;

- Gammon, S. T.; Piwnica-Worms, D.; Smith, B. D. *Angew. Chem., Int. Ed.* **2007**, *46*, 5528.
9. (a) Ros-Lis, J. V.; Garca, B.; Jimnez, D.; Martnez-Mez, R.; Sancenn, F.; Soto, J.; Gonzalvo, F.; Valldecabres, M. C. *J. Am. Chem. Soc.* **2004**, *126*, 4064. (b) Basheer, M. C.; Alex, S.; Thomas, K. G.; Suresh, C. H.; Das, S. *Tetrahedron* **2006**, *62*, 605. (c) Jisha, V. S.; Arun, K. T.; Hariharan, H.; Ramaiah, D. *J. Am. Chem. Soc.* **2006**, *128*, 6024. (d) Avirah, R. R.; Jyothish, K.; Ramaiah, D. *Org. Lett.* **2007**, *9*, 121. (e) Thomas, J.; Sherman, D. B.; Amiss, T. J.; Andaluz, S. A.; Pitner, J. B. *Bioconjugate Chem.* **2007**, *18*, 1841. (f) Sreejith, S.; Divya, K. P.; Ajayaghosh, A. *Angew. Chem.* **2008**, *120*, 8001. (g) Ros-Lis, J. V.; Martinez-Manez, R.; Sancenon, F.; Soto, Spielles, M.; Rurack, K. *Chem. Eur. J.* **2008**, *14*, 10101. (h) Sreejith, S.; Carol, P.; Chithra, P.; Ajayaghosh, A. *J. Mater. Chem.* **2008**, *18*, 264. (i) Climent, E.; Calero, P.; Marcos, M. D.; Martinez-Manez, R.; Sancenon, F.; Soto, J. *Chem. Eur. J.* **2009**, *15*, 1816.
10. Liu, L.-H.; Nakatani, K.; Pansu, R.; Vachan, J.-J.; Tauc, P.; Ishow, E. *Adv. Mater.* **2007**, *19*, 433.
11. (a) Ramaiah, D.; Eckert, I.; Arun, K. T.; Weidenfeller, L.; Epe, B. *Photochem. Photobiol.* **2002**, *76*, 672. (b) Ramaiah, D.; Eckert, I.; Arun, K. T.; Weidenfeller, L.; Epe, B. *Photochem. Photobiol.* **2004**, *79*, 99. (c) Jisha, V. S.; Arun, K. T.; Hariharan, M.; Ramaiah, D. *J. Am. Chem. Soc.*

- 2006**, *128*, 6024. (d) Beverina, L.; crippa, M.; Landenna, M.; Ruffo, R.; Salice, P.; Silvestri, F.; Versari, S.; Villa, A.; Ciaffoni, L.; Collini, E.; Ferrante, C.; Bradamante, S.; Mari, C. M.; Bozio, R.; Pagani, G. A. *J. Am. Chem. Soc.* **2008**, *130*, 1894.
12. (a) Scherer, D.; Dorfler, R.; Feldner, A.; Vogtmann, T.; Schwoerer, M.; Lawrentz, U.; Grahn, W.; Lambert, C. *Chem. Phys.* **2002**, *279*, 179. (b) Chung, S. J.; Zheng, S.; Odani, T.; Beverina, L.; Fu, J.; Padiha, L.; Biesso, A.; Hales, J. M.; Zhan, X.; Schmidt, K.; Ye, A.; Zojer, E.; Barlow, S.; Hagan, D. J.; Stryland, E. W. V.; Yi, Y.; Shuai, Z.; Pagani, G. A.; Bredas, J.-L.; Perry, J. W.; Marder, S. R. *J. Am. Chem. Soc.* **2006**, *128*, 14444. (c) Ohira, S.; Rudra, I.; Schmidt, K.; Barlow, S.; Chung, S.-J.; Zhang, Q.; Matichak, J.; Marder, S. R.; Bredas, J.-L. *Chem. Eur. J.* **2008**, *14*, 11082.
13. Renard, B.-L.; Aubert, Y.; Asseline, U. *Tetrahedron Lett.* **2009**, *50*, 1897.
14. (a) Cornelissen-Gude, C.; Rettig, W.; Lapouyade, R. *J. Phys. Chem.* **1997**, *101*, 9673. (b) Momicchioll, F.; Tatlkolov, A. S.; Vanossi, D.; Ponterini, G. *Photochem. Photobiol. Sci.* **2004**, *3*, 396.
15. Keil, D.; Hartmann, H. *Dyes Pigments* **2001**, *49*, 161.
16. (a) Stanescu, M.; Samha, H.; Perlstein, J.; Whitten, D. G. *Langmuir* **2000**, *16*, 275. (b) Yagi, S.; Nakai, K.; Hyodo, Y.; Nakazumi, H. *Synthesis* **2002**, *3*, 413. (c) Kim, J. J.; Funabiki, K.; Shiozaki, H.; Matsui, M. *Dyes Pigments* **2003**, *57*, 165. (d) Block, M. A. B.; Khan, A.; Hecht, S. *J. Org. Chem.* **2004**,

- 69, 184. (e) Tatarets, A. L.; Fedyunyaeva, I. A.; Terpetschnig, E.; Patsenker, L. D. *Dyes Pigments* **2005**, *64*, 125.
17. Xie, J.; Comeau, A. B.; Seto, C. T. *Org. Lett.* **2004**, *6*, 83.
18. (a) Jyothish, K.; Arun, K. T.; Ramaiah, D. *Org. Lett.* **2004**, *6*, 3965. (b) Jyothish, K.; Avirah, R. R.; Ramaiah, D. *Org. Lett.* **2006**, *8*, 111. (c) Jyothish, K.; Avirah, R. R.; Ramaiah, D. *Arkivoc* **2007**, *8*, 296. (d) Jyothish, K.; Hariharan, H.; Ramaiah, D. *Chem. Eur. J.* **2007**, *13*, 5944.
19. X-ray analysis was carried out at Sophisticated Analytical Instrument Facility, Indian Institute of Technology Madras, Chennai, India. The crystal was grown by the slow evaporation of the solvent in a 3:1 dichloromethane: ether mixture.
20. (a) Jyothish, K.; Hariharan, M.; Ramaiah, D. *Chem. Eur. J.* **2007**, *13*, 5944. (b) Kuruvilla, E.; Ramaiah, D. *J. Phys. Chem. B* **2007**, *111*, 6549. (c) Neelakandan, P. P.; Ramaiah, D. *Angew. Chem. Int. Ed.* **2008**, *47*, 8407. (d) Nair, A. K.; Neelakandan, P. P.; Ramaiah, D. *Chem. Commun.* **2009**, 6352.
21. Jha, B. N.; Banerji, J. C. *Dyes Pigments* **1983**, *4*, 77.

CHAPTER 3. NOVEL SEMISQUARAINES AND STUDY OF THEIR INTERACTIONS WITH MONO- AND DIVALENT METAL IONS



3.1. ABSTRACT

With the objective of evaluating the ability of the semisquaraine dyes as molecular probes, we have investigated the interaction of these dyes with various mono- and divalent metal ions. Due to the presence of highly electron rich carbonyl groups, both the E- and Z-isomers of the semisquaraine dyes **1** and **2** can function as bidentate ligands for various metal ions. Addition of mercuric ions to these semisquaraine dyes resulted in colour change as well as significant enhancement in fluorescence intensity in acetone. Interestingly, both these dyes (E- and Z- isomers)

show selective reversible interactions with mercuric ions, while negligible interactions were observed with other biologically and environmentally relevant mono- and divalent metal ions. Jobs plot analysis of the complexation showed that the semisquaraine dye **2a** showed a 1:1 binding stoichiometry, while its isomer **1a** formed both 1:1 as well as 2:1 complexes under similar conditions. Notably, of the two dyes, **1a** showed a higher binding affinity of $2.4 \pm 0.1 \times 10^5 \text{ M}^{-1}$ towards the Hg^{2+} ions as compared to **2a** which showed a binding affinity of $2.2 \pm 0.1 \times 10^4 \text{ M}^{-1}$. ^1H NMR and IR spectral analysis confirms that the binding of the semisquaraine dyes with the mercuric ions involves the participation of the carbonyl groups of the squaryl moiety. These studies demonstrate that the semisquaraine dyes can function as efficient probes for mercuric ions and signal the complexation event through visual colour change as well as 'turn-on' fluorescence intensity.

3.2. INTRODUCTION

Optical probes for the sensing and reporting of chemical species are of significant importance in chemical, biological and environmental sciences.¹ Of particular interest has been the development of specific probes for the detection of transition or heavy metal ions because they play important roles in living systems and have an extremely toxic impact on

the environment.² In this regard, the selective detection of Hg^{2+} ions gains increasing attention owing to the inherent toxicity of the Hg^{2+} ions which can result in severe environmental and human health hazards.³

Inorganic mercury, Hg° and Hg^{2+} ions, are released into the environment through a variety of anthropogenic and natural sources. The United States Environmental Protection Agency has mandated an upper limit of 2 ppb for Hg^{2+} ions in drinking water.^{3d} A fraction of Hg^{2+} ions is reduced to Hg° or methylmercury (CH_3HgX species), which gets biomagnified in the food chain.^{2c-f} Neurological problems associated with methylmercury intoxication include prenatal brain damage, cognitive and motion disorders, vision and hearing loss and death. At the molecular and cellular levels, methylmercury causes oxidative stress^{3e} and lipid peroxidation,^{3f} and it inhibits the division and migration of neurons. It accumulates in astrocytes, preventing glutamate uptake, and thereby causes excitotoxic injury to neurons.^{3g,3h} Inorganic mercury targets the renal epithelial cells of the kidney, causing tubular necrosis and proteinuria.^{3i,3j} It is also a neurotoxin and causes immune system dysfunction.^{3k} The Minamata disaster in Japan²ⁱ as well as the epidemic in Iraq^{2j} are indicative of the disastrous effects of mercury intoxication.

The recognition of toxic Hg^{2+} ions through optical methods has been an area of intense research in recent years. A number of reported Hg^{2+} sensors employing dual mode recognition in the aqueous medium employ

rhodamine based systems, where the initially colourless and non-fluorescent spirolactam ring undergoes ring opening to form the highly coloured and emissive open form.⁴ Modification of this framework with various receptor groups has afforded a number of Hg²⁺ ion probes.⁵ A few examples are shown in Chart 3.1.⁶ However, lack of solubility in the aqueous medium prevents the use of most of these sensors for the detection of Hg²⁺ ions.⁷

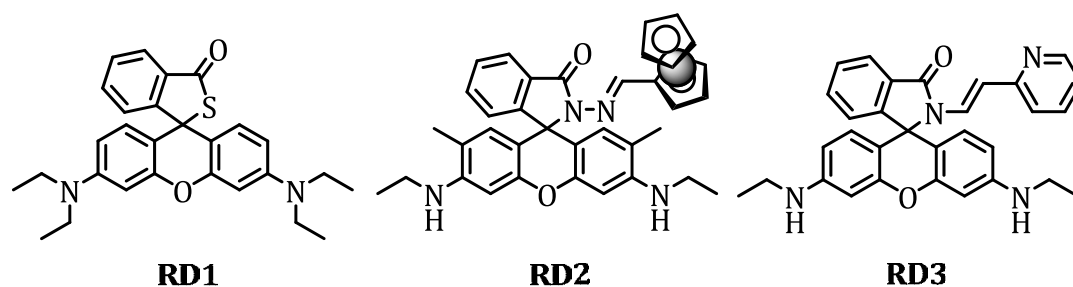
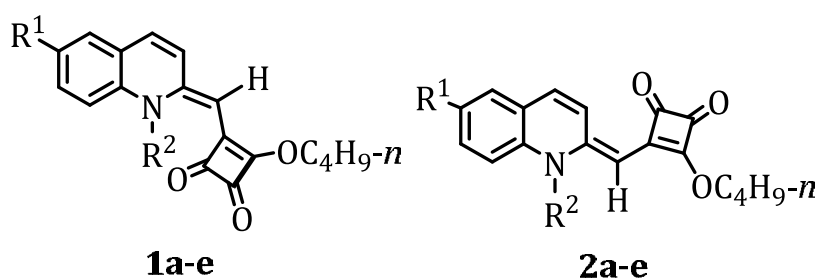


Chart 3.1

A number of selective probes for Hg²⁺ ions have been devised using redox, chromogenic or fluorogenic changes.⁸ Among these, fluorescence monitoring has received great interest because of the simplicity, selectivity, and sensitivity of the technique.⁹ In particular, the design of sensors that give fluorescence enhancement upon binding to Hg²⁺ ions is an intriguing challenge, since Hg²⁺ ions, like many heavy elements, can cause fluorescence quenching.¹⁰ Restriction of such 'turn-on' Hg²⁺ sensors to aqueous environments introduces additional complexity.¹¹ Moreover, the

development of specific probes for Hg^{2+} ions employing multichannel sensing is still a challenge.¹²

In this context, it was of our interest to investigate the interactions of semisquaraine dyes with metal ions and evaluate their potential as probes for metal ions. These systems are characterized by high electron density at the carbonyl group. Hence, these systems can, in principle, act as bidentate ligands for metal ions. Chart 3.2 shows the different semisquaraine derivatives that we have investigated. Of these, two semisquaraine dyes **1a** and **2a** have been chosen for detailed investigation as representatives of each class of isomers due to their higher solubility and stability (Chart 3.2). Our results indicate that, these two semisquaraine dyes bind selectively to Hg^{2+} ions as compared to other mono- and divalent metal ions. Of the two



- a)** $\text{R}^1 = \text{OC}_2\text{H}_5$, $\text{R}^2 = \text{CH}_3$
b) $\text{R}^1 = \text{OH}$, $\text{R}^2 = \text{CH}_3$
c) $\text{R}^1 = \text{O}(\text{CH}_2)_3\text{COOH}$, $\text{R}^2 = \text{CH}_3$
d) $\text{R}^1 = \text{H}$, $\text{R}_2 = \text{H}$, $\text{R}^2 = \text{CH}_2\text{CH}_2\text{OH}$
e) $\text{R}^1 = \text{Br}$, $\text{R}_2 = \text{H}$, $\text{R}^2 = \text{CH}_2\text{CH}_2\text{OH}$

Chart 3.2

isomeric systems, **1** showed one order higher binding affinity towards the Hg²⁺ ions as compared to **2**. Uniquely, such binding event was signaled through 'turn-on' fluorescence intensity, thereby demonstrating the potential of the dyes **1** and **2** as selective probes for the detection of Hg²⁺ ions.

3.3. RESULTS

3.3.1. Synthesis and Photophysical Properties

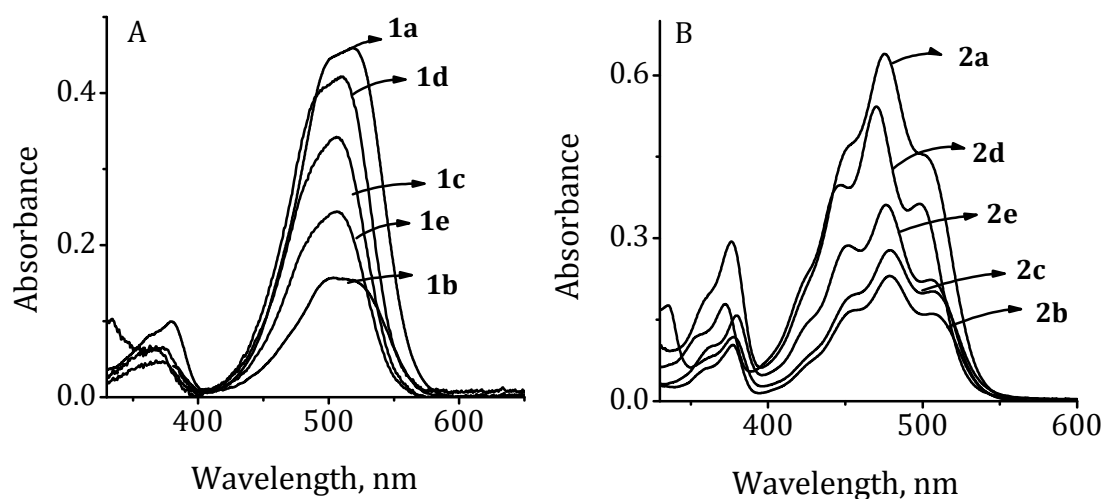
The synthesis of the semisquaraine dyes, **1a-e** and **2a-e** has been achieved, as described in Chapter 2 of the thesis, by the reaction between the corresponding quinaldinium salt and squaric acid/dibutyl squarate, respectively. These semisquaraine dyes exhibited good solubility in various organic solvents with absorption in the range 450-540 nm and molar extinction coefficients of $1-6 \times 10^4 \text{ M}^{-1}\text{cm}^{-1}$. The photophysical properties of these dyes are summarized in Table 3.1.

The absorption properties of the semisquaraines were found to be independent of the substituent present at the 6-position of the quinoline ring. For example, the ethoxy substituted semisquaraine derivative **1a** showed the absorption maximum at 515 nm in chloroform, while the absorption maximum of the semisquaraine derivative **1c** is at 508 nm (Figure 3.1). Compared to the Z-isomer, the E-isomer (**2a-e**) showed blue-

Table 3.1. Photophysical properties of the semisquaraine dyes.^a

No	Z-isomer	λ_{\max} (nm)	ϵ (M ⁻¹ cm ⁻¹)	E-isomer	λ_{\max} (nm)	ϵ (M ⁻¹ cm ⁻¹)
1	1a^b	478	2.93 x 10 ⁴	2a^b	476	1.91 x 10 ⁴
2	1b^b	479	4.12 x 10 ⁴	2b^b	475	1.90 x 10 ⁴
3	1c^c	501	3.21 x 10 ⁴	2c^c	478	9.23 x 10 ³
4	1d^d	509	3.43 x 10 ⁴	2d^d	471	5.81 x 10 ⁴
5	1e^d	512	2.23 x 10 ⁴	2e^d	475	5.83 x 10 ⁴

^aThe data are the average of more than two independent experiments and the error is ca. $\pm 5\%$. ^bCH₃OH. ^cDMSO. ^dCHCl₃.

**Figure 3.1.** Absorption spectra of the dyes in CHCl₃ (A) **1a-e** (B) **2a-e**.

shifted and vibrationally resolved absorption spectrum. For example, the ethoxy substituted dye **2a** has an absorption maximum at 476 nm in

chloroform, while the acid derivative **2c** exhibited absorption at 478 nm. All the semisquaraine derivatives were found to have negligible fluorescence quantum yields in the solution state.

3.3.2. Interactions of Semisquaraine Dyes with Metal Ions

The interaction of semisquaraine dyes **1a-e** and **2a-e** have been studied with various mono- and divalent metal ions in the organic and aqueous media in presence of micelles. Interestingly, it was observed that these semisquaraine dyes, showed an increase in fluorescence intensity upon complexation with mercuric ions. Figures 3.2 and 3.3 show the

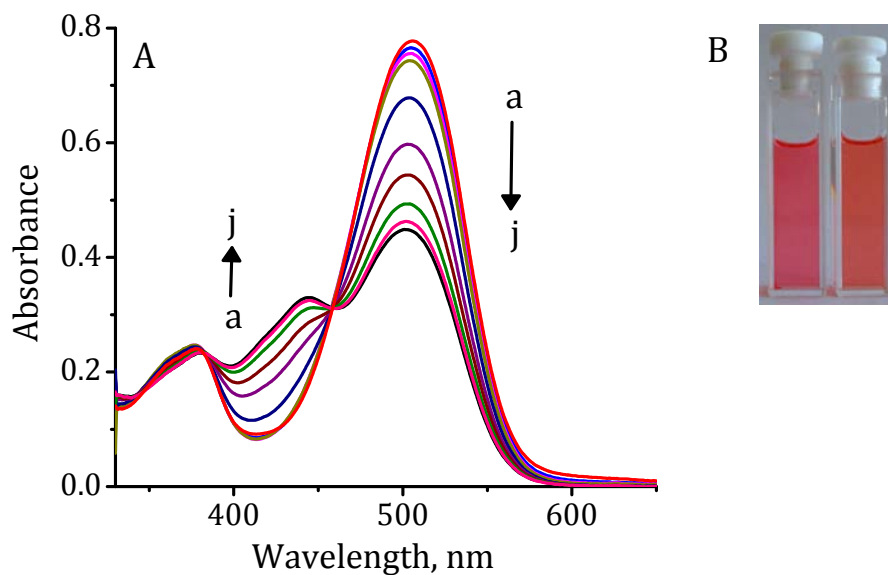


Figure 3.2. (A) Absorption spectra of **1a** (26.5 μM) in acetone with increase in concentration of $\text{Hg}(\text{ClO}_4)_2$. [$\text{Hg}(\text{ClO}_4)_2$]: a) 0 and j) 26.5 μM. (B) Photograph showing the visual colour change of **1a** alone and in the presence of one equivalent of $\text{Hg}(\text{ClO}_4)_2$.

changes in the absorption and emission spectra of the Z-isomer (**1a**) with the addition of Hg^{2+} ions. The solution of **1a** in acetone shows the absorption and emission maximum at 505 and 558 nm, respectively. Upon addition of increasing concentration of Hg^{2+} ions (in water) to **1a** in acetone, a decrease in the absorption at 505 nm was observed with a concomitant increase in absorption at 444 nm through an isosbestic point at 454 nm. After the addition of 0.5 equivalent of Hg^{2+} ions, we observed a shift in the isosbestic point from 454 nm to 455 nm. The changes reach saturation with the addition of 1 equivalent of Hg^{2+} ions. The appearance of the new absorption band at 444 nm as well as the decrease in absorption at

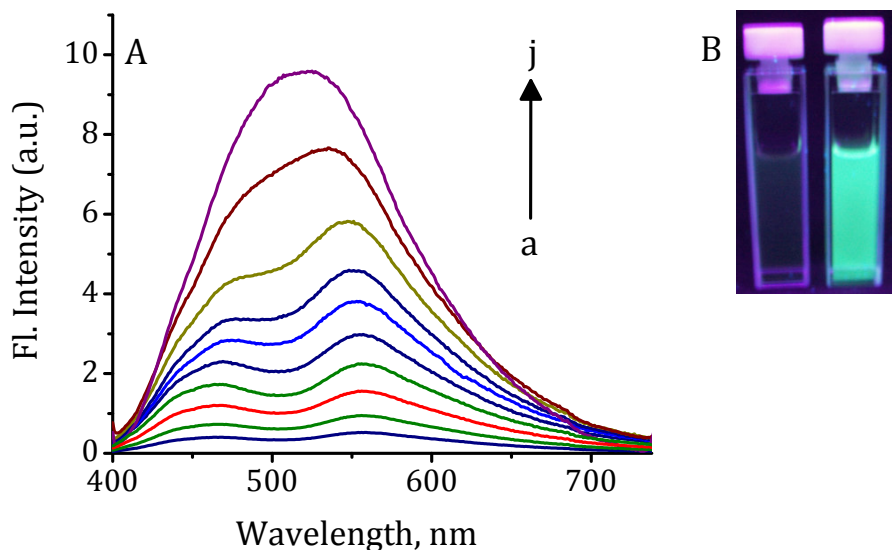


Figure 3.3. Fluorescence spectra of **1a** (26.5 μM) in acetone with increase in concentration of $\text{Hg}(\text{ClO}_4)_2$. [$\text{Hg}(\text{ClO}_4)_2$]: a) 0 and j) 26.5 μM . Excitation wavelength, 389 nm. (B) Photograph showing the visual fluorescence colour change of **2a** alone and in the presence of one equivalent of $\text{Hg}(\text{ClO}_4)_2$.

505 nm enables 'naked eye' detection of Hg^{2+} ions with a colour change from deep red to orange.

The corresponding changes in fluorescence are shown in Figure 3.3. With increasing concentration of Hg^{2+} ions, an enhancement in the fluorescence intensity (*ca.* 18 fold) with a blue shift of ~ 37 nm was observed. Similar observations in the absorption and emission spectra have been made for the dyes **1b-e** in the presence of Hg^{2+} ions, indicating that the Z-isomer of the semisquaraine dyes undergo efficient interactions with the Hg^{2+} ions.

Figure 3.4 shows the changes in the excitation spectra of the dye **1a** with increasing concentration of Hg^{2+} ions. Before the addition of Hg^{2+} ions, the excitation spectrum of the semisquaraine exactly matches with the

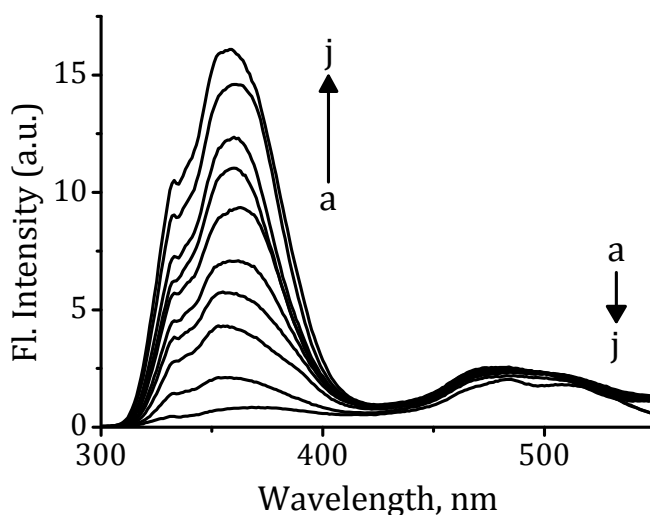


Figure 3.4. Excitation spectra of **1a** ($26.5 \mu\text{M}$) in acetone with the increase in concentration of $\text{Hg}(\text{ClO}_4)_2$. $[\text{Hg}(\text{ClO}_4)_2]$: a) 0 and j) $26.5 \mu\text{M}$.

absorption spectrum. As can be seen from the figure, in the presence of the metal ions, we observed an increase in the absorption at 358 nm and correspondingly an increase in the fluorescence intensity was observed.

Figure 3.5 shows the changes in the absorption spectrum of the E-isomer **2a** with the addition of Hg^{2+} ions. As observed in the case of the Z-isomer, when an aqueous solution of Hg^{2+} ions was added to **2a** in acetone, we observed gradual change in the colour and a significant increase in the fluorescence intensity. **2a** has absorption and emission maxima at 475 and 545 nm, respectively, in acetone. But when a solution of Hg^{2+} ions was added, we observed a decrease in the absorbance and colour change from deep orange to light yellow. In the fluorescence spectrum, we observed *ca.*

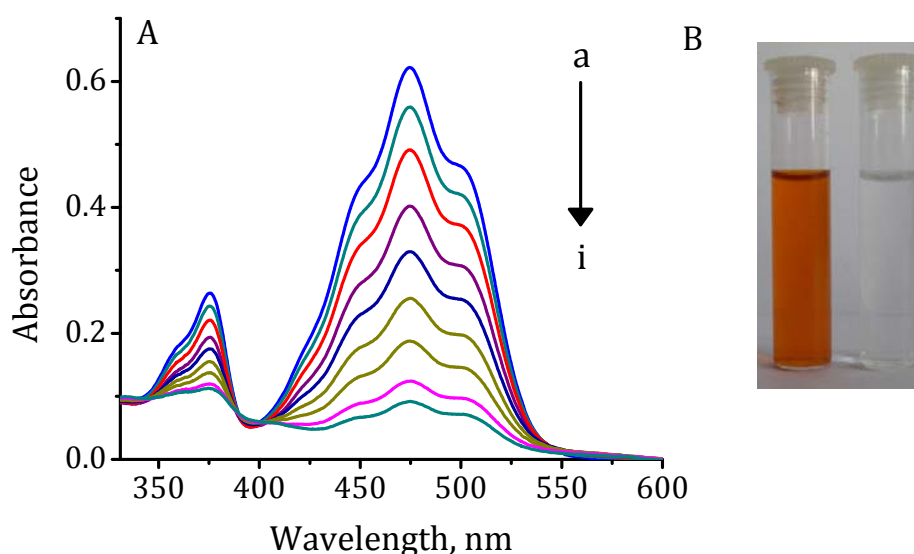


Figure 3.5. (A) Absorption spectra of **2a** (13.6 μM) in acetone with increase in concentration of $\text{Hg}(\text{ClO}_4)_2$. [$\text{Hg}(\text{ClO}_4)_2$]: a) 0 and i) 26.8 μM . (B) Photograph showing the visual colour change of **2a** alone and in the presence of one equivalent of $\text{Hg}(\text{ClO}_4)_2$.

41-fold enhancement in the fluorescence intensity along with a blue shift of ~ 78 nm under similar conditions (Figure 3.6). Similar observations have been made with the dyes **2b-e** in the presence of Hg^{2+} ions.

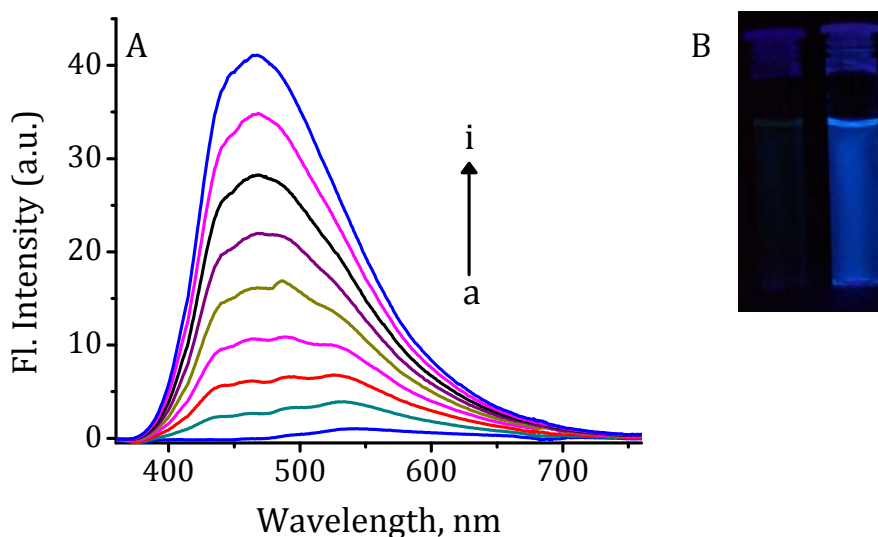


Figure 3.6 emission spectra of **2a** (13.6 μM) in acetone with increase in concentration of $\text{Hg}(\text{ClO}_4)_2$. [$\text{Hg}(\text{ClO}_4)_2$]: a) 0 and i) 26.8 μM . Excitation wavelength, 340 nm. (B) Photograph showing the visual fluorescence colour change of **2a** alone and in the presence of one equivalent of $\text{Hg}(\text{ClO}_4)_2$.

The changes in the excitation spectrum of **2a** with increasing concentration of Hg^{2+} ions are shown in Figure 3.7. Before the addition of mercuric ions, the excitation spectrum of the semisquaraine dye exactly matches with the absorption spectrum. However, with the addition of Hg^{2+} ions, we observed an increase in the band at 366 nm and a corresponding increase in the fluorescence intensity.

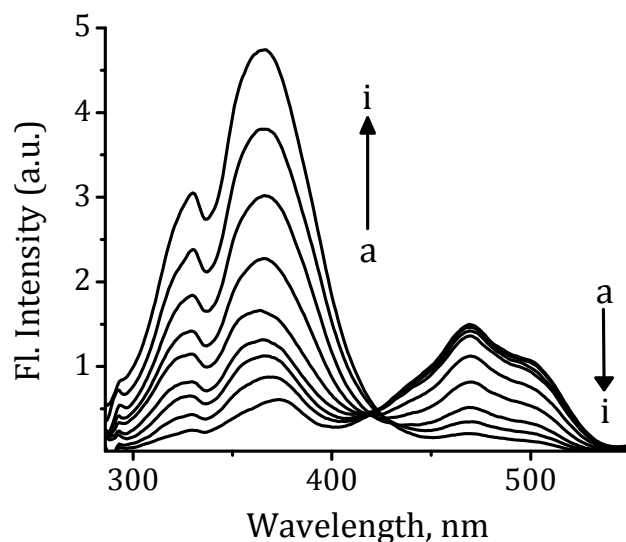


Figure 3.7. Excitation spectra of **2a** (13.6 μM) in acetone with increase in addition of $\text{Hg}(\text{ClO}_4)_2$. [$\text{Hg}(\text{ClO}_4)_2$]: a) 0 and i) 26.8 μM .

3.3.3. Stoichiometry and Reversibility of Complexation

The stoichiometry of the complex formed between the semisquaraine dyes **1a-e** and **2a-e** and Hg^{2+} ions were analyzed through Jobs plot and the binding constant was calculated through Benesi-Hildebrand analysis.¹³ The semisquaraine dye **1a** formed a 2:1 complex in the presence of 0.5 equivalents of Hg^{2+} ions, while a 1:1 complex formation was observed with one equivalent of Hg^{2+} ions. The Benesi-Hildebrand analysis gave an association constant (K) of $2.7 \pm 0.1 \times 10^5 \text{ M}^{-1}$ for the 2:1 complex, whereas it was calculated to be $2.4 \pm 0.1 \times 10^5 \text{ M}^{-1}$ for the 1:1 complex (Figure 3.8). In the case of the E-isomer, we observed a 1:1 stoichiometry with an association constant (K) of $2.2 \pm 0.1 \times 10^4 \text{ M}^{-1}$. These results indicate that

the Z-isomer shows one order higher binding affinity when compared to the E-isomer (Figure 3.9).

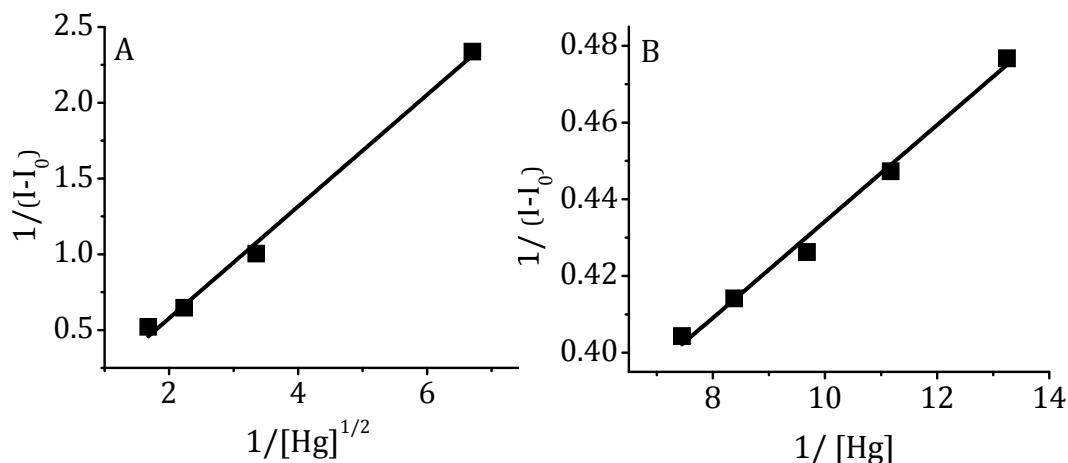


Figure 3.8. Benesi-Hildebrand analysis of the complexation between **1a** with Hg^{2+} ions in acetone for (A) 2:1 complex and (B) 1:1 complex.

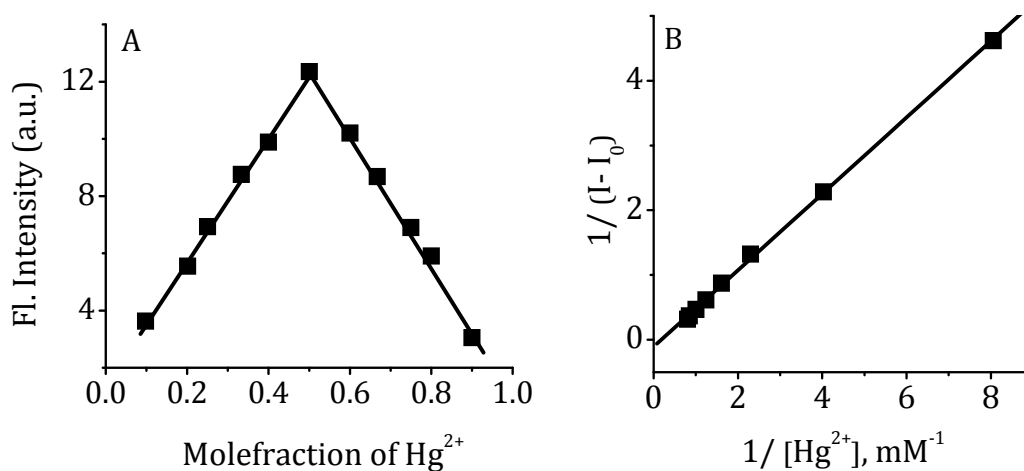


Figure 3.9. (A) Job's plot for the complexation of **2a** with Hg^{2+} ions in acetone. (B) Benesi-Hildebrand analysis of the complexation between **2a** with Hg^{2+} ions in acetone.

To investigate the reversibility of the complexation of the semisquaraine dyes **1a-e** and **2a-e** with mercuric ions, ethylenediamine tetraacetic acid (EDTA) was used as the complexating agent (Figures 3.10 and 3.11).¹⁴ Initially both these semisquaraine dyes showed negligible fluorescence emission. With the addition of one equivalent of Hg^{2+} ions, significant enhancement in the fluorescence intensity was observed (trace b in Figure 3.10B and Figure 3.11B). However, when EDTA was added to the solution of the $[\text{dye-Hg}^{2+}]$ complex, a decrease in the fluorescence intensity was observed. These results demonstrate that both the Z- and E-isomers show reversibility of the complexation in the presence of EDTA (trace c in Figure 3.10 and Figure 3.11).

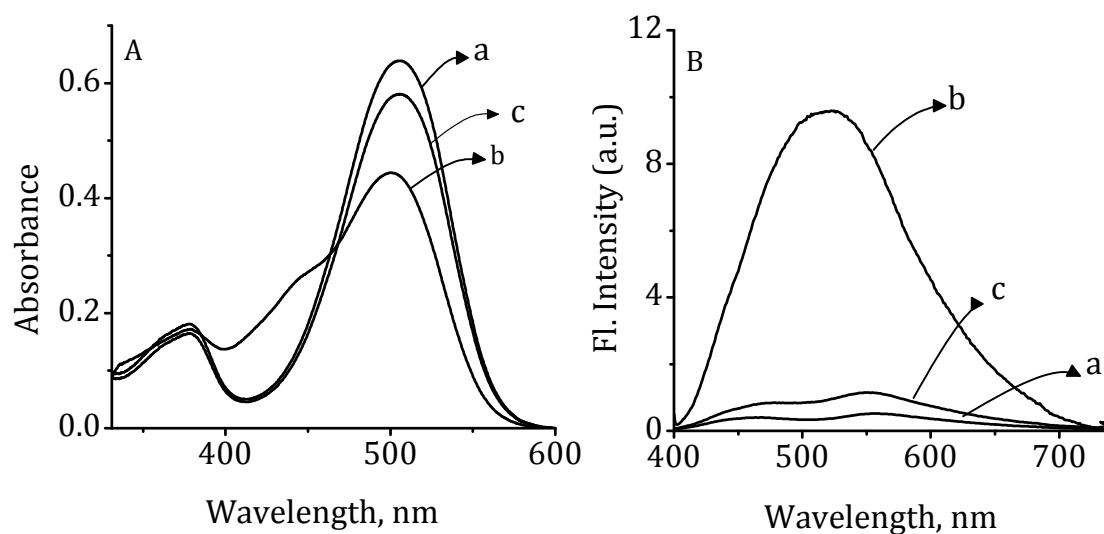


Figure 3.10. (A) Absorption and (B) emission spectra of **1a** showing reversibility of the complexation in acetone a) **1a**, b) $[\mathbf{1a-Hg}^{2+}]$ and c) $\mathbf{1a-Hg}^{2+}$ after the addition of EDTA (in water). Excitation wavelength, 389 nm.

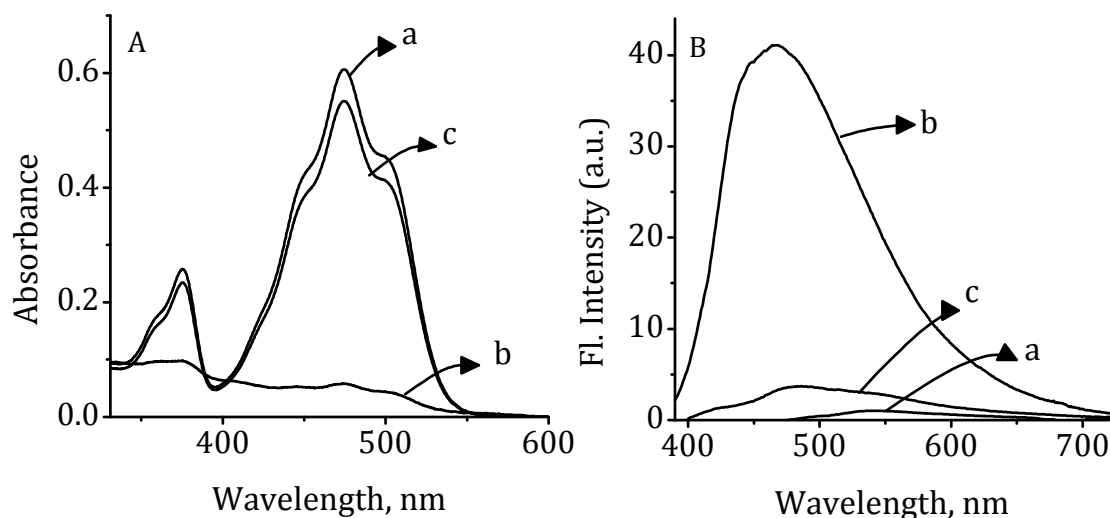


Figure 3.11. (A) Absorption and (B) emission spectra of **2a** showing reversibility of the complexation in acetone a) **2a**, b) [**2a**-Hg²⁺] and c) **2a**-Hg²⁺ after the addition of EDTA (in water). Excitation wavelength, 389 nm.

3.3.4. Nature of Complexation

To understand the nature of the complexation, we monitored the ¹H NMR spectral changes of the dyes **1a** and **2a** in the absence and presence of different concentrations of Hg²⁺ ions. Figure 3.12a shows the ¹H NMR spectrum of the semisquaraine dye **1a** in CDCl₃. The ¹H NMR spectrum of **1a** in CDCl₃ showed five aromatic protons as multiplets in the region between δ 7 and 9.5 ppm, whereas the olefinic and *N*-CH₃ protons appeared as singlets at δ 6.2 and 4.1 ppm, respectively. With the increase in the addition of Hg²⁺ ions, the aromatic proton at δ 9.45 ppm (3-H) showed a regular upfield shift ($\Delta\delta = 0.55$ at 1 equivalent of Hg²⁺ ions), and the other aromatic protons (4-H, 7-H, and 8-H) and the olefinic and *N*-methyl protons

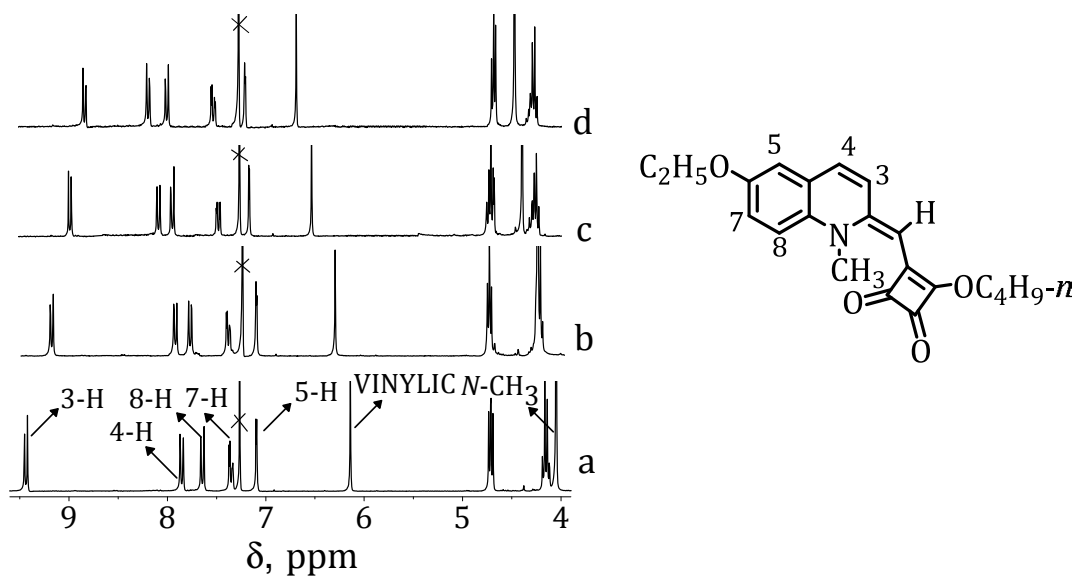


Figure 3.12. ^1H NMR spectra of **1a** (1 in CDCl_3 with increasing concentration of Hg^{2+} ions (in CD_3CN). The mole ratio of $[\text{Hg}^{2+}]$ to **[1a]** is a) 0, b) 0.36, c) 0.76 and d) 1.0, respectively.

exhibited downfield shifts in the range $\Delta\delta = 0.35\text{-}0.6$ ppm (Figure 3.12b-d). However, the 5-H aromatic proton and the aliphatic protons showed relatively negligible changes in their chemical shifts. Interestingly, with the addition of 1 equivalent of Hg^{2+} ions, the changes in the chemical shifts of the various protons reached saturation, confirming thereby the 1:1 stoichiometry for the **[1a-Hg $^{2+}$]** complex. The significant upfield shift of aromatic proton 3-H and the downfield shifts observed for the other aromatic, olefinic, and *N*-methyl protons clearly indicate the involvement of the carbonyl groups of the squaryl moiety of the dye **1a** in the complexation.

Figure 3.13a shows the ^1H NMR spectra of the E-isomer **2a** in CDCl_3 . The aromatic peaks of the semisquaraine dye **2a** are observed in the region δ 7.35-6.91 ppm in addition to a broad band at δ 8.55 ppm. The characteristic olefinic proton peak was observed at δ 5.2 ppm, while the *N*- CH_3 protons appeared as a singlet at δ 3.7 ppm. With the addition of $\text{Hg}(\text{ClO}_4)_2$ in CD_3CN , the peaks corresponding to the aromatic as well as the olefinic and *N*- CH_3 protons exhibited broadening together with a change in the chemical shift by $\Delta\delta = 0.01$ to 0.4 ppm (Figures 3.13b-d). The 3-H proton of the quinoline ring seen as a broad peak at 8.55 ppm undergoes an upfield shift of $\Delta\delta = 0.04$ ppm, while the olefinic proton showed a shift of 0.036 ppm. On the other hand, the aromatic protons such as 4-H, 5-H, 7-H

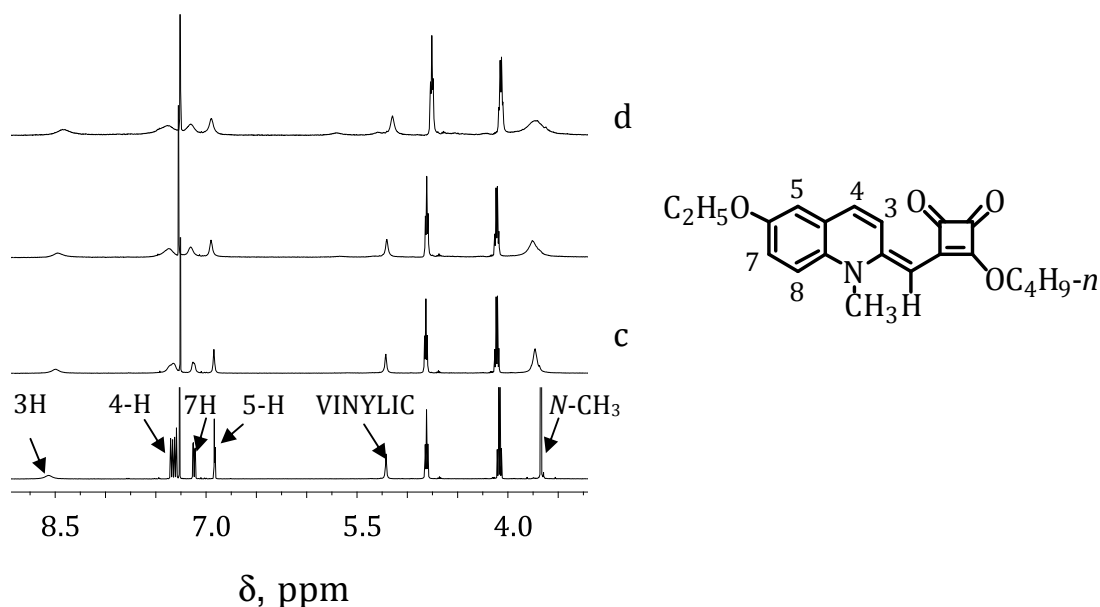


Figure 3.13. ^1H NMR spectra of **2a** in CDCl_3 with increasing concentration of Hg^{2+} ions (in CD_3CN). The mole ratio of $[\text{Hg}^{2+}]$ to $[\mathbf{2a}]$ is a) 0, b) 0.36, c) 0.76 and d) 1.0, respectively.

and 8-H showed deshielding by 0.09-0.17 ppm, while the *N*-CH₃ protons broadened and deshielded by 0.09 ppm. Furthermore, negligible changes are observed in the chemical shift values of the aliphatic protons indicating their non-involvement in the binding process. The changes in the ¹H NMR spectra of the isomer **2a** indicate that electron rich carbonyl groups are involved in the complexation.

The binding of the mercuric ions at the carbonyl group was also confirmed by ¹³C NMR experiments, where we could observe the downfield shift in the frequency of the carbonyl carbons of the semisquaraine isomer **1a** from 184 and 176 ppm to 195 and 185 ppm, respectively; while the isomer **2a** showed a shift from 193 and 185 ppm to 198 and 186 ppm, respectively. The involvement of carbonyl groups of the E- and Z-isomers in the complexation was also further confirmed through infrared spectral analysis (FTIR) of the dyes in the presence and absence of Hg²⁺ ions. The characteristic carbonyl peaks of the semisquaraine E-isomer **2a** were observed at 1766 and 1696 cm⁻¹ (Figure 3.14). However, the [**2a**-Hg²⁺] complex showed a shift in the carbonyl stretching frequencies to 1756 and 1676 cm⁻¹. Similar changes were observed in the case of the Z-isomer **1a**. The shift of the carbonyl stretching frequency of **1a** from 1760 cm⁻¹ to 1739 cm⁻¹ upon complexation confirms that the binding of the Hg²⁺ ions occur at the electron rich carbonyl groups of the squaryl ring. Further, the

formation of 1:1 complex was characterized through the observation of the peak at 591.43 and 591.52 for the dyes **1a** and **2a**, respectively.

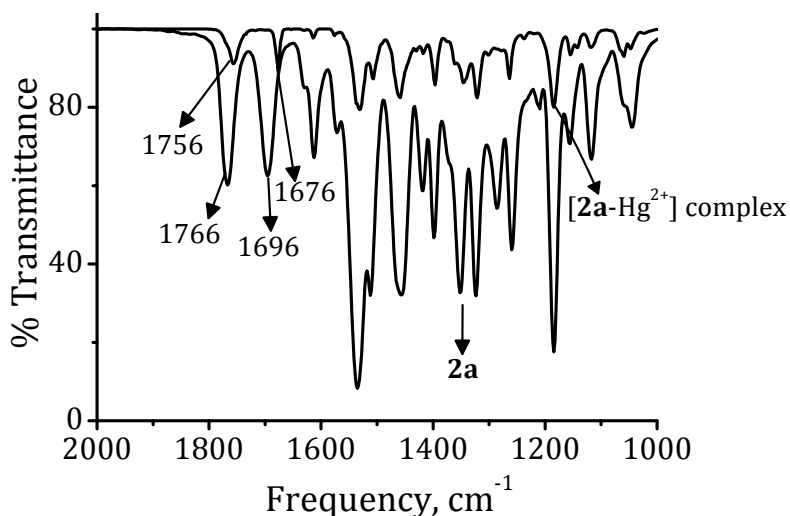


Figure 3.14. FTIR spectra of **2a** alone and in the presence of Hg(ClO₄)₂.

3.3.5. Selectivity of Recognition of Hg²⁺ ions

To demonstrate the selectivity of the semisquaraine dyes for Hg²⁺ ions, we have investigated the interactions of dyes **1a** and **2a** with other environmentally important metal ions such as Li⁺, Na⁺, K⁺, Ca²⁺, Ba²⁺, Mg²⁺, Zn²⁺, Pb²⁺ and Cd²⁺ ions in acetone. Figure 3.15 shows the relative changes in the fluorescence intensity of **1a** with the addition of one equivalent of different metal ions. As evident from the figure, the addition of other metal ions caused negligible changes in the fluorescence emission of **1a**. The selectivity of **1a** towards Hg²⁺ ions can be observed visually because the deep red colour and the fluorescence intensity of **1a** remained unchanged

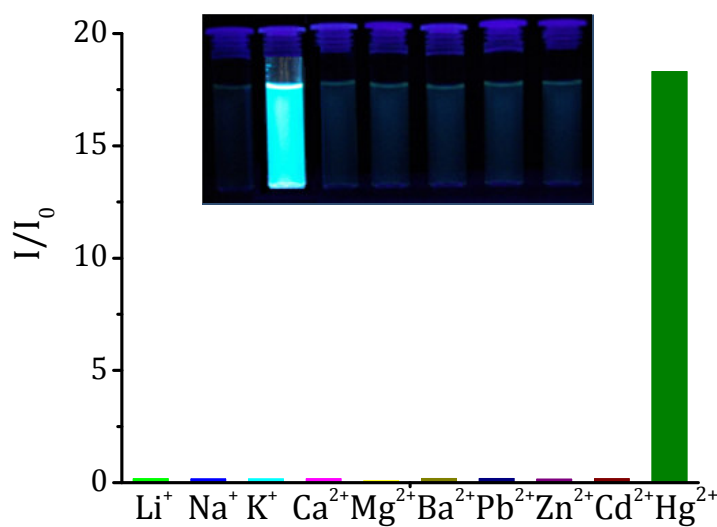


Figure 3.15. Fluorescence response of **1a** towards various metal ions in acetone. Excitation wavelength, 389 nm. Inset shows the fluorescence of **1a** on adding various metal ions. From left : **1a** alone, **1a** in presence of Hg^{2+} , Na^+ , Mg^{2+} , Pb^{2+} , Cd^{2+} , Zn^{2+} ions.

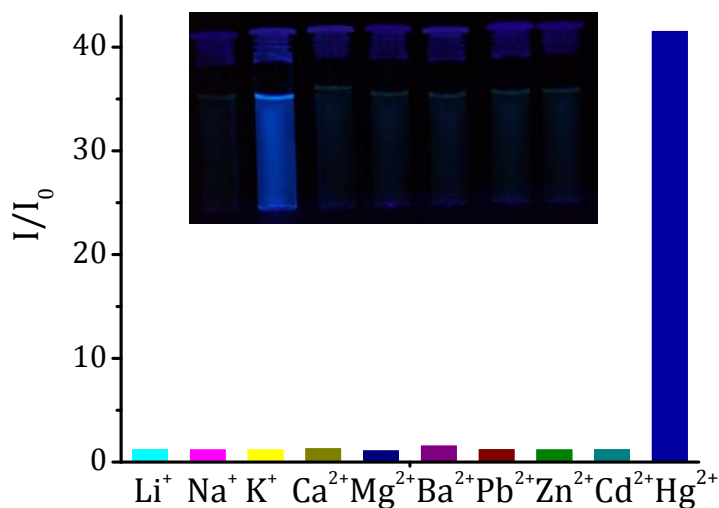


Figure 3.16. Fluorescence response of **2a** towards various metal ions in acetone. Excitation wavelength, 340 nm. Inset shows the fluorescence of **2a** on adding various metal ions, From left : **2a** alone, **2a** in presence of Hg^{2+} , Na^+ , Mg^{2+} , Pb^{2+} , Cd^{2+} , Zn^{2+} ions.

upon the addition of these metal ions, whereas with Hg^{2+} ions, we observed visual colour change as well as turn on fluorescence intensity. Similar observations have been made with the E-isomer **2a**, but the intensity of fluorescence enhancement observed was *ca.* 42-fold (Figure 3.16).

3.3.6. Detection of Hg^{2+} Ions in Aqueous Medium Containing Micelles

The semisquaraine dyes showed unusual selectivity for Hg^{2+} ions and hence it was our goal to identify the ideal conditions for the detection event in aqueous solutions. With the objective of demonstrating the potential of the semisquaraine dyes as probes, we have investigated the interactions of **1** and **2** with Hg^{2+} ions and other metal ions under different conditions including the micellar media. We chose three surfactants such as cetyltrimethylammonium bromide (CTAB), sodium dodecyl sulfate (SDS), and Triton X-100 (TX-100), which are representative examples of cationic, anionic, and neutral surfactants. Of the two series chosen for the study, it was observed that the Z-isomers **1a-e** showed significant changes in their absorption and fluorescence properties with the addition of Hg^{2+} ions in the aqueous medium. Of all the conditions examined, it has been observed that a solvent system consisting of a mixture (9:1) of water and acetone containing SDS has been found to be very effective with respect to the

stability of **1** as well as to the selectivity and sensitivity of the metal ion binding event.

Figure 3.17A shows the changes in the absorption spectra of **1a** in a mixture (9:1) of water and acetone containing SDS (12 mM) with the addition of Hg^{2+} ions. As the concentration of Hg^{2+} ions increased, we observed a regular decrease in the absorbance of **1a** at 472 nm with a concomitant increase in absorbance at 360 nm through an isosbestic point at 392 nm. Further addition of Hg^{2+} ions resulted in the complete disappearance of the absorbance at 472 nm, leading to a visual colour change from a deep yellow to a colourless solution. Similarly, with an increase in the concentration of Hg^{2+} ions, we observed a gradual increase in the fluorescence intensity of **1a** (Figure 3.17B). Addition of $19.8 \mu\text{M}$ Hg^{2+}

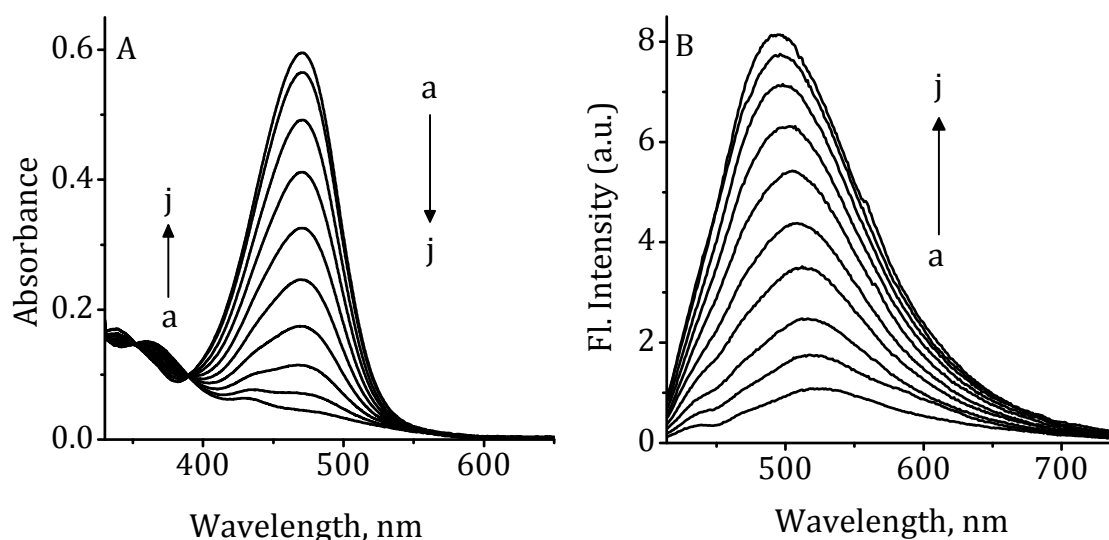


Figure 3.17. Changes in the (A) Absorption and (B) emission spectra of **1a** ($19.8 \mu\text{M}$) in 9:1 water/acetone mixture containing 12 mM SDS with increase in concentration of $\text{Hg}(\text{ClO}_4)_2$ a) 0, and j) $19.8 \mu\text{M}$. Excitation wavelength, 392 nm.

ions gave *ca.* 8-fold enhancement in the fluorescence intensity along with a hypsochromic shift of 30 nm. This significant 'turn-on' intensity led to the visual observation of the change in fluorescence intensity of **1a** in the presence of Hg^{2+} ions.

In order to understand the stoichiometry of the complex formed, Job's plot analysis was carried out. The stoichiometry of the complex formed between **1a** and Hg^{2+} ions was found to be 1:1 (Figure 3.18A). Benesi-Hildebrand analysis showed that the association constant for the complex formation is $K = 4.0 \pm 0.1 \times 10^4 \text{ M}^{-1}$ (Figure 3.18B).

To investigate the effect of a micellar medium on the sensitivity of the assay, the detection of Hg^{2+} ions by **1a** has been examined by varying the concentration of SDS. Thus, in the presence of 6 mM SDS, we observed *ca.*

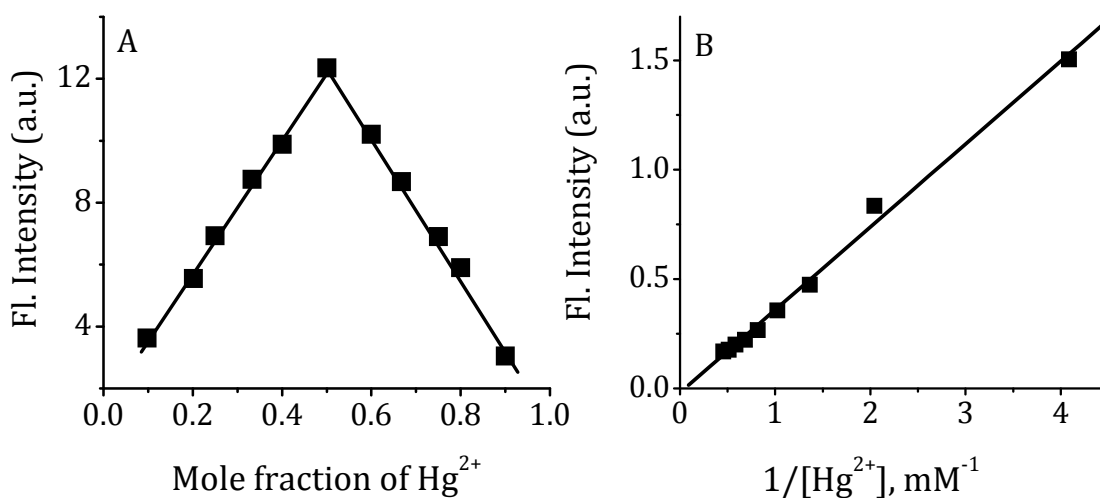


Figure 3.18. (A) Job's plot and (B) Benesi-Hildebrand analysis for the complexation of **1a** with Hg^{2+} ions in 9:1 water/acetone mixture containing 12 mM SDS.

2-fold enhancement in fluorescence intensity of **1a** upon binding with Hg^{2+} ions, and it reached a saturation with a maximum enhancement of *ca.* 8-fold at 12 mM SDS. Figure 3.19 show the relative changes in the fluorescence intensity of **1a** upon the addition of 1 equivalent of Hg^{2+} ions at different concentrations of SDS. With increase in concentration of SDS, the changes in the fluorescence intensity of **1a** upon addition of Hg^{2+} ions increased and reached saturation at and above the critical micellar concentration (CMC)¹⁵ of SDS.

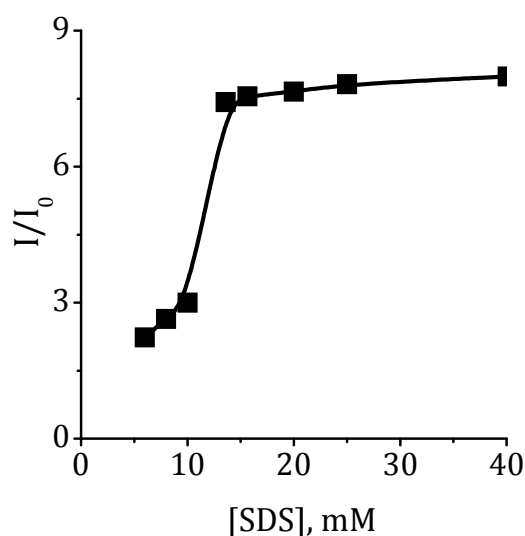


Figure 3.19. Relative changes in fluorescence of **1a** in 9:1 water/acetone on complexation with Hg^{2+} ions as a function of [SDS].

Figure 3.20 shows the plot of the variation of association constants with varying SDS concentrations for the semisquaraine isomer **1a**. As can be seen, the association constant (K) is clearly dependent upon the concentration of SDS. Interestingly, the association constant in SDS

solutions shows saturation at 12 mM of the surfactant. The CMC in mixed solvents and in the presence of free ions will be different from that in pure solvents.¹⁶ This might explain the higher value of the CMC observed. This variation in the CMC is reflected in the higher value of K observed at 12 mM of SDS.

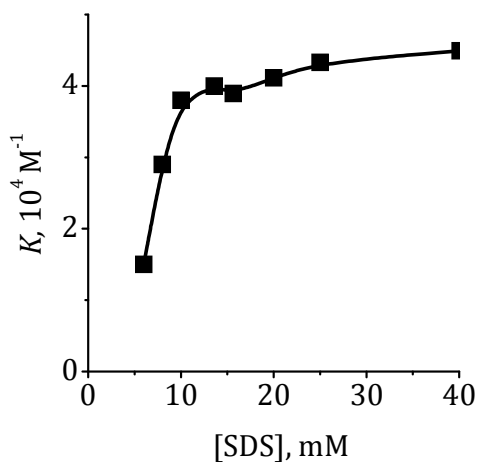


Figure 3.20. Variation of the association constant (K) with concentration of SDS on the addition of Hg^{2+} ions to a solution of **1a** in 9:1 water/acetone mixture containing SDS.

3.3.7. Selectivity of Hg^{2+} Ions Recognition in Aqueous Medium

To demonstrate the selectivity of the semisquaraine dyes for Hg^{2+} ions, we have investigated the interactions with other environmentally important metal ions such as Li^+ , Na^+ , K^+ , Ag^+ , Ca^{2+} , Mg^{2+} , Zn^{2+} , Pb^{2+} , Cd^{2+} , Cu^{2+} and Fe^{3+} ions in a mixture (9:1) of water and acetone containing 12 mM SDS. For example, the addition of K^+ and Cd^{2+} ions showed negligible changes in the absorption and fluorescence intensity of **1a** (Figures 3.21

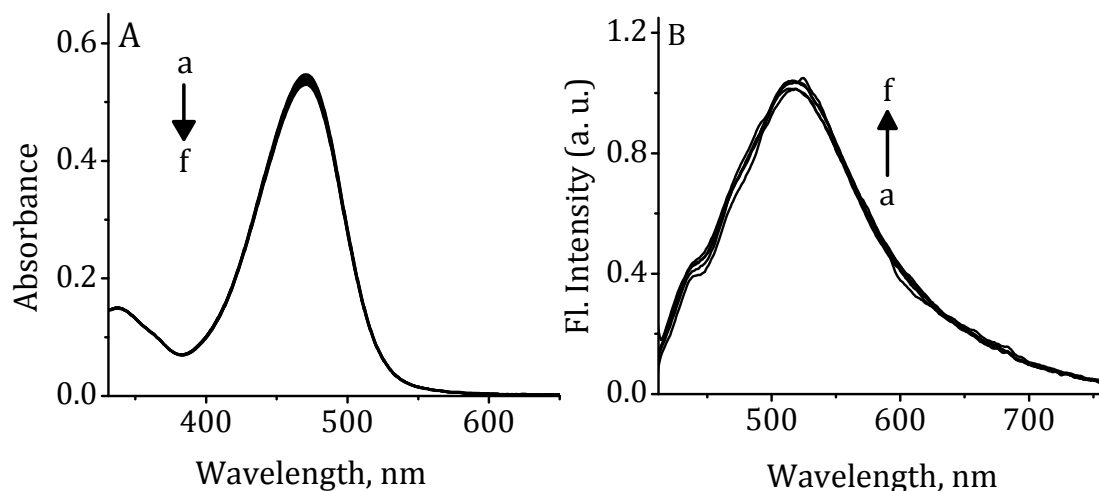


Figure 3.21. (A) Absorption and (B) the corresponding fluorescence spectra of **1a** (18 μM) in 9:1 water/acetone mixture containing 12 mM SDS with increase in concentration of KCl. $[\text{K}^+]$ (a) 0 and (f) 90 μM . Excitation wavelength, 392 nm.

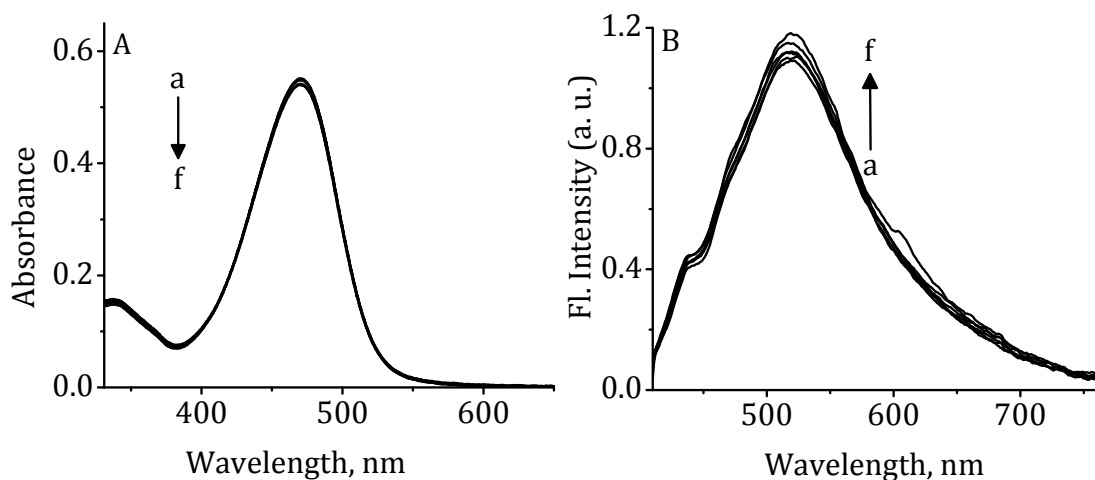


Figure 3.22. (A) Absorption and (B) the corresponding fluorescence spectra of **1a** (20 μM) in 9:1 water/acetone mixture containing 12 mM SDS with increase in concentration of $\text{Cd}(\text{ClO}_4)_2$. $[\text{Cd}^{2+}]$ (a) 0 and (f) 90 μM . Excitation wavelength, 392 nm.

and 3.22). Similar observations have been made with the divalent metal ions. Figure 3.23 shows the relative changes in the fluorescence intensity of **1a** with the addition of one equivalent of different metal ions. The selectivity of **1a** toward Hg^{2+} ions can be observed visually because the deep yellow colour and the fluorescence intensity of **1a** remained unchanged upon the addition of these metal ions, whereas with Hg^{2+} ions, we observed visual colour change as well as 'turn-on' fluorescence intensity (Inset, Figure 3.23). Further, the presence of equimolar concentrations of these metal ions in the sample showed negligible influence on the sensitivity of **1a** for Hg^{2+} ion detection in the aqueous solutions.

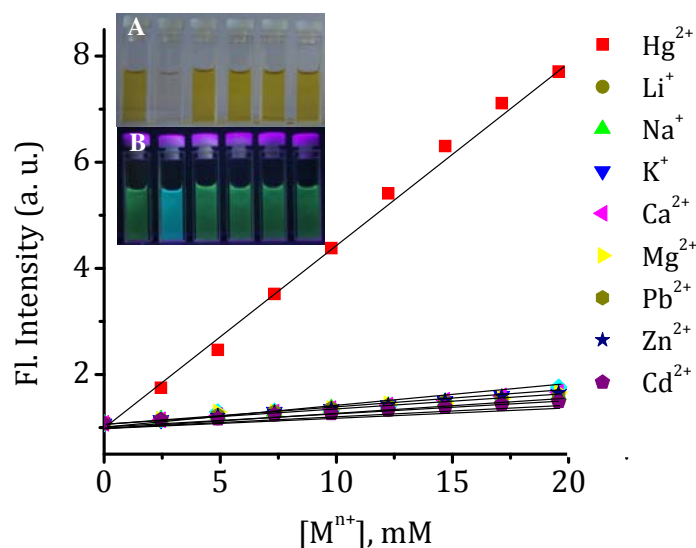


Figure 3.23. Fluorescence response of **1a** towards various metal ions in a mixture (9:1) of water and acetone containing SDS (12 mM). Inset shows the visual changes in (A) absorption and (B) fluorescence of **1a** on adding various metal ions, From left : **1a** alone, **1a** in presence of Hg^{2+} , Na^+ , Mg^{2+} , Pb^{2+} , Cd^{2+} ions.

3.4. DISCUSSION

The semisquaraine dye isomers **1a-e** and **2a-e** undergo selective interactions with mercuric ions resulting in visual colour change as well as enhancement in fluorescence intensity. Theoretical calculations have been carried out to understand the nature of the complex between the semisquaraines and Hg^{2+} ions.¹⁷ The electrostatic potential map showed the availability of lone pair of electrons at the carbonyl oxygen atoms, and the distance between the two carbonyl oxygen atoms is found to be 3.3 Å (Figure 3.24). The selectivity of the semisquaraines towards Hg^{2+} ions can be attributed to the soft acid nature¹⁸ as well as the size of the mercuric ions. The fixed distance of 3.3 Å between the two carbonyl groups of the squaryl moiety can ideally accommodate mercuric ions with a diameter of 2.2 Å. Moreover, the significant changes in the ^1H NMR, FTIR spectra of the semisquaraine dyes indicate that the binding of the mercuric ions involves the carbonyl groups in the metal ion complexation (Figure 3.25).

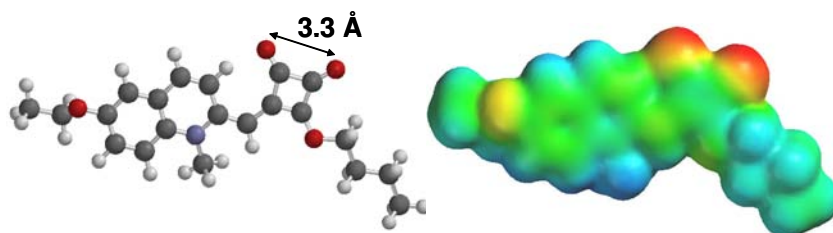


Figure 3.24. Geometry optimized structure as well as the electrostatic potential map of **2a**.

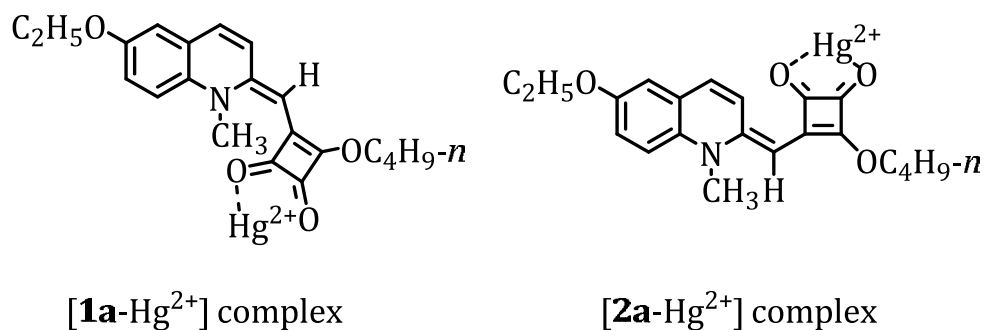


Figure 3.25. Structures of the complexes formed between Hg²⁺ ions and the semisquaraine dyes **1a** and **2a**.

A comparison of the metal ion binding ability of the two classes of semisquaraine dyes indicated that the efficiency of binding interaction is higher in the case of the Z-isomer. This is clear from the higher association constants observed for the complexation between the semisquaraine dye **1a** and Hg²⁺ ions as compared to the [2a-Hg²⁺] complex. This could be attributed to the absence of hydrogen bonding between the carbonyl oxygen and the quinoline proton in the Z-isomer (**1a**), resulting in greater electron density at the carbonyl group as compared to the E-isomer (**2a**). Notably, the higher complexation ability of the Z-isomer with mercuric ions is also retained under aqueous conditions, whereas the E-isomer exhibits less significant interactions with Hg²⁺ ions under similar conditions. This could be due to the fact that in poorly coordinating organic solvents, there is no competition by the solvent molecules towards the coordination of the probe to the metal ions, so that effective binding takes place between the probe and metal ions.¹⁹ However, in organic solvent-water mixtures or in

neat water, the competitive nature of the solvent increases, resulting in decreased complexation ability of the probe. This is due to the strong solvation energy of the metal ions in the presence of water, which disfavours metal-ligand interactions. Hence, only a strongly coordinating ligand can induce a favourable response towards the metal ions. In the present case, due to the stronger complexation ability of the Z-isomer to the Hg²⁺ ions, we were able to observe significant changes in its absorption and fluorescence property, as compared to the E-isomer, albeit with lower association constants.

The semisquaraine dye **1a** shows significant binding with the mercuric ions in aqueous solution containing anionic micelles. In the case of anionic surfactants, the anionic charges are present at the micellar interface, and hence this micellar region becomes favourable as a complexation field for cations.²⁰ By taking into account the binding of the dye with the metal ions, we propose that these dye molecules distribute within the micellar structure but close to the surface near the polar head groups (Figure 3.26). In such a situation, the hydrophobicity rendered by the aromatic moieties can be overcome by the hydrophilicity of the carbonyl oxygen atoms. This would enhance the affinity of the dye molecules toward polar ends so that stable complex formation between the dye and Hg²⁺ ions could occur at the interface involving water molecules as

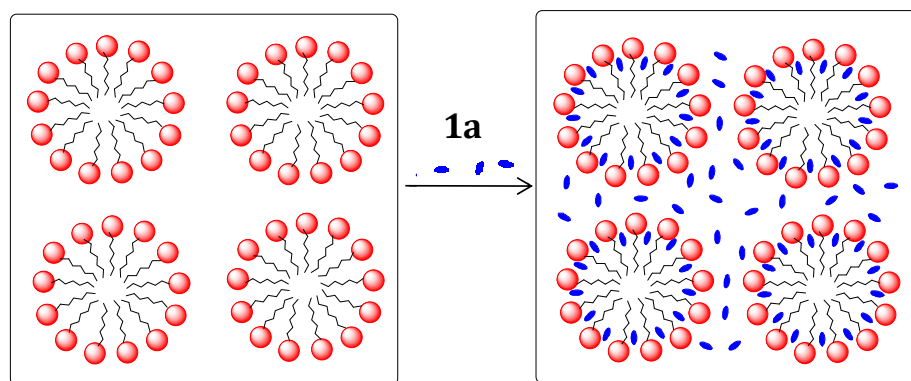


Figure 3.26. Schematic representation of the micellization of the dye **1a**.

other coordinates. The observed significant signaling efficiency of **1a** for Hg^{2+} ions in the presence of SDS as compared to the aqueous medium could be attributed to the microencapsulation of the complex. This results in the decrease in the rotational as well as translational freedom of the excited state of the complex leading to the significant fluorescence enhancement in the presence of the surfactant.

To rationalize the variation in the activity of the semisquaraine dye towards the Hg^{2+} ions in various SDS concentrations, it is important to consider two competing processes: the first is the electrostatic interaction between the anionic SDS micellar surface and the positively charged metal ion (Hg^{2+} ions) and the second factor is the lesser accessibility of the probe molecules toward the metal ions within the micellar environment.²¹ The electrostatic interaction between the SDS micellar surface and the Hg^{2+} ions leads to an increase in the local concentration of the metal ions in the near

vicinity of the probe. This close proximity of **1a** and the metal ions in micellar aggregates ensure effective communication between the probe and the metal ions. Thus, with the formation of the micellar units, an efficient complexation was observed between the semisquaraine dyes and Hg²⁺ ions when compared to the aqueous medium.

3.5. CONCLUSIONS

We have synthesized a series of novel semisquaraine dyes **1a-e** and **2a-e** and investigated their metal ion binding properties with various mono- and bivalent metal ions. These systems are characterized by the presence of electron rich carbonyl group in the squaryl ring, due to which these semisquaraine dyes act as bidentate ligands for metal ions. Both the semisquaraine derivatives displayed unusual selectivity for the Hg²⁺ ions among the various metal ions investigated. Our investigations revealed that the metal ion complexation involves the electron rich carbonyl groups of the semisquaraine derivatives as characterized by ¹H, ¹³C NMR and FTIR spectral analysis. The unusual selectivity of the semisquaraine dyes for the Hg²⁺ ions could be rationalized due to the soft acid nature and size of the metal ion. This binding of the semisquaraine derivatives to Hg²⁺ ions could be visualized through visual colour change as well as 'turn-on' fluorescence intensity. These results demonstrate that the semisquaraine dyes can

function as efficient dual chromogenic and fluorogenic probes for the detection of Hg²⁺ ions.

3.6. EXPERIMENTAL SECTION

3.6.1. General Techniques

The equipment and procedure for spectral recordings are described elsewhere.²² All melting points were determined on a Mel-Temp II melting point apparatus. The IR spectra were recorded on a Perkin Elmer Model 882 infrared spectrometer. The electronic absorption spectra were recorded on a Shimadzu UV-3101 or 2401 PC UV-VIS-NIR scanning spectrophotometer. The fluorescence spectra were recorded on a SPEX-Fluorolog F112X spectrofluorimeter.

3.6.2. Materials

Hg(ClO₄)₂, Pb(ClO₄)₂, Cu(ClO₄)₂, Zn(ClO₄)₂, Ca(ClO₄)₂, NaClO₄, KClO₄, LiClO₄, Mg(ClO₄)₂ was purchased from Aldrich, India and used as received. The synthesis of the semisquaraine dyes **1a** (mp 202-204 °C), **1b** (mp 205-207 °C), **1c** (mp 167-169 °C), **1d** (mp 170-172 °C), **1e** (mp 230-232 °C), **2a** (mp 184-186 °C), **2b** (mp 150-152 °C), **2c** (mp 152-154 °C), **2d** (mp 182-184 °C), **2e** (mp 208-210 °C) used in the present study was achieved as

described in Chapter 2 of the present thesis. All the solvents used were purified and distilled before use.

3.6.3. Determination of Stoichiometry of Complexation

In the Jobs plot method, the total molar concentration of the two binding partners (e.g. dye and metal ions) are held constant, but their mole fractions are varied. The fluorescence intensity (or peak area) that is proportional to complex formation is plotted against the mole fractions of these two components. The maximum on the plot corresponds to the stoichiometry of the two species if sufficiently high concentrations are used.

3.6.4. Determination of Association Constants

The binding affinities of the semisquaraine dyes were calculated using Benesi-Hildebrand equation 3.1 for 1:1 stoichiometry and equation 3.2 for 2:1 stoichiometry, where K is the equilibrium constant, I_0 is the fluorescence intensity of the free dye, I is the observed fluorescence intensity in the presence of metal ions and I_s is the fluorescence intensity at saturation. The linear dependence of on the reciprocal (or its square root) of the metal ion concentration indicates the formation of a 1:1 or 2:1 complex between the dye and the metal ion.

$$\frac{1}{I - I_0} = \frac{1}{I - I_s} + \frac{1}{K(I - I_0)[M^{n+}]} \quad \text{eq (3.1)}$$

$$\frac{1}{I - I_0} = \frac{1}{I - I_s} + \frac{1}{K(I - I_0)[M^{n+}]^{1/2}} \quad \text{eq (3.2)}$$

3.7. REFERENCES AND NOTES

1. (a) Ludwig, R.; Dzung, N. T. K. *Sensors* **2002**, *2*, 397. (b) Gokel, G. W.; Leevy, W. M.; Weber, M. E. *Chem. Rev.* **2004**, *104*, 2723. (c) Ros-Lis, J. V.; Martinez-Manez, R.; Sancenon, F.; Soto, J.; Spieles, M.; Rurack, K. *Chem. Eur. J.* **2008**, *14*, 10101.
2. (a) Takeuchi, T.; Morikawa, N.; Matsumoto, H.; Shiraishi, Y. *Acta Neuropathologica* **1962**, *2*, 40. (b) Bakir, F.; Damluji, S. F.; Amin-Zaki, L.; Murtadha, M.; Khalidi, A.; Al-Rawi, N. Y.; Tikriti, S.; Dhahir, H. I.; Clarkson, T. W.; Smith, J. C.; Doherty, R. A. *Science* **1973**, *181*, 230. (c) Mason, R. P.; Morel, F. M. M.; Hemond, H. F. *Water, Air, Soil Pollut.* **1995**, *80*, 775. (d) Mason, R. P.; Reinfelder, J. R.; Morel, F. M. M. *Water, Air, Soil Pollut.* **1995**, *80*, 915. (e) Harris, H. H.; Pickering, I. J.; George, G. N. *Science* **2003**, *301*, 1203. (f) Kraepiel, A. M. L.; Keller, K.; Chin, H. B.; Malcolm, E. G.; Morel, F. M. M. *Environ. Sci. Technol.* **2003**, *37*, 5551. (g) Montvydiene, D.; Marciulioniene, D. *Environmental Toxicology* **2004**, 351. (h) Burger, J.; Gochfeld, M. *Environ. Res.* **2004**, *96*, 239. (i) Hylander, L. D.; Goodsite, M. E. *Science of the Total Environment* **2006**,

- 368, 352. (j) Kuwabara, J. S.; Arai, Y.; Topping, B. R.; Pickering, I. J.; George, G. N. *Environ. Sci. Technol.* **2007**, *41*, 2745.
3. (a) Frumkin, H.; Letz, R.; Williams, P. L.; Gerr, F.; Pierce, M.; Sanders, A.; Elon, L.; Manning, C. C.; Woods, J. S.; Hertzberg, V. S.; Mueller, P.; Taylor, B. B. *American Journal of Industrial Medicine* **2001**, *39*, 1. (b) Mercury Update: Impact of Fish Advisories. EPA Fact Sheet EPA-823-F-01-011; EPA, Office of Water: Washington, DC, **2001**. (c) Shanker, G.; Mutkus, L. A.; Walker, S. J.; Aschner, M. *Mol. Brain Res.* **2002**, *106*, 1. (d) Tchounwou, P. B.; Ayensu, W. K.; Ninashvili, N.; Sutton, D. *Environmental Toxicology*, **2003**, *18*, 149. (e) Clarkson, T. W.; Magos, L.; Myers, G. J. *The Journal of Trace Elements in Experimental Medicine* **2003**, *16*, 321. (f) Clarkson, T. W.; Magos, L.; Myers, G. J. *New Engl. J. Med.* **2003**, *349*, 1731. (g) Zalups, R. K.; Ahmad, S. J. *Am. Soc. Nephrol.* **2004**, *15*, 2023. (h) Silbergeld, E. K.; Silva, I. A.; Nyland, J. F. *Toxicol. Appl. Pharmacol.* **2005**, *207*, S282. (i) Kaur, P.; Aschner, M.; Syversen, T. *Neurotoxicol.* **2006**, *27*, 492. (j) Zalups, R. K.; Lash, L. H. *Toxicol. Appl. Pharmacol.* **2006**, *214*, 88. (k) Milaeva, E. R. *J. Inorg. Biochem.* **2006**, *100*, 905.
4. (a) Yoon, S.; Miller, E. W.; He, Q.; Do, P. H.; Chang, C. J. *Angew. Chem., Int. Ed.* **2007**, *46*, 6658. (b) Kim, H. N.; Lee, M. H.; Kim, H. J.; Kim, J. S.; Yoon, J. *Chem. Soc. Rev.* **2008**, *37*, 1465.

5. (a) Chae, M.-Y.; Czarnik, A. W. *J. Am. Chem. Soc.* **1992**, *114*, 9704. (b) Nolan, E. M.; Lippard, S. J. *J. Mater. Chem.* **2005**, *15*, 2778. (c) Nolan, E. M.; Lippard, S. J. *J. Am. Chem. Soc.* **2007**, *129*, 5910. (d) Yang, H.; Zhou, Z.; Huang, K.; Yu, M.; Li, F.; Yi, T.; Huang, C. *Org. Lett.* **2007**, *9*, 4729. (e) Wu, D.; Huang, W.; Duan, C.; Lin, Z.; Meng, Q. *Inorg. Chem.* **2007**, *46*, 1538. (f) Zhang, X.; Shiraishi, Y.; Hirai, T. *Tetrahedron Lett.* **2007**, *48*, 5455. (g) Soh, J. H.; Swamy, K. M. K.; Kim, S. K.; Kim, S.; Lee, S.-H.; Yoon, J. *Tetrahedron Lett.* **2007**, *48*, 5966. (h) Yang, H.; Zhou, Z.; Huang, K.; Yu, M.; Li, F.; Yi, T.; Huang, C. *Org. Lett.* **2007**, *9*, 4729.
6. Shi, W.; Ma, H. *Chem. Commun.* **2008**, 1856.
7. (a) Lee, M. H.; Wu, J.-H.; Lee, J. W.; Jung, J. H.; Kim, J. S. *Org. Lett.* **2007**, *9*, 2501. (b) Shiraishi, Y.; Sumiya, S.; Kohno, Y.; Hirai, T. *J. Org. Chem.* **2008**, *73*, 8571.
8. (a) Chae, M.-Y.; Czarnik, A. W. *J. Am. Chem. Soc.* **1992**, *114*, 9704. (b) Jiang, P.; Guo, Z. *Coord. Chem. Rev.* **2004**, *248*, 205. (c) Ros-Lis, J. V.; Marcos, M. D.; Martinez-Manez, R.; Rurack, K.; Soto, J. *Angew. Chem. Int. Ed.* **2005**, *44*, 4405. (d) Coronado, E.; Galan-Mascaros, J. R.; Marti-Gastaldo, C.; Palomares, E.; Durrant, J. R.; Vilar, R.; Gratzel, M.; Nazeeruddin, Md. K. *J. Am. Chem. Soc.* **2005**, *127*, 12351. (e) Zhao, Q.; Cao, T.; Li, F.; Li, X. Jing, H.; Yi, T.; Huang, C. *Organometallics* **2007**, *26*, 2077. (f) Ye, B.-C.; Yin, B.-C. *Angew. Chem. Int. Ed.* **2008**, *47*, 8386. (g)

- Nolan, E. W.; Lippard, S. J. *Chem. Rev.* **2009**, *108*, 3443.
9. (a) de Silva, A. P.; Gunaratne, H. Q. N.; Gunnlaugsson, T.; Huxley, A. J. M.; McCoy, C. P.; Rademacher, J. T.; Rice, T. E. *Chem. Rev.* **1997**, *97*, 1515. (b) Yoon, S.; Albers, A. E.; Wong, A. P.; Chang, C. J. *J. Am. Chem. Soc.* **2005**, *127*, 16030. (c) Yang, Y.-K.; Yook, K.-J.; Tae, J. *J. Am. Chem. Soc.* **2005**, *127*, 16760.
10. (a) Pesek, J. J.; Abpikar, H.; Becker, J. F. *Appl. Spectrosc.* **1988**, *42*, 473. (b) Descalzo, A. B.; Martínez-Máñez, R.; Radeaglia, R.; Rurack, K.; Soto, J. *J. Am. Chem. Soc.* **2003**, *125*, 3418. (c) Métivier, R.; Leray, I.; Valeur, B. *Chem. Eur. J.* **2004**, *10*, 4480. (d) Saito, S.; Suzuki, R.; Danzaka, N.; Hikichi, A.; Yoshimoto, K.; Maeda, M.; Aoyama, M. *Electrophoresis* **2007**, *28*, 2448. (e) Park, S. M.; Kim, M. H.; Choe, J.-I.; No, K. T.; Chang, S.-K. *J. Org. Chem.* **2007**, *72*, 3550. (f) Bag, B.; Bharadwaj, P. K. *J. Lumin.* **2007**, *126*, 27. (g) Ma, L.-J.; Li, Y.; Sun, J.; Tian, C.; Wu, Y. *Chem. Commun.* **2008**, 6345.
11. (a) Costero, A. M.; Andreu, R.; Monrabal, E.; Martínez-Máñez, R.; Sancenón, F.; Soto, J. *J. Chem. Soc., Dalton Trans.* **2002**, 1769. (b) Wu, Z.; Chen, Q.; Xiong, S.; Xin, B.; Zhao, Z.; Jiang, L.; Ma, J. S. *Angew. Chem., Int. Ed.* **2003**, *42*, 3271. (c) Ryu, E.-H.; Zhao, Y. *Org. Lett.* **2004**, *6*, 3187. (d) Metivier, R.; Leray, I.; Valeur, B. *Chem.-Eur. J.* **2004**, *10*, 4480. (e) Ros-Lis, J. V.; Martinez-Manez, R.; Rurack, K.; Sancenon, F.; Soto, J.; Spielles,

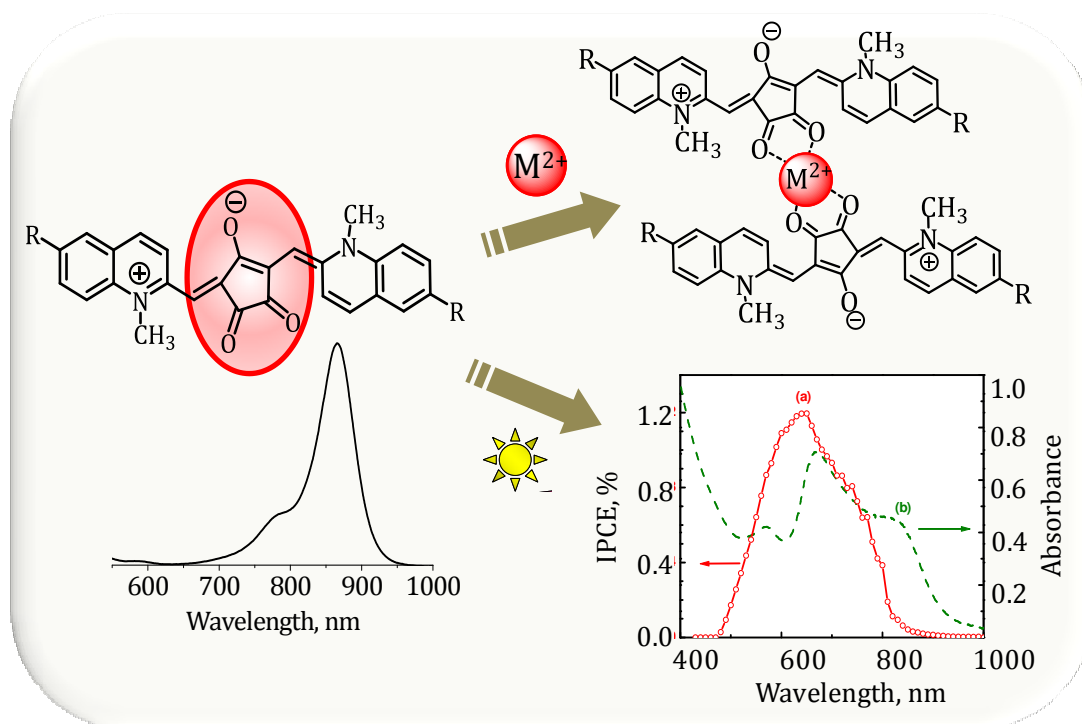
- M. *Inorg. Chem.* **2004**, *43*, 5183. (f) Ono, A.; Togashi, H. *Angew. Chem., Int. Ed.* **2004**, *43*, 4300. (g) Zhu, X.-J.; Fu, S.-T.; Wong, W.-K.; Guo, J.-P.; Wong, W.-Y. *Angew. Chem., Int. Ed.* **2006**, *45*, 3150. (h) Zhao, Y.; Zhong, Z. *J. Am. Chem. Soc.* **2006**, *128*, 9988. (i) Zhu, X.-J.; Fu, S.-T.; Wong, W.-K.; Guo, J.-P.; Wong, W.-Y. *Angew. Chem., Int. Ed.* **2006**, *45*, 3150. (j) Wu, Z.; Zhang, Y.; Ma, J. S.; Yang, G. *Inorg. Chem.* **2006**, *45*, 3140.
12. (a) Avirah, R. R.; Jyothish, K.; Ramaiah, D. *Org. Lett.* **2007**, *9*, 121. (b) Bae, J.-S.; Son, Y.-A.; Kim, S.-H. *Fibers Polym.* **2009**, *10*, 403. (c) Bae, J.-S.; Gwon, S.-Y.; Son, Y.-A.; Kim, S.-H. *Dyes Pigments* **2009**, *83*, 324.
13. (a) Jisha, V. S.; Thomas, A. J.; Ramaiah, D. *J. Org. Chem.* **2009**, *74*, 6667. (b) Nair, A. K.; Neelakandan, P. P.; Ramaiah, D. *Chem. Commun.* **2009**, 6352.
14. Arunkumar, E.; Chithra, P. ; Ajayaghosh, A. *J. Am. Chem. Soc.* **2004**, *126*, 6590.
15. (a) Kalyanasundaram, K. *Photochemistry in Microheterogeneous Systems*; Academic Press: New York, **1987**. (b) Arun, K. T.; Ramaiah, D. *J. Phys. Chem. A* **2005**, *109*, 5571.
16. Sarkar, B.; Lam, S.; Alexandridis, P. *Langmuir* **2010**, DOI: 10.1021/la100544w.
17. All geometries are optimized using semiempirical AM1 calculations. DFT B3LYP/6-31.G* single-point energy calculations were used to

obtain the electrostatic potential surfaces using Titan (Wavefunction, Inc.). The color at each point on these surfaces reflects the interaction energy between a positive test charge at that point. Red indicates an attractive potential, whereas blue represents a repulsive potential. The areas of red therefore indicate a “negative” region, and yellow/green indicates a more neutral or “positive” region, depending on how blueish the color is.

18. (a) Huang, J.-H.; Wen, W.-H.; Sun, Y.-Y.; Chou, P.-T.; Fang, J.-M. *J. Org. Chem.* **2005**, *70*, 5827. (b) Kunze, A.; Gleiter, R.; Rominger, F. *Eur. J. Inorg. Chem.* **2006**, 621. (c) Lee, J. Y.; Lee, S. Y.; Park, S.; Kwon, J.; Sim, W.; Lee, S. S. *Inorg. Chem.* **2009**, *48*, 8934.
19. (a) Nakahara, Y.; Kida, T.; Nakatsuji, Y.; Akashi, M. *Chem. Commun.* **2004**, 224. (b) Nakahara, Y.; Kida, T.; Nakatsuji, Y.; Akashi, M. *Org. Biomol. Chem.* **2005**, *3*, 1787.
20. (a) Fernandez, Y. D.; Gramatges, A. P.; Amendola, V.; Foti, F.; Mangano, C.; Pallavicini, P.; Patroni, S. *Chem. Commun.* **2004**, 1650. (b) Zhao, Y.; Zhong, Z. *Org. Lett.* **2006**, *8*, 4715.
21. Mallick, A.; Mandal, M. C.; Haldar, B.; Chakrabarty, A.; Das, P.; Chattopadhyay, N. *J. Am. Chem. Soc.* **2006**, *128*, 3126.
22. (a) Joseph, J.; Eldho, N. V.; Ramaiah, D. *Chem. Eur. J.* **2003**, *9*, 5926. (b) Kuruvilla, E.; Joseph, J.; Ramaiah, D. *J. Phys. Chem. B* **2005**, *109*, 21997.

(c) Neelakandan, P. P.; Hariharan, M.; Ramaiah, D. *J. Am. Chem. Soc.* **2006**, *128*, 11334. (d) Hariharan, M.; Suneesh, C. K.; Ramaiah, D. *Org. Lett.* **2007**, *9*, 417.

CHAPTER 4. NOVEL CROCONAINE DYES AND STUDY OF THEIR METAL ION BINDING AND LIGHT HARVESTING PROPERTIES



4.1. ABSTRACT

With an objective to develop infrared absorbing dyes as probes for metal ions and sensitizers in solar cells, we synthesized a few quinaldine based croconaine dyes. These dyes exhibited absorption maximum in the infrared region (840-870 nm) with high molar extinction coefficients ($1-5 \times 10^5 \text{ M}^{-1}\text{cm}^{-1}$). Upon interaction with divalent metal ions these dyes were

found to form complexes with a 2:1 stoichiometry having high association constants in the order 10^5 - 10^7 M⁻¹, while the monovalent metal ions caused negligible changes in their spectral properties. As characterized through FTIR and NMR, the complex formation with divalent metal ions involves the participation of the croconyl moiety and results in strong chelation enhanced fluorescence emission.

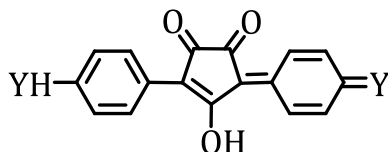
Another interesting aspect of these dye molecules is their ability to undergo intermolecular interactions and form H-type and J-type aggregates. By making use of this property, we have demonstrated the possibility of tuning the absorptive range of a photoelectrochemical cell. These dyes when deposited as thin film on optically transparent electrodes or on nanostructured TiO₂ film resulted in H-aggregates with a blue-shifted absorption maximum at 660 nm. The excitons formed upon excitation of the dye aggregates undergo charge separation at the TiO₂ and SnO₂ interfaces. The H-aggregates in the thin film are photoactive and produce anodic current when employed in a photoelectrochemical cell. Our results reveal that the suitably substituted croconaine dyes can have potential applications as probes for divalent metal ions and also in dye sensitized solar cells.

4.2. INTRODUCTION

Dyes that absorb or emit in the long wavelength (> 650 nm) region of the optical spectrum have gained increasing attention in the last few years,¹ especially because of their potential optoelectronic² and biomedical³ applications.⁴ Several attempts have been made towards developing compounds that absorb in the near-infrared (NIR) region. One commonly employed approach is to increase the extent of π conjugation, however, this would eventually lead to its convergence limit.⁵ Further, most of the near-infrared absorbing dyes require tedious synthetic methodologies.⁶ Of these, cyanine dyes have received considerable attention as NIR dyes due to their remarkable absorption and emission properties.⁷ However, photobleaching and low chemical stability of these dyes has necessitated the development of alternate dyes with absorption in the infrared (IR) region including squaraines and croconaines.⁸

The interest in IR dyes as indicators and labels grew strongly in the last decade,⁹ triggered by significant advances in optical detection and imaging technologies.¹⁰ Two of the main advantages of operating in the IR region are the virtually negligible background absorption and the absence of autofluorescence.¹¹ In this context, there is an intense search for potent IR fluorophores.^{12,13} On the other hand, most IR dyes show intense

absorption bands because their chromophores are characterized by a highly conjugated and often largely extended π -electron system.¹⁴

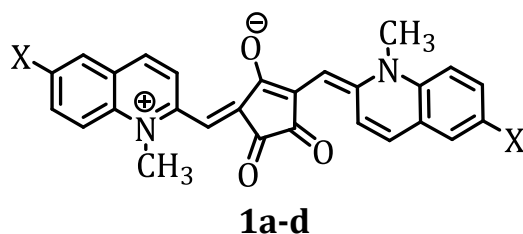


Croconaine dye (**CR**)

Chart 4.1

Croconaines are a class of dyes possessing sharp and intense absorption bands in the near-infrared to infrared region (Chart 4.1) and can, in general, be considered as an acceptor in conjugation with two donors, D-A-D.¹⁵ Although, croconaine dyes are the higher homologues of squaraine dyes, the photophysical and photochemical properties of these dyes have not been studied extensively.¹⁶ These dyes are usually prepared by the condensation between croconic acid and an electron rich aromatic, heteroaromatic or olefinic compounds in a one-step reaction. In this context, we synthesized quinoline based croconaine dyes **1a-d**, absorbing in the infrared region (Chart 4.2) and examined the potential use of these dyes as probes for metal ions and also in solar cell applications. Our results indicate that the croconaine dyes undergoes efficient interactions with various metal ions leading to chelation enhanced fluorescence intensity.^{17a}

In addition to this, the thin films of the croconaine dyes can generate photocurrent when employed in an electrochemical cell.^{17b}



a) X= H , **b)** X= Br , **c)** X= I,

d) X =

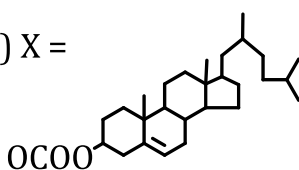
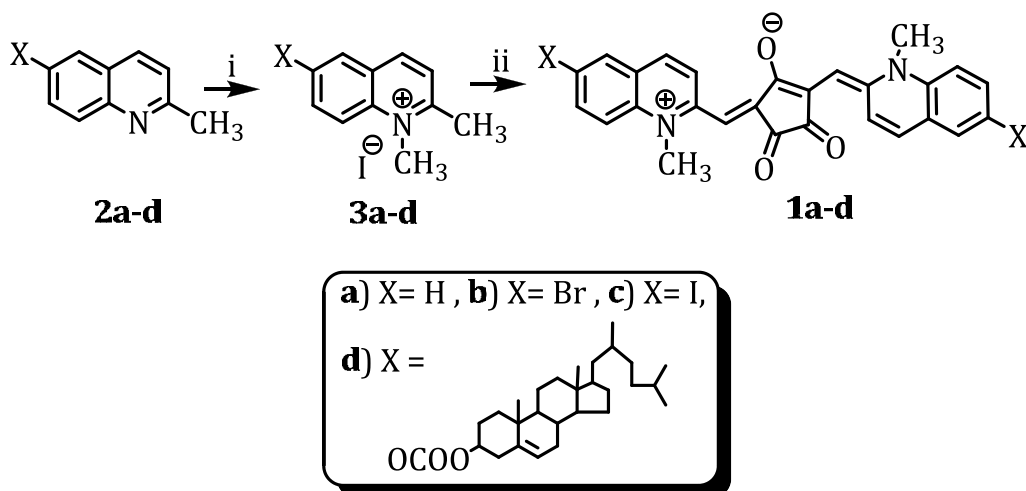


Chart 4.2

4.3. RESULTS

4.3.1. Synthesis of Croconaine Dyes

The synthesis of the dyes **1a-c** has been achieved by the condensation reaction between 2:1 equivalents of the quinaldinium salts **3a-c** and croconic acid in ethanol at 80 °C using quinoline as catalyst. The quinaldinium salts **3a-d**, in turn, was isolated by the reaction of the substituted quinaldines **2a-d** with methyl iodide at 100 °C in a sealed tube.¹⁸ With a view to improving the solubility and cellular permeability of the dyes, cholesterol anchored croconaine dye **1d** was synthesized from the corresponding quinaldinium salt **3d**, following the same synthetic strategy



i) Methyl iodide, 100 °C, 12 h; ii) croconic acid, ethanol, quinoline, 80 °C, 12 h

Scheme 4.1

as in the previous cases. The reaction mixture following work up and column chromatography gave the cholesterol linked croconaine dye **1d** in 75% yield. All the croconaine dyes were characterized on the basis of analytical and spectral techniques. For example, in the ^1H NMR spectrum of the unsubstituted croconaine dye **1a** in $\text{DMF-}d_6$, showed the aromatic protons in the range from δ 7.5-7.3 ppm, while the 3-H proton appeared as a doublet at 8.9 ppm with $J = 9.4$ Hz. In addition, the olefinic proton can be seen as a sharp peak at δ 6.4 ppm, while the *N*-methyl protons appear as a singlet at δ 3.9 ppm. In the FTIR spectrum, the characteristic carbonyl stretching frequency of the croconyl ring appeared at 1604 and 1558 cm^{-1} . The FAB mass analysis showed a molecular mass of 420.14, which corresponds to the molecular formula $\text{C}_{27}\text{H}_{20}\text{N}_2\text{O}_3$ of the croconaine dye **1a**.

4.3.2. Photophysical Properties of Croconaine Dyes

The croconaine dyes **1a-d** showed sharp and intense absorption in the infrared window with absorption maximum ranging from 840-875 nm and high molar extinction coefficients in the range $\epsilon = 1-5 \times 10^5 \text{ M}^{-1} \text{ cm}^{-1}$. Figure 4.1 shows the absorption spectra of the various croconaine dyes. The unsubstituted croconaine dye **1a** showed absorption maximum at 840 nm in DMF, while the halogenated dyes **1b** and **1c** exhibited absorption maximum, which is *ca.* 20 nm red-shifted from the parent unsubstituted derivative, 860 and 865 nm, respectively (Table 4.1). The dyes **1a-c** have low solubility in common organic solvents. However, the substitution of quinaldine ring with the cholesterol moiety resulted in increased solubility of the dye **1d** in THF and CHCl_3 . The dye **1d** showed an absorption maximum at 871 nm in THF.

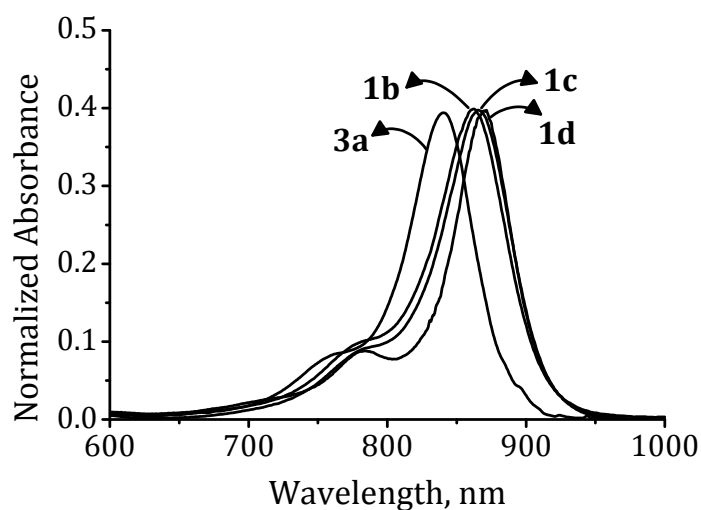


Figure 4.1. Normalized absorption spectra of the croconaine dyes **1a-d**.

All these dyes were found to have negligible fluorescence quantum yields and hence their singlet excited state characterization using emission spectroscopy was difficult and femtosecond transient absorption spectroscopy was employed to probe the excited state behaviour of the croconaine dyes. The time-resolved spectra of the transients recorded following 775 nm laser pulse excitation of the croconaine dye **1d** in CH₂Cl₂ are shown in Figure 4.2. The formation of singlet excited state can be seen from the transient absorption spectrum recorded immediately after 130 fs laser pulse excitation. The difference in the absorption spectra shows a broad absorption peak in the visible region with split maxima at 630 and 720 nm. The decay of this absorption band in the visible region parallels

Table 4.1. Excited-State Properties of Croconaine Dyes^a

Dye	λ_{max} , nm Abs	ϵ , M ⁻¹ cm ⁻¹	S ₁ -S _n abs max, nm	Excited singlet lifetime (ps)
1a ^b	842	1.3 x 10 ⁵	-	-
1b ^b	861	1.9 x 10 ⁵	630, 720	7.3
1c ^b	865	1.4 x 10 ⁵	635, 685	4.4
1d ^c	865	4.2 x 10 ⁵	630, 720	4.1

^aAverage of more than 2 experiments and the error is ca. \pm 5 %. ^bDMF. ^cCHCl₃.

the bleaching recovery at 860 nm. The excited state lifetime, as monitored from the decay at 630 nm, is 7.3 ps. The excited singlets of **1b** and **1c** also show similar broad absorption in the 600-720 nm region and exhibit lifetimes of 4.4 and 4.1 ps in DMF, respectively. The decreased lifetime of these dye singlets as compared to **1d** is expected to arise from the difference in the solvent medium.

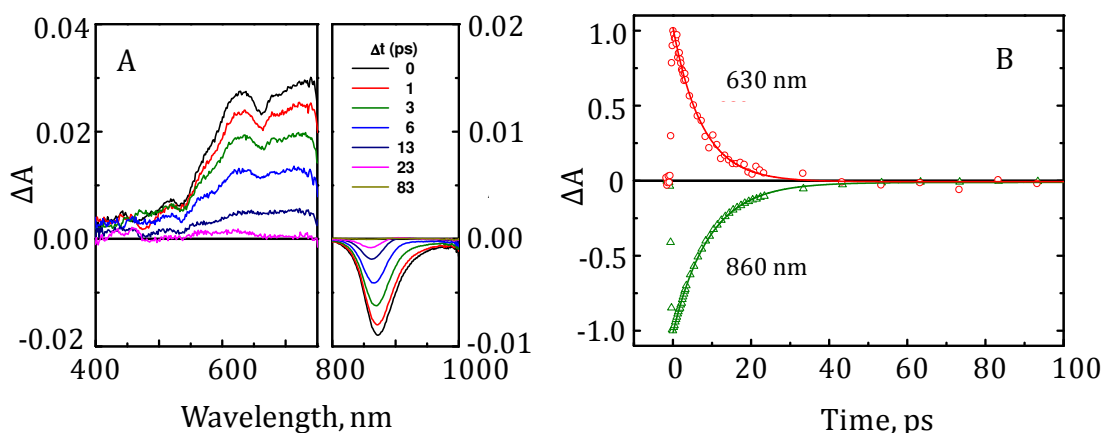
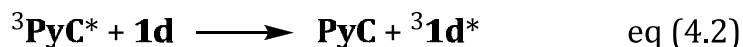


Figure 4.2. Transient absorption spectra recorded following the 775 nm laser pulse excitation of **1d** in CH_2Cl_2 . (A) Time resolved absorption spectra recorded at 0, 1, 3, 6, 13, 23 and 83 ps and (B) absorption-time profiles recorded at 630 and 860 nm.

The bleaching recovery for all three dyes was completed within ~ 40 ps. This complete recovery of the ground state in turn indicates the absence of long-lived transients and confirms that the singlet excited state is the only transient formed when monomer croconaine dye is excited with 775 nm laser pulse. Absence of long-lived transient rules out the possibility of intersystem crossing in the formation of triplet excited state. The side chain

modification with Br, I or cholesterol group had little effect on the formation or deactivation of the croconaine dye singlet excited states.

Since the intersystem crossing efficiency was found to be negligible under direct excitation of the croconaine dyes, triplet-triplet (T-T) energy transfer method was adopted to characterize the triplet excited state of these dyes.¹⁹ Pyrenecarboxaldehyde, **PyC** ($E_T = 186$ kcal/mole; $\lambda_{\max} = 440$ nm and $\epsilon_{\max} = 20000$ M⁻¹cm⁻¹) in CH₂Cl₂ was used as a sensitizer to transfer triplet energy to **1d** in a nanosecond laser flash photolysis set up (equations 4.1 and 4.2).



The transient absorption spectrum recorded immediately after 355 nm laser pulse excitation of **PyC** shows absorption maximum at 440 nm, corresponds to the triplet excited state (spectrum *a* in Figure 4.3). In presence of **1d**, the deactivation of the pyrene triplet proceeds via T-T energy transfer as illustrated in equation 4.2. This is evident from the growth of a new absorption band in the visible region (spectra *b* and *c* in Figure 4.3). The broad absorption band seen around 500 and 680 nm corresponds to the triplet of excited state of **1d**. The bimolecular rate as determined from the dependence of pseudo-first order decay rate constant

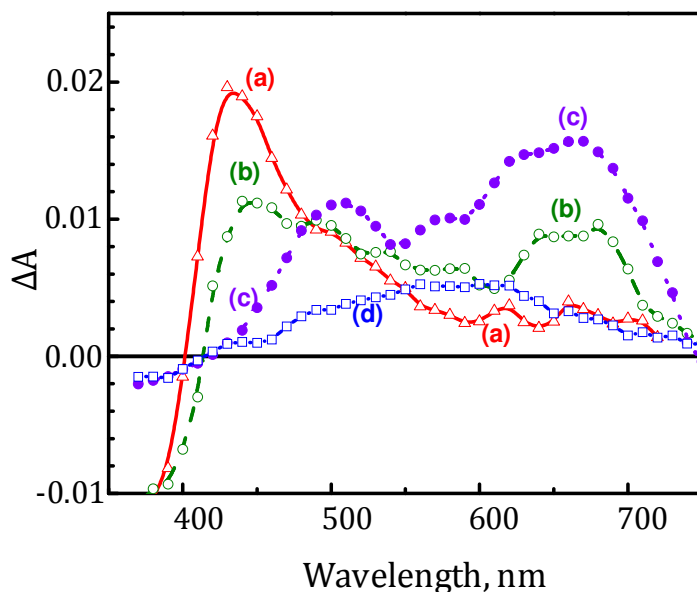


Figure 4.3. T-T energy transfer between excited 0.1 mM **PyC** and 0.02 mM **1d** in dichloromethane. Time-resolved spectra were recorded following 355 nm laser pulse excitation: (a) 50 ns (b) 500 ns (c) 5 μ s and (d) 20 μ s.

of **PyC** triplet on the concentration of **1d** is $1.8 \times 10^{10} \text{ M}^{-1}\text{s}^{-1}$. If we assume energy transfer to be 100%, we can determine the extinction coefficient of triplet excited state of **1d**. By comparing the maximum absorbance values and the extinction coefficient of **PyC** triplet, we obtained a value of 15500 $\text{M}^{-1}\text{cm}^{-1}$ for **1d** triplet at 680 nm. The triplet excited state of **1d** is relatively long lived (lifetime of 7.2 μ s) compared to its singlet excited state (7.3 ps). Spectrum *d* in Figure 4.3 shows the residual absorption following the decay of triplet excited state. The formation of the photoproduct is an indication of the photochemical reactivity of triplet excited state. Since the triplet excited state has a longlife, if formed under direct excitation, we could have seen a long-lived transient in Figure 4.2. These results further confirm that

the intersystem crossing is a minor pathway in the deactivation of the singlet excited state of the croconaine dyes.

4.3.3. Study of Interactions with Mono- and Divalent Metal Ions

With a view to investigate the ability of the croconaine dyes **1a-d** as bidentate ligands and thereby their potential use as probes, we have carried out their interactions with various mono- and divalent metal ions such as Li⁺, Na⁺, K⁺, Ag⁺, Ca²⁺, Mg²⁺, Zn²⁺, Pb²⁺ and Cd²⁺ ions. The derivative **1d** was selected as a representative example, because of its higher solubility and stability. Figure 4.4A shows the changes in the absorption spectrum of the dye **1d** on addition of Zn²⁺ ions. With increasing concentration of Zn²⁺ ions, we observed a decrease in the absorption band at 871 nm, with the concomitant formation of the band at 788 nm. The corresponding changes in the fluorescence spectra of the dye **1d** with increasing addition of the metal ions are shown in Figure 4.4B. The dye **1d** alone is weakly fluorescent. With the addition of Zn²⁺ ions, a significant increase in the fluorescence intensity was observed with an emission maximum at 814 nm.

The progressive increase in the fluorescence intensity reached saturation with the addition of 0.5 equivalents of the metal ions and *ca.* 28-fold fluorescence enhancement could be observed with Zn²⁺ ions ($\Phi = 2.5 \times$

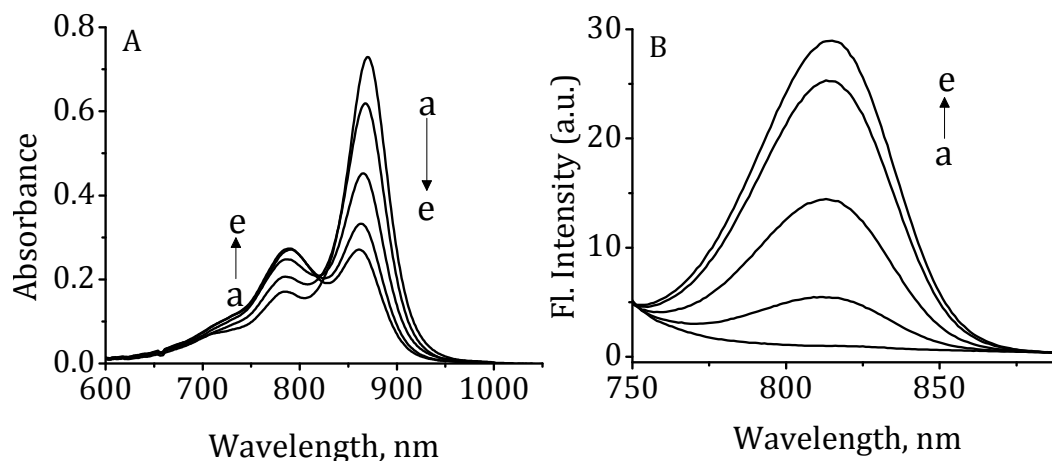


Figure 4.4. Changes in the (A) absorption and (B) emission spectra of the croconaine dye **1d** (7.75 μM) in THF with the addition of Zn^{2+} ions, a) 0, and e) 3.87 μM . Excitation wavelength, 700 nm.

10^{-3}). The stoichiometry of the complex formed between the croconaine dye **1d** and the representative metal ion Zn^{2+} ions was found to be 2:1 as evident from the Job's plot (Figure 4.5).^{1c} Benesi-Hildebrand analysis²⁰ of the complex formation between the dye **1d** and Zn^{2+} ions was studied by following the changes in the fluorescence spectra. These analysis gave a binding constant of $1.1 \pm 0.3 \times 10^7 \text{ M}^{-1}$, which is in good agreement with the value obtained from the absorption changes.

The interaction of the dye **1d** with different alkali, alkaline earth, transition and heavy metal ions was also examined. The complexation of **1d** with other metal ions led to the formation of a new absorption band characteristic of the complexation with the corresponding metal ions. For example, with the addition of Pb^{2+} ions to the dye solution in THF, a decrease in the band corresponding to the dye at 871 nm was observed,

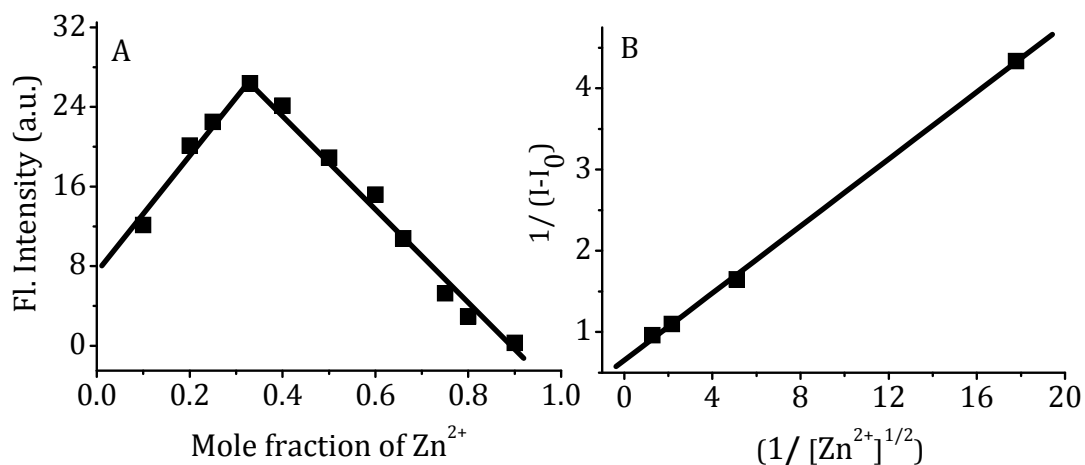


Figure 4.5. (A) Job's plot for the complexation of the croconaine dye **1d** with Zn²⁺ ions in THF. Figure B shows the Benesi-Hildebrand analysis of the emission changes for the complexation between the dye **1d** and Zn²⁺ ions.

with the concomitant formation of a new band at 735 nm (Figure 4.6A). With increasing concentration of Pb²⁺ ions, the initially weakly fluorescent dye showed *ca.* 26-fold enhancement in fluorescence intensity ($\Phi = 2.2 \times 10^{-3}$) with the emission maxima at 816 nm (Figure 4.6B). Similar observations have been made with Cd²⁺ ions; however, the new band corresponding to the [**1d**-Cd²⁺] complex was observed at 804 nm and *ca.* 14-fold fluorescence enhancement ($\Phi = 1.4 \times 10^{-3}$) was observed with emission maxima at 818 nm. Based on the fluorescence data, the binding constants for Pb²⁺ and Cd²⁺ ions were calculated and these values are found to be $6.5 \pm 0.5 \times 10^6 \text{ M}^{-1}$ and $2.6 \pm 0.3 \times 10^6 \text{ M}^{-1}$, respectively. The relative changes in the fluorescence intensity of the croconaine dye **1d** upon the addition of different metal ions are shown in Figure 4.7.

The monovalent metal ions such as Li^+ , Na^+ and K^+ ions caused negligible changes in the absorption and fluorescence spectra. In contrast, the addition of other divalent metal ions like Pb^{2+} , Cd^{2+} , Mg^{2+} , Hg^{2+} , Ca^{2+} and Ba^{2+} ions showed significant affinity for the dye resulting in the chelation

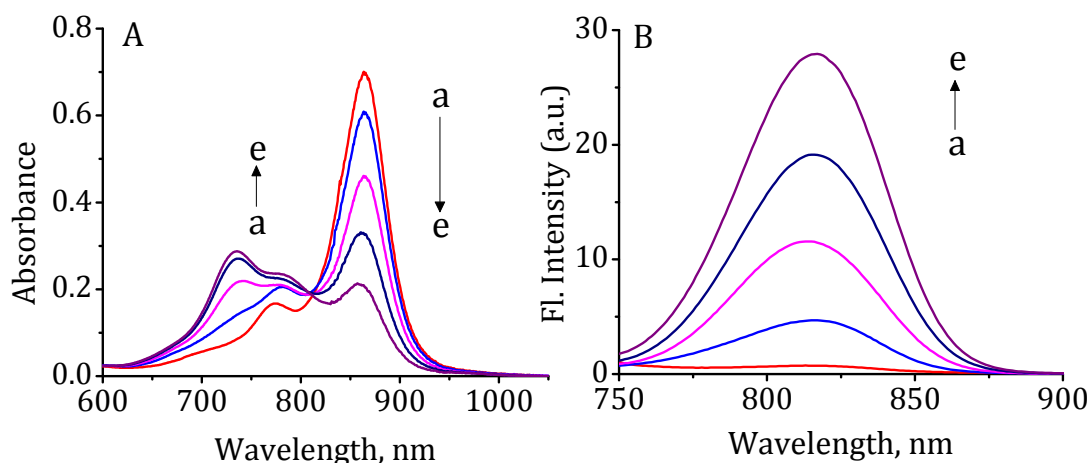


Figure 4.6. Changes in the (A) absorption and (B) emission spectra of the dye **1d** ($7.75 \mu\text{M}$) in THF with the addition of Pb^{2+} ions. $[\text{Pb}^{2+}]$ a) 0, and e) $3.87 \mu\text{M}$. Excitation wavelength, 700 nm.

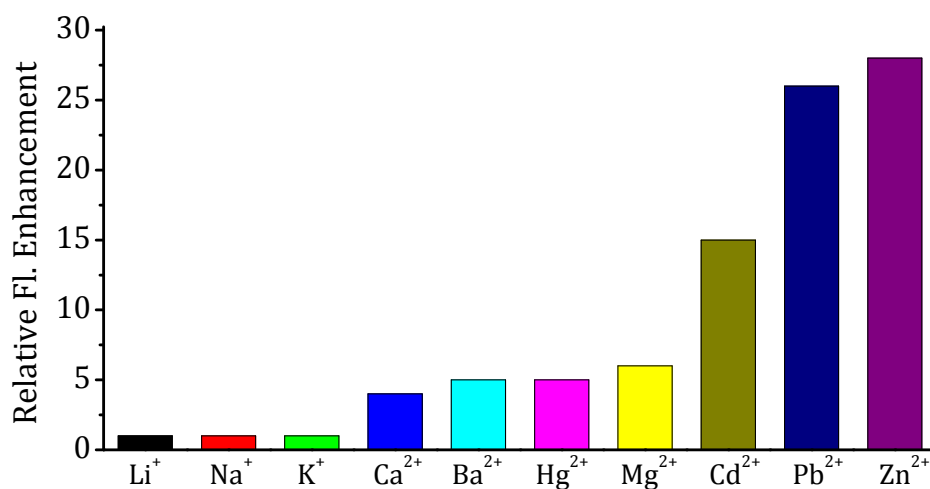


Figure 4.7. Relative fluorescence enhancement of the croconaine dye **1d** ($7.75 \mu\text{M}$) upon interaction with different metal ions.

enhanced fluorescence intensity. However, the relative changes were found to vary with different metal ions. Similar, but less significant effects were observed in the absorption and emission spectra of the dye **1d** upon adding other divalent metal ions like Mg²⁺, Hg²⁺, Ba²⁺ and Ca²⁺ ions. The absorption and emission maxima as well as the association constants calculated for the various metal complexes of **1d** are summarized in Table 4.2. As shown in

TABLE 4.2. Absorption and fluorescence maxima, association constants and quantum yields of the various metal ion complexes of **1d** in THF.^a

Complex	λ_{\max} , nm		Φ_F^b	Association constant (K), ^c M ⁻¹
	Abs	Em		
[1d -Zn ²⁺]	788	814	2.5×10^{-3}	$1.1 \pm 0.3 \times 10^7$
[1d -Pb ²⁺]	735	816	2.2×10^{-3}	$6.5 \pm 0.5 \times 10^6$
[1d -Cd ²⁺]	804	818	1.4×10^{-3}	$2.6 \pm 0.3 \times 10^6$
[1d -Mg ²⁺]	805	815	5.5×10^{-4}	$3.2 \pm 0.4 \times 10^6$
[1d -Ba ²⁺]	750	818	4.7×10^{-4}	$8.0 \pm 0.2 \times 10^5$
[1d -Hg ²⁺]	735	812	4.2×10^{-4}	$2.6 \pm 0.3 \times 10^5$
[1d -Ca ²⁺]	755	820	3.2×10^{-4}	$1.3 \pm 0.4 \times 10^5$

^aAverage of more than 2 experiments and the error is ca. $\pm 5\%$. ^bFluorescence quantum yields were calculated using indocyanine-green (IR-125) as the standard ($\Phi = 0.13$, in DMSO). ^cAssociation constants were calculated based on fluorescence changes.

the table, the [**1d**-Mⁿ⁺] complexes have absorption maxima in the range 735-805 nm, while the emission maxima is in the range 812-820 nm. For example, the absorption and emission maxima for the complex [**1d**-Zn²⁺] was observed at 788 and 814 nm with association constant $1.1 \pm 0.3 \times 10^7$ M⁻¹, while for the [**1d**-Ba²⁺] complex, we observed a lower value of $8.0 \pm 0.2 \times 10^5$ M⁻¹.

4.3.4. Characterization of Metal Ion Complexation

The complexation between various metal ions and the dye **1d** was confirmed through ¹H NMR and infrared (FTIR) spectral analysis of the complex. The ¹H NMR spectrum of the croconaine dye **1d** in CDCl₃ showed five aromatic protons as multiplets in the region between δ 7-9.1 ppm,

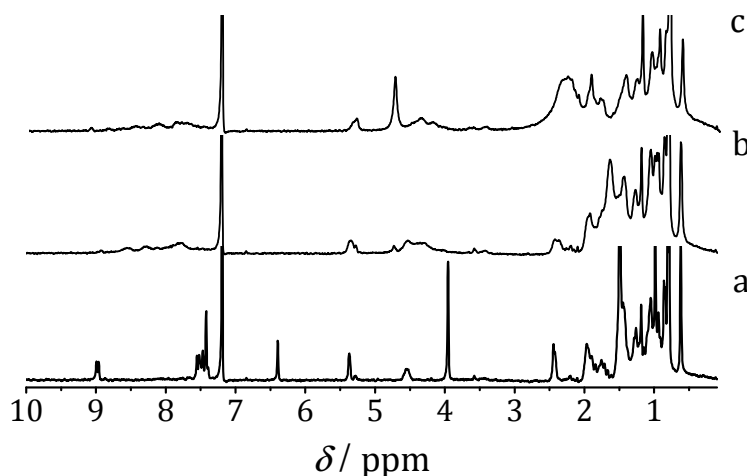


Figure 4.8. ¹H NMR spectra of the dye **1d** in CDCl₃ with increasing concentration of Zn²⁺ ions in CD₃CN. The mole ratio of [Zn²⁺] to [**1d**] is a) 0, b) 0.25 and c) 0.5.

while the olefinic and *N*-methyl protons appeared as singlets at δ 6.4 and 3.9 ppm, respectively (Figure 4.8). With the addition of Zn^{2+} ions, a broadening of the aromatic signals as well as the olefinic and *N*-methyl protons could be observed.

The infrared (FTIR) spectrum of the dye **1d** is shown in Figure 4.9. The bands at 1660, 1598 and 1560 cm^{-1} , are characteristic of the carbonyl groups of the croconyl moiety, while the band at 1755 cm^{-1} is assigned to the carbonyl group attached to the cholesterol moiety. The FTIR spectrum of the [**1d**- Zn^{2+}] complex showed the carbonyl band at 1610 cm^{-1} , while the bands at 1598 and 1560 cm^{-1} were merged to give a new band at 1564 cm^{-1} . This clearly indicates the involvement of two carbonyl groups of the croconyl moiety of **1d** in the complexation with Zn^{2+} ions. As expected, the

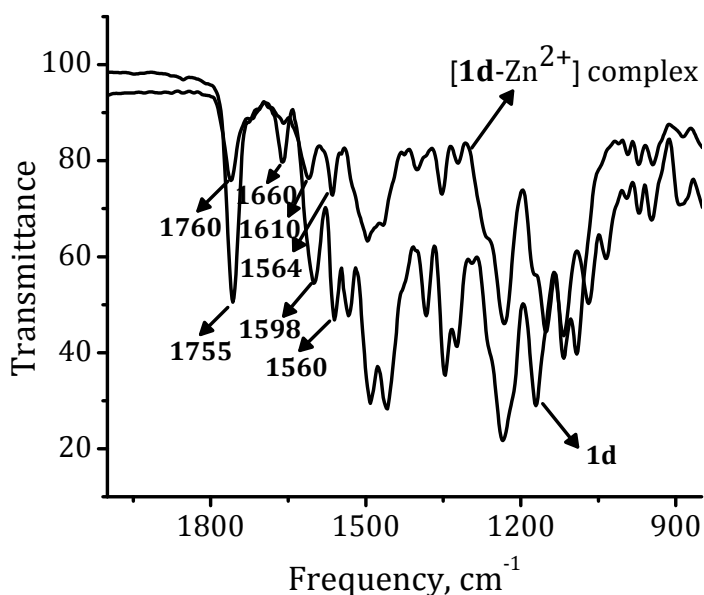


Figure 4.9. IR spectra of the croconaine dye **1d** and the [**1d**- Zn^{2+}] complex.

band at 1755 cm⁻¹ corresponding to the carbonyl group attached to the cholesterol moiety showed negligible changes. Moreover, no significant changes were observed in the protons of the aliphatic region in the ¹H NMR spectrum of the [**1d**-Zn²⁺] complex, indicating that the cholesterol moiety has no significant interactions with the metal ions.

4.3.5. Light Harvesting Properties of Croconaine Dyes

Dye sensitization of nanocrystalline semiconductors have attracted considerable attention since Grätzel first reported on the highly efficient ruthenium complex sensitized nanocrystalline TiO₂-based dye sensitized solar cell (DSSC).²¹ Polypyridyl complexes of ruthenium, such as N3 dye,^{21a} and the 'black dye'^{21e} have been reported to have solar energy to electricity conversion of up to 10.4%. Various sensitizers based on coumarin,²² indoline,²³ cyanine,²⁴ hemicyanine,²⁵ merocyanine,²⁶ perylene,²⁷ xanthene,²⁸ triarylamine,²⁹ squaraine³⁰ and thiophene³¹ have been explored. Since the croconaine dyes under investigation exhibit intense absorption in the infrared region, it was our interest to investigate the potential of these dyes as sensitizers in solar cells.

One of the possible ways to utilize the croconaine dyes for harvesting infrared photons (in a photoelectrochemical cell) is to cast thin films on the electrode surface. Two different approaches were adopted for casting the

films of the croconaine dye **1d** in the electrode surface. A drop cast method was employed to cast thin film of **1d** on glass slide by applying the chloroform solution and air drying, while the other method involved the assembling of the dye molecules as thin films on nanostructured TiO₂ and SnO₂. The absorption spectra of the dye film cast on conducting glass and the dye molecules deposited on TiO₂ and SnO₂ films are shown in the Figure 4.10. The dye film cast on the conducting glass exhibits blue-shifted absorption band with a maximum at 660 nm, indicating thereby, the formation of H-aggregates under these conditions.³² The presence of both monomer and aggregate forms are evident from the absorption spectra as shown in Figure 4.10 (traces b and c).

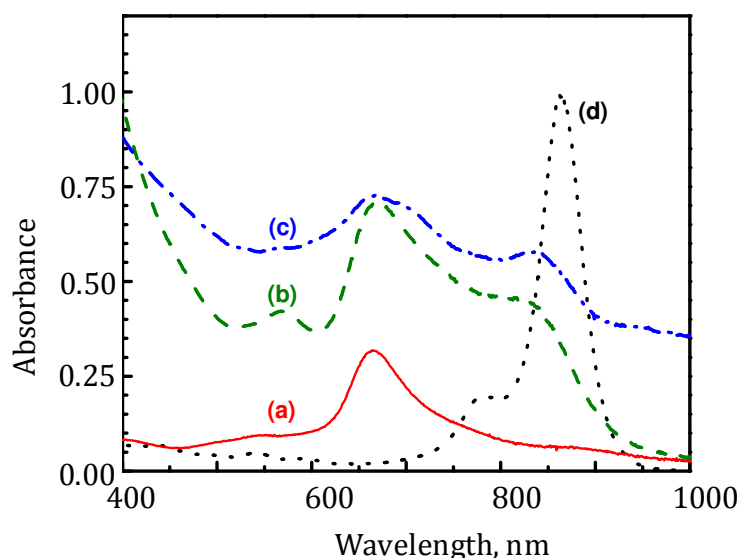


Figure 4.10. Absorption spectra of the croconaine dye **1d** cast or deposited on (a) glass slide using drop cast method, (b) nanostructured TiO₂ film, (c) nanostructured SnO₂ film using dip-adsorption method and (d) monomer solution spectrum.

The observation of smaller peaks in the higher energy region (e.g., 560 nm) is indicative of higher ordered aggregates such as trimer and tetramer of **1d**. The broadness of the aggregation peak indicates the degree of randomness of the aggregates formed in these films. As compared to the solution spectrum, the absorption peak of the monomer dye on TiO₂ and SnO₂ surface is slightly blue shifted with maximum around 840 nm. The presence of monomer form in these films indicates that the surface of the oxide particles promotes dispersion of dye molecules without aggregation.

The excited state behaviour of the croconaine dye films were further investigated using pump-probe spectroscopy. Figure 4.11 shows the time-resolved absorption spectra recorded following 775 nm excitation of **1d** film cast on conducting glass electrode. A difference absorption peak at 610

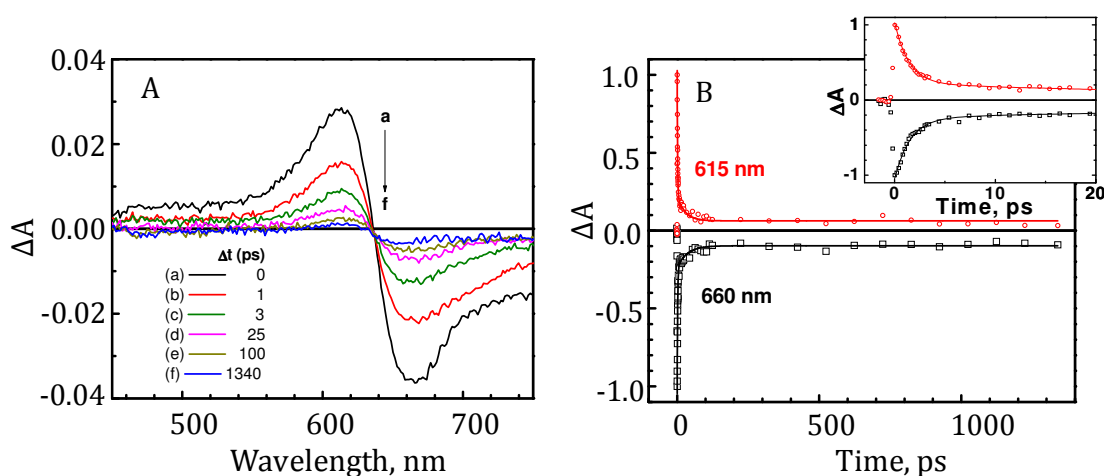


Figure 4.11. Transient absorption spectra recorded following the 775 nm laser pulse excitation of **1d** film on glass. (A) Time resolved absorption spectra recorded at 0, 1, 3, 25, 100 and 1340 ps and (B) the absorption-time profiles recorded at 615 and 660 nm.

nm and bleaching at 670 nm can be seen as the excitonic state of the dye aggregate is generated using infrared laser excitation. The transient decay when fitted to biexponential decay analysis, gave lifetime values of 1.1 and 7.6 ps. The inhomogeneity of the aggregates in the film is expected to influence the decay kinetics and contribute to the deviation from the monoexponential decay behaviour.

The excited singlet of H-aggregate is nonfluorescent because of the forbidden transition between the lower excited singlet level and ground state.³³ Thus, the excited H-aggregates undergo intersystem crossing to produce relatively long-lived triplet species. More than 98% of the bleached dye is recovered in ~30 ps. Based on this observation, we can conclude that the intersystem crossing is not a dominant deactivation pathway for the excited dimer of **1d**. Further, the excited state or excitonic state formed with direct excitation of the dye aggregate on a glass surface undergoes rapid annihilation without producing charge separated state or triplet excited state. In order to see whether the semiconducting property of TiO₂ and SnO₂ can influence the charge separation process, we evaluated the transient spectra following laser pulse excitation of **1d** films.

Figure 4.12 compares the transient spectra recorded following the 387 nm laser pulse excitation of the **1d** film on glass and TiO₂ surface. The higher energy of the laser pulse chosen for this experiment ensured the excitation of all aggregated forms of the dye in the film. Neither the SnO₂ or

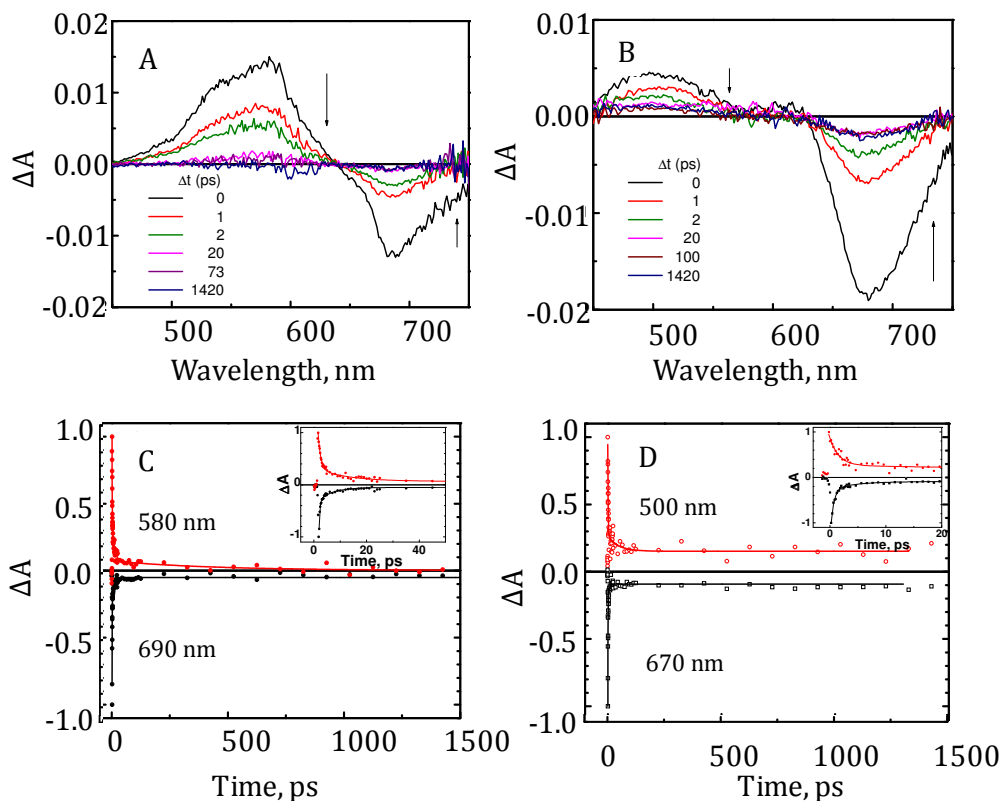
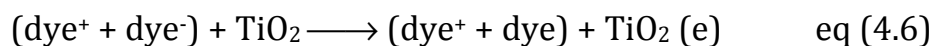
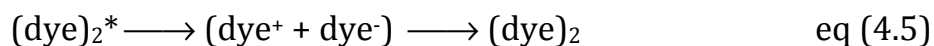


Figure 4.12. Transient absorption spectra recorded following the 387 nm laser pulse excitation of **1d** film on (A) glass and (B) nanostructured TiO_2 film. The absorption-time profiles recorded for (C) **1d** film on glass at 580 and 690 nm and (D) nanostructured TiO_2 film at 500 and 670 nm.

TiO_2 ($E_g > 3.5$ eV) substrate can be directly excited with 387 nm laser pulse. The transient absorption and decay behavior of the **1d** films on the glass surface was similar to the one observed with 775 nm laser pulse excitation. Any higher energy states formed during 387 nm laser pulse excitation are quickly relaxed to form the excitonic state similar to the 775 nm laser pulse excitation. The transient decay deviates from the monoexponential behavior. The biexponential kinetic analysis of the transient decay yielded lifetimes of 1 and 11 ps.

Interestingly, a different type of transient absorption behaviour was observed on the TiO₂ surface with a broad maximum around 500 nm. The bleaching in the 670 nm confirms that the origin of the transient is still centered on the dimer of **1d**. Upon fitting the transient decay at 500 nm to biexponential kinetic analysis, we obtain lifetimes of 0.5 and 3.4 ps. Two notable differences emerge from these experiments. (i) The transient observed on the TiO₂ and SnO₂ surface exhibits blue shifted absorption compared to the excitonic absorption on the glass surface. (ii) The initial decay times of the transient on the TiO₂ and SnO₂ surface are shorter than the one observed on the glass surface and formation of long-lived transient is also visualized from the residual bleaching at 690 nm. These results suggest that a significant fraction of the excitonic state of the aggregate dye dissociates at the TiO₂ surface to generate the charge separated pair.

The transient absorption around 500 nm is attributed to the charge separated state. Most of these separated charges undergo recombination, however, a small fraction (<10%) of the charge separated state is stabilized as the electrons are trapped within the TiO₂ particles. The possible reaction pathways with which the excited dye aggregates in the film undergo deactivations are summarized in equations 4.3-4.6. If indeed TiO₂ is capable of accepting electrons from the charge separated dye aggregate, we should be able to collect these charges at the electrode surface in a photoelectrochemical cell.



4.3.6. Photocurrent Generation at Dye Modified TiO₂ Electrode

The nanostructured TiO₂ film was first cast on a conducting glass electrode (OTE/TiO₂) using TiO₂ colloids. The dye **1d** deposited on the TiO₂ surface (referred as OTE/TiO₂/**1d**) was found to be photoactive and generates photocurrent in a photoelectrochemical cell when irradiated with light. Figure 4.13 shows the photocurrent response to On-Off cycles of illumination and the power characteristics of the cell. The photocurrent response is prompt and reproducible at several cycles of illumination. As the electrons are transported towards the collecting electrode surface, the dye is regenerated by the redox couple (I₃⁻/I⁻) at the electrolyte interface. A maximum current of 0.23 mA/cm² and a photovoltage of 190 mV was observed for visible-IR illumination (100 mW/cm²) of the electrode. Although overall power conversion efficiency is small (<0.1%), the generation of anodic photocurrent confirms the light initiated electron flow towards TiO₂ film and the collecting OTE surface.

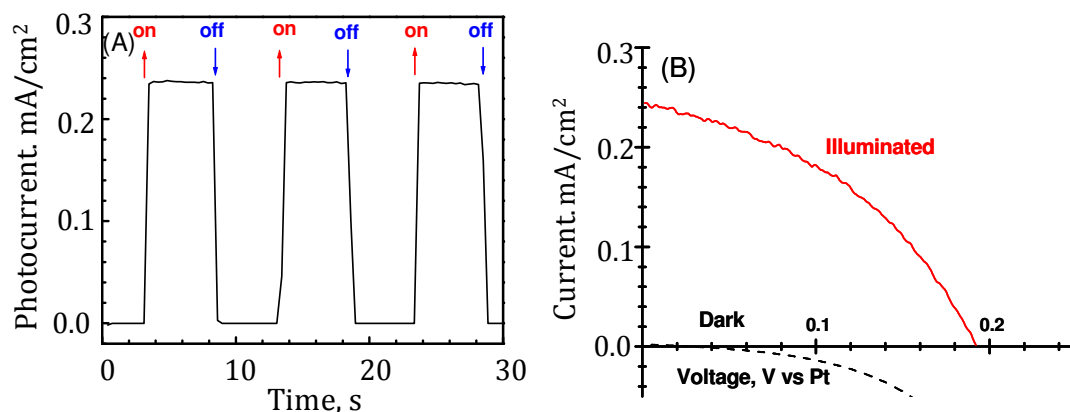


Figure 4.13. (A) Photocurrent response and (B) power characteristics of OTE/TiO₂/CR-1 electrode. Excitation wavelength, >400 nm, 100 mW/cm². Electrolyte: 0.5 M LiI and 0.05 M I₂ in acetonitrile.

The incident photon to charge carrier generation efficiency (*IPCE*) of OTE/TiO₂/**1d** electrode and OTE/SnO₂/**1d** electrode is shown in Figure 4.14. These experiments were carried out in a two arm flat cell and the illumination area was limited to 0.28 cm². The dye **1d** modified OTE/TiO₂ electrode shows photocurrent response in the 500-800 nm region, thus matching the absorption of the H-aggregates. The maximum *IPCE* was ~1.2 % (curve *a*) at 650 nm. The performance of OTE/SnO₂/**1d** electrode was relatively poor with maximum *IPCE* of 0.6%. It is interesting to note that the *IPCE* at longer wavelengths (> 800 nm) is relatively low and there was no contribution from the monomer dye to the photocurrent generation. The blue-shift in the *IPCE* peak compared to the absorption maximum indicate that higher aggregates of dye **1d** contribute to the photocurrent

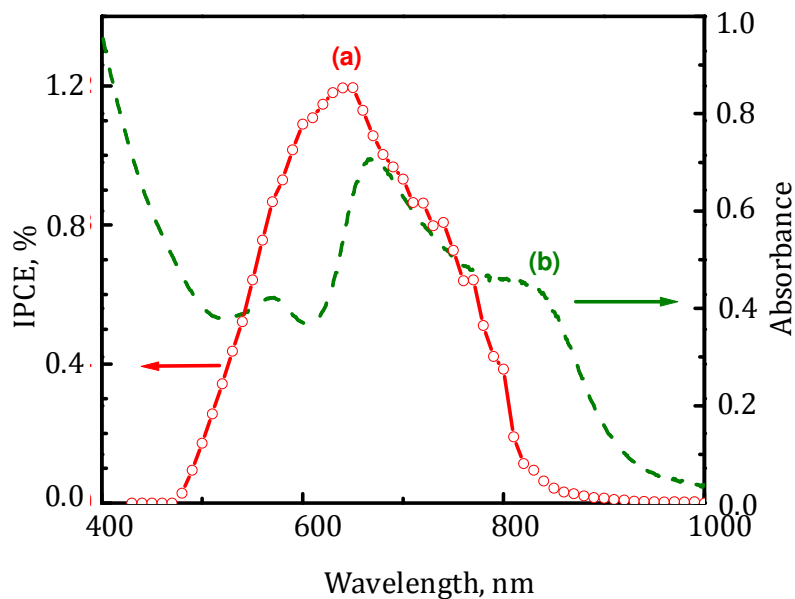


Figure 4.14. Photocurrent response of the OTE/TiO₂/**1d** electrode to monochromatic illumination. The comparison of (a) *IPCE* and (b) absorbance traces show the primary species responsible for photocurrent generation.

generation with greater efficiency. The varying photocurrent generation efficiency of monomers aggregates has been elucidated in earlier studies.³⁴ Compared to the dye **1d**, the other croconaine dyes, **1b** and **1c**, performed poorly and no attempt was made to further evaluate the photoelectrochemical performance of these two dyes.

4.4. DISCUSSION

The ground (S_0) and excited states (S_1) of the croconaine dyes are intramolecular D-A-D charge transfer (ICT) states.³⁵ The S_0 - S_1 electronic excitation in these systems involves a CT process that is primarily confined to the central C₅O₃ cyclopentane ring. The intramolecular charge transfer

character (ICT) of this transition, combined with an extended π conjugation is responsible for the sharp and intense absorption bands of these dyes.

The interaction of the metal ions at the carbonyl group lowers the π conjugation as well as the CT character, resulting in the formation of a hypsochromically shifted absorption band for the dye-metal complex. The formation of the $[1\mathbf{d}-\text{M}^{2+}]$ complex reduced the bond energy of the conjugated C=O bond, leading to the reduction of the carbonyl stretching frequency as seen in the FTIR analysis. In addition, in the ^1H NMR spectra, the peaks corresponding to the aromatic, olefinic and *N*-methyl protons get broadened upon metal ion binding. The presence of electron rich carbonyl oxygen allow only the interaction with divalent metal ions, in a 2:1 binding mode as evidenced through Jobs and Benesi-Hildebrand analysis and the sensitivity of the binding follows the order, $\text{Zn}^{2+} > \text{Pb}^{2+} \gg \text{Cd}^{2+} \gg \text{Mg}^{2+} \approx \text{Hg}^{2+} \approx \text{Ca}^{2+} \approx \text{Ba}^{2+}$ ions (Figure 4.15).

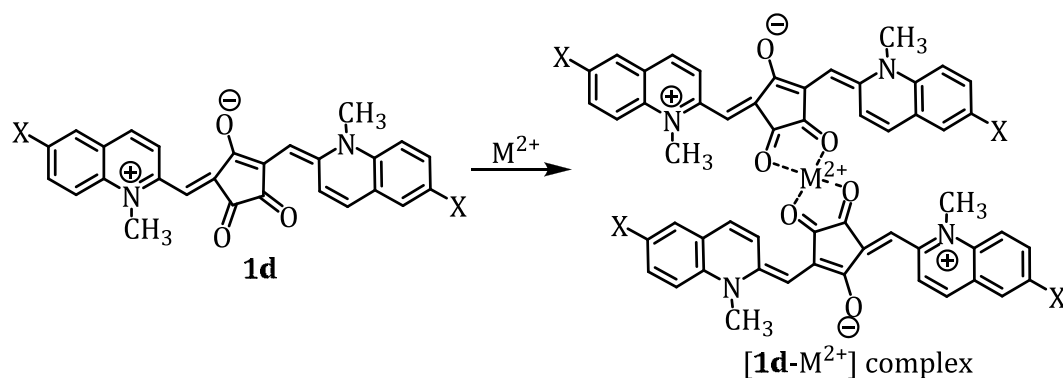


Figure 4.15. Schematic representation of the complexation between divalent metal ion, M^{2+} and the croconaine dye **1d**.

Depending on the nature of substituents and the medium, squaraine and croconaine dyes can form H-aggregates or J-aggregates, (Figure 4.16);³⁶ the formation of which have been explained by the molecular exciton theory. According to this theory, the dye molecule is regarded as a point dipole and the excitonic state of the dye aggregate splits into two levels through the interaction of transition dipoles. The dye molecules can aggregate in a parallel way (plane-to plane stacking) to form a H-aggregate (sandwich-type arrangement) or in a head-to-tail arrangement (end-to end stacking) to form a J-aggregate. A transition to the upper state having parallel transition moments (in parallel aggregates) and to a lower state with perpendicular transition moments (in a head-to-tail arrangement) leads to hypsochromic (blue) and bathochromic (red) shifts, respectively.³⁷

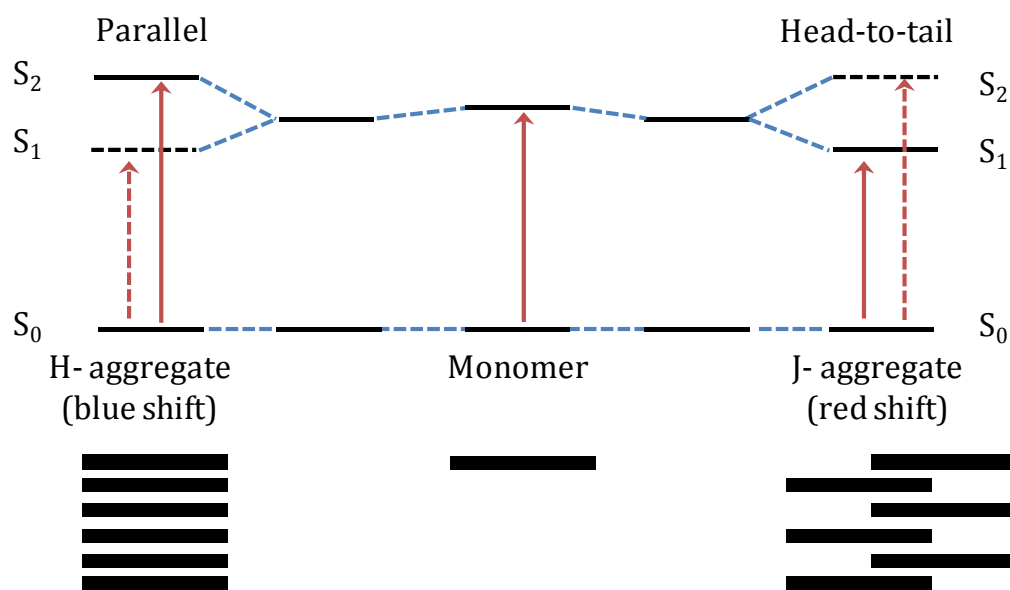


Figure 4.16. Exciton band energy diagram for molecular excitons for H- and J-aggregates.

In the case of the croconaine dye **1d**, it is the H-aggregate of the dye that undergo charge separation over TiO₂ electrode, rather than the monomer dye. In a dye-sensitized photocurrent generation mechanism, the excited singlet of the sensitizing dye directly injects electrons into the TiO₂ particles. The oxidation potential of the ground state dye (**1d**) as determined from the cyclic voltammetry experiment is 1.22 V vs. NHE. This value corresponds to ~ 0.23 V for the oxidation potential of the excited monomer (assuming the singlet energy as 1.45 eV). Since the conduction band energy of TiO₂ (0.5 V vs. NHE) is more negative than the oxidation potential, the excited monomer form of the dye cannot directly participate in the charge injection process. As a result of this energy mismatch, we are not able to observe sensitized photocurrent generation from the monomer. However, the dye aggregates are capable of generating photocurrent as the excitons undergo charge separation and thus contribute to the photocurrent generation.³⁸

4.5. CONCLUSIONS

In conclusion, a new class of substituted quinoline based croconaine dyes was synthesized and their interactions with metal ions and light harvesting properties have been investigated. Due to the presence of a stronger acceptor moiety, these croconaine dyes exhibited around 100 nm

red-shifted absorption compared to the corresponding squaraine dyes. The presence of the two carbonyl groups facilitates complex formation of the croconaine dyes with divalent metal ions. The lowered ICT character and decreased conjugation in the ring resulted in the formation of a new absorption band at lower wavelength region for the dye-metal ion complex and the metal binding is signaled through 'turn on' fluorescence intensity.

The photophysical properties of the croconaine dyes in the monomeric and aggregated forms have been characterized using femtosecond spectroscopy. The excitation of the H-aggregate of the thin films produces excitons, which are capable of undergoing charge separation on the TiO_2 and SnO_2 surface. When the dye molecules adsorbed on TiO_2 films were excited with visible-IR light anodic current generation was observed, wherein only the aggregates contribute to the photocurrent generation. The low *IPCE* of the croconaine dye film shows that the net charge separation is poor. Improvement in the dye aggregate/semiconductor heterojunction is necessary to further improve the efficiency of charge separation. Results of the investigations demonstrate that croconaine dyes act as potential probes for metal ions in the infrared region and also in light harvesting applications.

4.6. EXPERIMENTAL SECTION

4.6.1. General Techniques

The equipment and procedure for spectral recordings are described elsewhere.³⁹ All melting points were determined on a Mel-Temp II melting point apparatus. The IR spectra were recorded on a Perkin Elmer Model 882 infrared spectrometer. The electronic absorption spectra were recorded on a Shimadzu UV-3101 or 2401 PC UV-VIS-NIR scanning spectrophotometer. The fluorescence spectra were recorded on a SPEX-Fluorolog F112X spectrofluorimeter. ¹H and ¹³C NMR spectra were measured on a 300 MHz Bruker advanced DPX spectrometer. Ultrafast (femtosecond) transient absorption experiments were conducted using a Clark-MXR 2010 laser system and an optical detection system provided by Ultrafast Systems (Helios). The source for the pump and probe pulses is the fundamental of the Clark laser system (775 nm, 1 mJ/pulse, fwhm 130 fs, 1 kHz repetition rate). Nanosecond laser flash photolysis experiments were performed with a 355 nm laser pulse (5 mJ, pulse width 6 ns) from a Quanta Ray Nd:YAG laser system. All the solvents used were purified and distilled before use. Fluorescence quantum yields were calculated using IR-125 as the standard (Φ DMSO = 0.13).⁴⁰ Metal ion binding studies were carried out by the addition of equal aliquots of metal ion stock solution in

water to 3 mL of dye in THF.

4.6.2. Materials

Cholester-3-yl-2-methylquinoline-6-yl carbonate (**2d**), mp 101-102 °C (lit. mp 101-102 °C),^{18b} 6-iodo-2-methylquinoline (**2c**), mp 108-109 °C (lit. mp 108-109 °C),⁴¹ 6-bromo-2-methylquinoline (**2b**), mp 95-96 °C (lit. mp 95-96 °C),⁴¹ cholester-3-yl-*N*-methyl-2-quinaldinium-6-yl carbonate iodide (**3d**), mp 216-217 °C (lit. mp 216-217 °C),^{18b} 6-iodo-*N*-methyl-2-quinaldinium iodide (**3c**), mp 222-223 °C (lit. mp 222-223 °C),⁴¹ and 6-bromo-*N*-methyl-2-quinaldinium iodide (**3b**), mp 237-239 °C (lit. mp 237-239 °C)⁴¹ were prepared by modifying the reported procedures. Croconic acid, Hg(ClO₄)₂, Pb(ClO₄)₂, Cu(ClO₄)₂, Zn(ClO₄)₂, Ca(ClO₄)₂, NaClO₄, KClO₄, LiClO₄, Mg(ClO₄)₂ were purchased from Aldrich and used as such.

4.6.3. General Procedure for Synthesis of Croconaine Dyes **1a-d**

A mixture of the corresponding quinaldinium salt (0.06 mmol), croconic acid (0.03 mmol) and quinoline (0.5 mL) was refluxed in ethanol (6 mL) for 24 h. The solvent was distilled off under reduced pressure to obtain a residue, which was washed with methanol and DMSO to give the corresponding croconaine dyes **1a-c**.

1a (80%, based on conversion): mp >300 °C, IR (KBr) ν_{\max} cm⁻¹ 3035, 1604, 1558, 1454; ¹H NMR (DMF-*d*₆, 300 MHz) δ 9.14 (1H, d, *J* = 9.4 Hz), 7.9

(2H, d, $J = 9$ Hz), 7.82 (2H, m), 7.53 (1H, m), 6.46 (1H, s), 4.14 (3H, s); FAB-MS: m/z Calcd for $C_{27}H_{20}N_2O_3$: 420.14. Found: 420.06. Anal. Calcd for $C_{27}H_{20}N_2O_3$: C, 77.13; H, 4.79; N, 6.66. Found: C, 76.92; H, 4.65; N, 6.54.

1b (85%): mp >300 °C, IR (KBr) ν_{\max} cm^{-1} 3055, 1654, 1608, 1543; FAB-MS: m/z Calcd for $C_{27}H_{18}Br_2N_2O_3$: 578.25. Found: 579.35. Anal. Calcd for $C_{27}H_{18}Br_2N_2O_3$: C, 56.08; H, 3.14; N, 4.84. Found: C, 55.74; H, 2.97; N, 5.10.

1c (85%): mp >300 °C, IR (KBr) ν_{\max} cm^{-1} 3055, 1653, 1606, 1546; FAB-MS: m/z Calcd for $C_{27}H_{18}I_2N_2O_3$: 672.25. Found: 672.31. Anal. Calcd for $C_{27}H_{18}I_2N_2O_3$: C, 48.04; H, 2.70; N, 4.17. Found: C, 48.21; H, 2.90; N, 4.16.

Procedure for the synthesis of dye 1d: A mixture of the cholesterol linked quinaldinium salt **3d** (0.06 mmol), croconic acid (0.03 mmol) and quinoline (0.5 mL) was refluxed in ethanol (6 mL) for 24 h. The solvent was distilled off under reduced pressure to obtain a residue, which was then subjected to column chromatography over silica gel. Elution of the column with a mixture (1:9) of methanol and chloroform gave 75% of the croconaine dye **1d**, mp 290-292 °C, IR (KBr) ν_{\max} cm^{-1} 2947, 1755, 1660, 1598, 1560; 1H NMR ($CDCl_3$, 300 MHz) δ 8.99 (2H, d, $J = 9.4$ Hz), 7.55-7.39 (8H, m), 6.39 (2H, s), 5.37 (2H, s), 4.55 (2H, s), 3.95 (6H, s), 2.44 (4H, s), 1.96-0.75 (82H, m); ^{13}C NMR ($CDCl_3$, 75 MHz) δ 196.6, 188.3, 186.8, 183.2, 154.1, 153.1, 140.4, 130.3, 128.2, 124.9, 123.2, 121.4, 118.2, 117.5, 114.3, 111.1, 108.4, 103.3, 81, 73.3, 72.1, 58.2, 57.7, 51.5, 43.8, 41, 37.7, 37.3, 33.4,

31.2, 30.9, 29.7, 29.5, 25.8, 25.4, 24.4, 24.2, 24.1, 22.6, 20.8, 20.3, 13; FAB-MS: m/z Calcd for $C_{83}H_{108}N_2O_7$: 1277.75. Found: 1277.69. Anal. Calcd for $C_{83}H_{108}N_2O_7$: C, 78.02; H, 8.52; N, 2.19. Found: C, 77.85 ; H, 8.3; N, 2.13.

4.6.4. Determination of Stoichiometry of Complexation

In the Jobs plot method, the total molar concentration of the two binding partners (e.g. dye and metal ions) is held constant, but their mole fractions are varied. The fluorescence intensity (or peak area) that is proportional to complex formation is plotted against the mole fractions of these two components. The maximum on the plot corresponds to the stoichiometry of the two species if sufficiently high concentrations are used.

4.6.5. Determination of Association Constants

The binding affinities of the semisquaraine dyes were calculated using Benesi-Hildebrand equation 4.7 for 2:1 stoichiometry, where K is the equilibrium constant, I_0 is the fluorescence intensity of the free dye, I is the observed fluorescence intensity in the presence of metal ions and I_s is the fluorescence intensity at saturation. The linear dependence of on the reciprocal of square root of the metal ion concentration indicates the formation of a 2:1 complex between the dye and the metal ion.

$$\frac{1}{I - I_0} = \frac{1}{I - I_s} + \frac{1}{K(I - I_0)[M^{n+}]^{1/2}} \quad \text{eq (4.7)}$$

4.6.6. Preparation of Electrodes

To prepare the SnO₂ Electrodes (OTE/SnO₂), the SnO₂ (15%) suspension obtained from Alfa chemicals was first diluted (1 mL of SnO₂ solution with 47 mL of water and 2 mL of ammonium hydroxide) to obtain 0.3% solution. 500 μL of this diluted suspension was spread over 2 cm² area of an optically transparent electrode (OTE). These electrodes were then air-dried on a warm plate and annealed in an oven at 673 K for 1 h. Details on the preparation of electrodes can be found elsewhere.⁴²

To prepare the TiO₂ Electrodes (OTE/TiO₂), TiO₂ colloids were first prepared by hydrolyzing titanium isopropoxide in glacial acetic acid solution followed by autoclaving the suspension at 507 K for 12 h. The details of the procedure can be found elsewhere.⁴³ 500 μL of the suspension was spread over the OTE plate using a syringe. After air drying the electrodes were annealed in an oven at 673 K for 1 h.

4.6.7. Photoelectrochemical Measurements

Photoelectrochemical measurements were performed using a standard two-compartment cell consisting of a working electrode and Pt wire gauze counter electrode. All photoelectrochemical measurements

were carried out in acetonitrile containing 0.5 M LiI and 0.05 M I₂. Photocurrents were measured using a Keithley model 2601 source meter. A collimated light beam from a 150 W Xenon lamp with a 400 nm cut-off filter was used for excitation of the electrodes. A Bausch and Lomb high intensity grating monochromator was introduced into the path of the excitation beam for selecting appropriate wavelength. The incident photon-to-photocurrent efficiency (*IPCE*) at various excitation wavelengths was determined from the equation 4.8, where *i*_{sc} is the short-circuit photocurrent (A/cm²), *I*_{inc} is the incident light intensity (W/cm²) and λ is the excitation wavelength.

$$IPCE(\%) = \frac{i_{sc}}{I_{inc}} \frac{1240}{\lambda} \times 100 \quad \text{eq (4.8)}$$

4.7. REFERENCES

1. (a) Fabian, J.; Nakazumi, H.; Matsuoka, M. *Chem. Rev.* **1992**, *92*, 1197. (b) Kiyose, K.; Kojima, H.; Urano, Y.; Nagano, T. *J. Am. Chem. Soc.* **2006**, *128*, 6548. (c) Basheer, M. C.; Alex, S.; Thomas, K. G.; Suresh, C. H.; Das, S. *Tetrahedron* **2006**, *62*, 605. (d) Coskun, A.; Ylimaz, M. D.; Akkaya, E. U. *Org. Lett.* **2007**, *9*, 607.
2. (a) Tian, M.; Tatsuura, S.; Furuki, M.; Sato, Y.; Iwasa, I.; Pu, L. S. *J. Am. Chem. Soc.* **2003**, *125*, 348. (b) Kang, H.; Facchetti, A.; Jiang, H.; Cariati,

- E.; Righetto, S.; Ugo, R.; Zuccaccia, C.; Macchioni, A.; Stern, C. L.; Liu, Z.; Ho, S.-T.; Brown, E. C.; Ratner, M. A.; Marks, T. J. *J. Am. Chem. Soc.* **2007**, *129*, 3267.
3. (a) Achilefu, S.; Jimenez, H. N.; Dorshow, R. B.; Bugaj, J. E.; Webb, E. G. Wilhelm, R. R.; Rajagopalan, R.; Johler, J.; Erion, J. L. *J. Med. Chem.* **2002**, *45*, 2003. (b) Chen, J.; Corbin, I. R.; Li, H.; Cao, W.; Glickson, J. D.; Zheng, G. *J. Am. Chem. Soc.* **2007**, *129*, 5798.
4. (a) Murakami, H.; Nagasaki, T.; Hamachi, I.; Shinkai, S. *J. Chem. Soc. Perkin Trans. 2* **1994**, 975. (b) Ajayaghosh, A.; Arunkumar, E.; Daub, J. *Angew. Chem.* **2002**, *114*, 1844. *Angew. Chem. Int. Ed.* **2002**, *41*, 1766. (c) Ros-Lis, J. V.; Martnez-Manez, R.; Rurack, K.; Sancenon, F.; Soto, J.; Spieles, M. *Inorg. Chem.* **2004**, *43*, 5183. (d) Jelinek, R.; Kolusheva, S. *Top. Curr. Chem.* **2007**, *277*, 155.
5. (a) Meier, H.; Petermann, R.; Gerold, J. *Chem. Comm.* **1999**, 977. (b) Adachi, M.; Nagao, Y. *Chem. Mater.* **2001**, *13*, 662.
6. Kohl, C.; Becker, S.; Mullen, K. *Chem. Commun.* **2002**, 2278.
7. Mishra, A, Behera, R. K.; Behera, P. K.; Mishra, B. K.; Behera, G. B. *Chem. Rev.* **2000**, *100*, 1973.
8. (a) Meier, H.; Dullweber, U. *J. Org. Chem.* **1997**, *42*, 4821. (b) Prabhakar, C.; Chaitanya, G. K.; Sitha, S.; Bhanuprakash, K.; Rao, V. J. *J. Phys. Chem. A* **2005**, *109*, 8604. (c) Ajayaghosh, A. *Acc. Chem. Res.* **2005**, *38*, 449-459.

9. (a) Gomez-Hens, A.; Aguilar-Caballos, M. P. *TrAC Trends Anal. Chem.* **2004**, *24*, 127. (b) Achilefu, S. *Technol. Cancer Res. Treat.* **2004**, *3*, 393. (c) Patonay, G.; Salon, J.; Sowell, J.; Strekowski, L. *Molecules* **2004**, *9*, 40. (d) Johnsson, N.; Johnsson, K. *ACS Chem. Biol.* **2007**, *2*, 31. (e) Kiyose, K.; Kojima, H.; Nagano, T. *Chem. Asian J.* **2008**, *3*, 506. (f) Descalzo, A. B.; Xu, H.-J.; Shen, Z.; Rurack, K. *Ann. N. Y. Acad. Sci.* **2008**, *1130*, 164. (g) Amiot, C. L.; Xu, S.; Liang, S.; Pan, L.; Zhao, J. X. *Sensors* **2008**, *8*, 3082.
10. (a) McWhorter, S.; Soper, S. A. *Electrophoresis* **2000**, *21*, 1267. (b) Fricker, M.; Runions, J. *Annu. Rev. Plant Biol.* **2006**, *57*, 79. (c) Rao, J. H.; Dragulescu-Andrasi, A.; Yao, H. Q. *Curr. Opin. Biotechnol.* **2007**, *18*, 17.
11. Near-Infrared Applications in Biotechnology (Ed.: R. Raghavachari), Marcel Dekker, New York, 2001.
12. (a) Siebrand, W.; *J. Chem. Phys.* **1967**, *46*, 440. (b) Yu, Y.-H.; Descalzo, A. B.; Shen, Z.; Rohr, H.; Liu, Q.; Wang, Y.-W.; Spieles, M.; Li, Y.-Z.; Rurack, K.; You, X.-Z. *Chem. Asian J.* **2006**, *1*, 176.
13. (a) Werts, M. H. V.; Woudenberg, R. H.; Emmerink, P. G.; van Gassel, R.; Hofstraat, J. W.; Verhoeven, J. W. *Angew. Chem.* **2000**, *112*, 4716; *Angew. Chem. Int. Ed.* **2000**, *39*, 4542. (b) Fischer, G. M.; Ehlers, A. P.; Zumbusch, A.; Daltrozzo, E. *Angew. Chem.* **2007**, *119*, 3824; *Angew. Chem. Int. Ed.* **2007**, *46*, 3750. (c) Johnson, J. R.; Fu, N.; Arunkumar, E.; Leevy, W. M.; Gammon, S. T.; Piwnica-Worms, D.; Smith, B. D. *Angew.*

- Chem.* **2007**, *119*, 5624; *Angew. Chem. Int. Ed.* **2007**, *46*, 5528. (d) Harriman, A.; Mallon, L. J.; Goeb, S.; Ziessel, R. *Phys. Chem. Chem. Phys.* **2007**, *9*, 5199. (e) Umezawa, K.; Nakamura, Y.; Makino, H.; Citterio, D.; Suzuki, K. *J. Am. Chem. Soc.* **2008**, *130*, 1550. (f) Killoran, J.; McDonnell, S. O.; Gallagher, J. F.; O'Shea, D. F. *New J. Chem.* **2008**, *32*, 483. (g) Song, X.; Kassaye, D. S.; Foley, J. W. *J. Fluoresc.* **2008**, *18*, 513. (h) Yang, Y.; Lowry, M.; Xu, X.; Escobedo, J. O.; Sibrian- Vazcluez, M.; Wong, L.; Schowalter, C. M.; Jensen, T. J.; Fronczek, F. R.; Warner, I. M.; Strongin, R. M. *Proc. Natl. Acad. Sci. USA* **2008**, *105*, 8829.
14. Fabian, J.; Nakazumi, H.; Matsuoka, M. *Chem. Rev.* **1992**, *92*, 1197.
15. (a) Yasui, S.; Matsuoka, M.; Kitao, T. *Dyes Pigments* **1988**, *10*, 13. (b) Gorman, A.; Killoran, J.; O'Shea, C.; Kenna, T.; Gallagher, W. M.; O'Shea, D. F. *J. Am. Chem. Soc.* **2004**, *126*, 10624.
16. Puyol, M.; Encinas, C.; Rivera, L.; Miltsov, Alonso, J. *Dyes Pigments* **2007**, *73*, 383.
17. (a) Avirah R. R.; Jyothish, K.; Ramaiah, D. *J. Org. Chem.* **2008**, *73*, 274. (b) Takechi. K.; Kamat P. V.; Avirah R. R.; Jyothish, K.; Ramaiah, D. *Chem. Mater.* **2008**, *20*, 265.
18. (a) Jyothish, K.; Arun, K. T.; Ramaiah, D. *Org. Lett.* **2004**, *6*, 3965. (b) Jyothish, K.; Avirah, R, R.; Ramaiah, D. *Org. Lett.* **2007**, *8*, 111. (c) Jyothish, K.; Avirah, R, R.; Ramaiah, D. *Arkivoc* **2007**, *8*, 296.

19. Sauve, G.; Kamat, P. V.; Thomas, K. G.; Thomas, J.; Das, S.; George, M. V. *J. Phys. Chem.* **1996**, *100*, 2117.
20. (a) Jisha, V. S.; Thomas, A. J.; Ramaiah, D. *J. Org. Chem.* **2009**, *74*, 6667. (b) Nair, A. K.; Neelakandan, P. P.; Ramaiah, D. *Chem. Commun.* **2009**, 6352.
21. (a) Nazeeruddin, M. K. Kay, A.; Rodicio, R.; Humphry-Baker, R.; Muller, P.; Liska, P.; Vlachopoulos, N.; Gratzel, M. *J. Am. Chem. Soc.* **1993**, *115*, 6382. (b) Hagfeldt, A; Graetzel, M. *Chem. Rev.* **1995**, *95*, 49. (c) Hagfeldt, A; Graetzel, M. *Acc. Chem. Res.* **2000**, *33*, 269. (d) Graetzel, M. *Nature* **2001**, *414*, 338. (e) Graetzel, M. *J. Photochem. Photobiol. C: Photochem. Rev.* **2003**, *4*, 145.
22. (a) Hara, K.; Sayama, K.; Ohga, Y.; Shinpo, A.; Suga, S.; Arakawa, H. *Chem. Commun.* **2001**, 569. (b) Hara, K.; Kurashige, M.; Dan-oh, Y.; Kasada, C.; Shinpo, A.; Suga, S.; Sayama, K.; Arakawa, H. *New J. Chem.* **2003**, *27*, 783.
23. (a) Ito, S.; Zakeeruddin, S. M.; Humphrey-Baker, R.; Liska, P.; Charvet, R.; Comte, P.; Nazeeruddin, M. K.; Péchy, P.; Takata, M.; Miura, H.; Uchida, S.; Grätzel, M. *Adv. Mater.* **2006**, *18*, 1202. (b) Horiuchi, T.; Miura, H.; Sumioka, K.; Uchida, S. *J. Am. Chem. Soc.* **2004**, *126*, 12218.
24. (a) Ehret, A.; Stuhl, L.; Spitler, M. T. *J. Phys. Chem. B* **2001**, *105*, 9960. (b) Sayama, K.; Hara, K.; Ohga, Y.; Shinpou, A.; Suga, S.; Arakawa, H. *New J. Chem.* **2001**, *26*, 200.

25. (a) Wang, Z.-S.; Li, F.-Y.; Huang, C.-H. *Chem. Commun.* **2000**, 2063. (b) Stathatos, E.; Lianos, P. *Chem. Mater.* **2001**, *13*, 3888. (c) Yao, Q.-H.; Meng, F.-S.; Li, F.-Y.; Tian, H.; Huang, C.-H. *J. Mater. Chem.* **2003**, *13*, 1048.
26. (a) Khazraji, A. C.; Kotchandani, S.; Das, S.; Kamat, P. V. *J. Phys. Chem. B.* **1997**, *103*, 4693. (b) Sayama, K.; Tsukagoshi, S.; Mori, T.; Hara, K.; Ohga, Y.; Shinpou, A.; Abe, Y.; Suga, S.; Arakawa, H. *Sol. Energy Mater. Sol. Cells* **2003**, *80*, 47.
27. (a) Ferrere, S.; Zaban, A.; Gregg, B. A. *J. Phys. Chem. B* **1997**, *101*, 4490. (b) Ferrere, S.; Gregg, B. A. *New J. Chem.* **2002**, *26*, 1155.
28. Hara, K.; Horiguchi, T.; Kinoshita, T.; Sayama, K.; Sugihara, H.; Arakawa, H. *Chem. Lett.* **2000**, *29*, 316.
29. Liang, M.; Wu, W.; Cai, F.; Chen, P.; Peng, B.; Chen, J.; Li, Z. *J. Phys. Chem. C* **2007**, *111*, 4465.
30. (a) Hagberg, D. P.; Edvinsson, T.; Marinado, T.; Boschloo, G.; Hagfeldt, A.; Sun, L. *Chem. Commun.* **2006**, 2245. (b) Li, S.-L.; Jiang, K.-J.; Shao, K.-F.; Yang, L.-M. *Chem. Commun.* **2006**, 2792. (c) Koumura, N.; Wang, Z.-S.; Mori, S.; Miyashita, M.; Suzuki, E.; Hara, K. *J. Am. Chem. Soc.* **2006**, *128*, 14256. (d) Kim, S.; Lee, J. K.; Kang, S. O.; Ko, J.; Yum, J.-H.; Fantacci, S.; De Angelis, F.; Censo, D. D.; Nazeeruddin, M. K.; Grätzel, M. *J. Am. Chem. Soc.* **2006**, *128*, 16701. (e) Chen, C.-Y.; Wu, S.-J.; Wu, C.-G.; Chen, J.-G.; Ho, K.-C. *Angew. Chem., Int. Ed.* **2006**, *45*, 1. (f) Qin, P.;

- Yang, X.; Chen, R.; Sun, L.; Marinado, T.; Edvinsson, T.; Boschloo, G.; Hagfeldt, A. *J. Phys. Chem. C* **2007**, *111*, 1853. (g) Chen, R.; Yang, X.; Tian, H.; Sun, L. *J. Photochem. Photobiol., A* **2007**, *189*, 295. (h) Thomas, K. R. J.; Hsu, Y.-C.; Lin, J. T.; Lee, K.-M.; Ho, K.-C.; Lai, C.-H.; Cheng, Y.-M.; Chou, P.-T. *Chem. Mater.* **2008**, *20*, 1830.
31. (a) Alex, S.; Santhosh, U.; Das, S. *J. Photochem. Photobiol. A* **2005**, *172*, 63. (b) Yum, J. H.; Walter, P.; Huber, S.; Rentsch, D.; Geiger, T.; Nlesch, F.; De Angelis, F.; Gratzel, M.; Nazeeruddin, M. K. *J. Am. Chem. Soc.* **2007**, *129*, 10320. (c) Silvestri, F.; Irwin, M. D.; Beverina, L.; Facchetti, A.; Pagani, G. A.; Marks, T. J. *J. Am. Chem. Soc.* **2008**, *130*, 17640. (d) Geiger, T.; Kuster, S.; Yum, J.-H.; Moon, S.-J.; Nazeeruddin, M. K.; Gratzel, M.; Nuesch, F. *Adv. Funct. Mater.* **2009**, *19*, 1.
32. (a) Chen, S.-Y.; Horng, M.-L.; Quitevis, E. L. *J. Phys. Chem.* **1989**, *93*, 3683. (b) Das, S.; Thanulingam, T. L.; Thomas, K. G.; Kamat, P. V.; George, M. V. *J. Phys. Chem.* **1993**, *97*, 13620. (c) Barazzouk, S.; Lee, H.; Hotchandani, S.; Kamat, P. V. *J. Chem. Phys. B* **2000**, *104*, 3616. (d) Das, S.; Thomas, J.; Thomas, K. G.; Madhavan, V.; Liu, D.; Kamat, P. V.; George, M. V. *J. Phys. Chem.* **1996**, *100*, 17310. (e) Arun, K. T.; Epe, B.; Ramaiah, D. *J. Phys. Chem. B* **2002**, *106*, 11622. (f) Takechi, K.; Sudeep, S.; Kamat, P. V. *J. Phys. Chem. B* **2006**, *110*, 16169.
33. (a) McRae, E. G.; Kasha, M. *J. Chem. Phys.* **1958**, *28*, 721. (b) Kasha, M.; Rawls, H. R.; El-Bayoumi, M. A. *Pure Appl. Chem.* **1965**, *11*, 371.

34. (a) Natoli, L. M.; Ryan, M. A.; Spitler, M. T. *J. Phys. Chem.* **1985**, *89*, 1448.
(b) Khazraji, A. C.; Hotchandani, S.; Das, S.; Kamat, P. V. *J. Phys. Chem. B* **1999**, *103*, 4693. (c) Sayama, K.; Tsukagoshi, S.; Hara, K.; Ohga, Y.; A, S.; Abe, Y.; Suga, S.; Arakawa, H. *J. Phys. Chem. B.* **2002**, *106*, 1363. (d) Toerne, K.; von Wandruszka, R. *Langmuir* **2002**, *18*, 7349.
35. Bigelow, R. W.; Freund, H. -J. *Chem. Phys.* **1986**, *107*, 159.
36. (a) Farnum, D. G.; Neuman, M. A.; Suggs, W. T., Jr. *J. Cryst. Mol. Struct.* **1974**, *4*, 199. (c) Wingard, R. E. *IEEE Ind. Appl.* **1982**, 1251. (b) McKerrow, A. J.; Buncel, E.; Kazmaier, P. M. *Can. J. Chem.* **1995**, *73*, 1605.
37. (a) Tristani-Kendra, M.; Eckhardt, C. J. *J. Chem. Phys.* **1984**, *81*, 1160.
(b) Law, K. Y. *J. Phys. Chem.* **1988**, *92*, 4226. (c) Bernstein, J.; Goldstein, E. *Mol. Cryst. Liq. Cryst.* **1988**, *164*, 213.
38. Liang, K.; Farahat, M. S.; Peristein, J.; Law, K. Y.; Whitten, D. G.; *J. Am. Chem. Soc.* **1997**, *119*, 830.
39. (a) Joseph, J.; Eldho, N. V.; Ramaiah, D. *Chem. Eur. J.* **2003**, *9*, 5926. (b) Joseph, J.; Eldho, N. V.; Ramaiah, D. *J. Phys. Chem. B* **2003**, *107*, 4444. (c) Kuruvilla, E.; Joseph, J.; Ramaiah, D. *J. Phys. Chem. B* **2005**, *109*, 21997.
(d) Neelakandan, P. P.; Ramaiah, D. *Angew. Chem. Int. Ed.* **2008**, *47*, 8407. (e) Kuruvilla, E.; Nandajan, P. C.; Schuster, G. B.; Ramaiah, D. *Org. Lett.* **2008**, *10*, 4295. (f) Neelakandan, P. P.; Sanju, K. S.; Ramaiah, D. *Photochem. Photobiol.* **2010**, *86*, 282.

40. Peng, X.; Song, F.; Lu, E.; Wang, Y.; Zhou, W.; Fan, J.; Gao, Y. *J. Am. Chem. Soc.* **2005**, *127*, 4170.
41. Jha, B. N.; Banerji, J. C. *Dyes Pigments* **1983**, *4*, 77.
42. Chibisov, A. K.; Zakharova, G. V.; Goerner, H.; Sogulyaev, Y. A.; Mushkalo, I. L.; Tolmachev, A. I. *J. Phys. Chem.* **1995**, *99*, 886.
43. Trosken, B.; Wiilig, F.; Schwarzburg, K.; Ehret, A.; Spitler, M. *J. Phys. Chem.* **1995**, *99*, 5152.

LIST OF PUBLICATIONS OF Ms. REKHA RACHEL AVIRAH

1. Synthesis of new cholesterol- and sugar-anchored squaraine dyes: Further evidence of how electronic factors influence dye formation, Jyothish Kuthanapillil, **Rekha Rachel Avirah**, Danaboyina Ramaiah, *Org. Lett.* **2006**, *8*, 111-114.
2. Dual-mode semisquaraine-based sensor for selective detection of Hg²⁺ in a micellar medium, **Rekha Rachel Avirah**, Jyothish Kuthanapillil, Danaboyina Ramaiah, *Org. Lett.* **2007**, *9*, 121-124.
3. Development of squaraine dyes for photodynamic therapeutical applications: Synthesis and study of electronic factors in the dye formation reaction, Jyothish Kuthanapillil, **Rekha Rachel Avirah**, Danaboyina Ramaiah, *Arkivoc* **2007**, *8*, 296-310.
4. Infrared absorbing croconaine dyes: Synthesis and metal ion binding properties, **Rekha Rachel Avirah**, Jyothish Kuthanapillil, Danaboyina Ramaiah, *J. Org. Chem.* **2008**, *73*, 274-279.
5. Harvesting infrared photons with croconate dyes, Kensuke Takechia, Prashant V. Kamat, **Rekha Rachel Avirah**, Jyothish Kuthanapillil, Danaboyina Ramaiah, *Chem. Mater.* **2008**, *20*, 265-272.
6. Functional cyclophanes: Promising hosts for optical biomolecular recognition, Danaboyina Ramaiah, Prakash P. Neelakandan, Akhil K. Nair, **Rekha Rachel Avirah**, *Chem. Soc. Rev.* **2010**, 39, 000 (In press).
7. Semisquaraine isomers: Implications on reactivity pattern, photophysical and metal ion binding properties, **Rekha Rachel Avirah**, Jyothish Kuthanapillil, Danaboyina Ramaiah (Communicated).
8. Aggregation and solid state fluorescence properties of a few novel semisquaraine dyes, **Rekha Rachel Avirah**, Jyothish Kuthanapillil, Nagappanpillai Adarsh, Danaboyina Ramaiah (Under preparation).

PAPERS PRESENTED AT CONFERENCE

1. Synthesis of novel quinoline based squaraine dyes: Experimental and theoretical investigation of the effect of substituents in the dye formation reaction, Jyothish Kuthanapillil, **Rekha Rachel Avirah**, Danaboyina Ramaiah, a poster presented at "*International Conference on Frontiers of Radiation and Photochemistry*," Mahatma Gandhi University, Kottayam, India, **2007**, February 8-11.
2. Synthesis, metal ion binding and light harvesting properties of novel infrared absorbing dyes, **Rekha Rachel Avirah**, Jyothish Kuthanapillil, Kensuke Takechi, Prashant V. Kamat and Danaboyina Ramaiah, a poster presented at the *11th CRSI National Symposium in Chemistry*, National Chemical Laboratory, Pune, India, **2009**, February 6-8.

